

# Lower Cretaceous Geothermal Reservoirs in the North German Basin

Dissertation  
zur Erlangung des mathematisch-naturwissenschaftlichen Doktorgrades  
"Doctor rerum naturalium"  
der Georg-August-Universität Göttingen  
im Promotionsstudiengang Geoscience  
der Georg-August University School of Science (GAUSS)

vorgelegt von

Sandra Franke

geboren in Saalfeld (Saale), Thüringen

Göttingen, 31.03.2023

**Betreuungsausschuss:**

Prof. Dr. Martin Sauter

Abt. Angewandte Geologie,  
Georg-August-Universität Göttingen

Dr. Matthias Franz

Abt. Angewandte Geologie,  
Georg-August-Universität Göttingen

**Mitglieder der Prüfungskommission:**

Referent: Dr. Matthias Franz

Abt. Angewandte Geologie,  
Georg-August-Universität Göttingen

Korreferent: Prof. Dr. Jonas Kley

Abt. Strukturgeologie,  
Georg-August-Universität Göttingen

2. Korreferent: Dr. Thomas Voigt

Institut für Geowissenschaften,  
Friedrich-Schiller-Universität Jena

Weitere Mitglieder der Prüfungskommission:

Prof. Dr. Martin Sauter

Abt. Angewandte Geologie,  
Georg-August-Universität Göttingen

Dr. Bettina Wiegand

Abt. Angewandte Geologie,  
Georg-August-Universität Göttingen

Prof. Dr. Inga Moeck

Abt. Angewandte Geothermik und  
Geohydraulik,  
Georg-August-Universität Göttingen

**Tag der mündlichen Prüfung: 23.05.2023**

## **Eidesstattliche Erklärung**

Hiermit versichere ich, dass ich die vorliegende Dissertation mit dem Titel 'Lower Cretaceous Geothermal Reservoirs in the North German Basin' selbstständig und ohne unzulässige Hilfe Dritter sowie ohne Benutzung anderer als der angegebenen Quellen und Hilfsmittel angefertigt habe. Alle Ausführungen, die wörtlich oder sinngemäß übernommen wurden, sind als solche gekennzeichnet. Die Arbeit hat in gleicher oder ähnlicher Form noch keiner anderen Prüfungsbehörde vorgelegen.

Jena, den 30.03.2023

Sandra Franke

## **Abstract**

This thesis contributes to the strategic effort to make Germany's energy supply more sustainable. The primary focus of this study was to enhance and update the geological knowledge of the Mesozoic deep geothermal sandstone aquifer complexes. The economically important Mesozoic deposits have been studied for decades, for example, the Buntsandstein, the Keuper, the Jurassic and the Lower and Upper Cretaceous. A comprehensive data base is provided by the data resulting from intensive hydrocarbon exploration since the last century. However, previous detailed work on Lower Cretaceous deposits had been done over 50 years ago, making new investigations applying new methods and techniques necessary.

Therefore, lithofacies analysis and determination of depositional environments were required to enhance the understanding of sand body architecture, sediment distribution and basin-scale configuration. Granulometric and petrophysical properties of lithofacies types and depositional environments were determined correlations and dependencies were differentiated according to available data. This work will contribute to reconstructing the primary basin extension in the eastern North German Basin and the basin history to predict the location, thickness and facies of Lower Cretaceous geothermal reservoirs. The results of this study show the importance of evaluating how tectono-stratigraphic and eustatic features influence the present-day petrophysical characteristics, distribution and thickness of Lower Cretaceous sandstone aquifers.

The eastern North German Basin was well connected to boreal and tethyal waters, although regressive conditions temporarily hampered faunal migration. Dominating terrestrial and shallow-marine conditions do not enable completely the same biostratigraphic time control as applied in the western North German Basin. However, characteristic ostracod, spore, pollen, foraminifera and dinocyst species could be identified combined with lithostratigraphic characteristics a time control on the Lower Cretaceous strata is enabled.

Despite the dominating extensional tectonic regime assigned to Lower Cretaceous times, the study area revealed widespread erosional patterns implying differential uplift and erosion. The formation and activity of the swell regions and salt movement contributed much to basin differentiation, the formation of local sub-basins and strata thickness. Three main unconformities could be figured out. Generally, the stratigraphic most complete successions kept preserved in syn-tectonic graben structures in northeast Germany and the rim synclines of salt plugs.

Petrographic analysis shows that the investigated sandstones are highly mature and influenced by diagenetic features, which enable high porosities and permeabilities depending

on the depositional environment. The grain fabric was stabilised by an eodiagenetic carbonate cement, which was dissolved during telodiagenetic uplift. The analysis of the grain-size distribution shows a constant trend, which suggests a relatively stable sediment source area. Corresponding to the heavy mineral assemblage, characterised by an ultrastable heavy mineral assemblage located on the Fennoscandian High.

The analysis of the depositional environments revealed deposits from a lagoonal or tidal flat, deltaic channel belt facies and alternating sand-, silt- and claystone successions from an upper and lower delta plain. Furthermore, delta front, prodelta and shoreface deposits were analysed. The ongoing subordinated basin extension and flooding are characterised by the formation of shoreface sands, fine clastics from the shelf transition zone, and pelagic limestones and mudrocks combined to a fully marine microfauna.

Finally, all information was combined to develop cumulative sandstone thickness maps, a schematic facies map for the Berriasian (Wealden 3-horizon) and the proposal of three potential exploration sites to minimise financial and exploration risks for deep geothermal aquifer exploration in the North German Basin.

## **Acknowledgement**

I acknowledge funding by the 'Bundesministerium für Wirtschaft und Energie', BMWI (grant 0325920). I want to thank Dr. Matthias Franz and Prof. Martin Sauter for the very interesting research opportunity. Dr. Matthias Franz is gratefully acknowledged for his supervising me the last years and for the numerous scientific discussions we had, I have really learned a lot during this time. I thank Dr. Thomas Voigt for his ideas, support, and cooperation during the last years and review work.

Likewise, many thanks to the further members of the committee: Prof. Dr. Jonas Kley for acting as the second reviewer, Dr. Bettina Wiegand, and Prof. Dr. Inga Moeck.

I am grateful to Dr. Marcus Wolfgramm, Kerstin Nowak and Christian Buse (GtN) for scientific discussions, lab work and support during SEM/EDX work; Dr. K. Obst and Juliane Brandes (Güstrow), M. Göthel (Wünsdorf), T. Tischner (Hannover), G. Notbohm (Grubenhagen) for access to core repositories of geological state surveys and well reports. I want to thank M. Magnus (Freiberg) for the preparation of thin sections, Dr. G. Sosa and Dr. A. van den Kerkhof (Göttingen) for their support during microscopy work and cathodoluminescence microscopy, F. W. Luppold, Dr. C. Heunisch and Dr. A. Bornemann (Hannover) for lab work in microfossil classification.

Many thanks to my colleagues from the Geoscience Centre Göttingen, especially to my colleague and friend Sebastian for the scientific discussions and support.

I am grateful to my friends Wiebke, Florian, Vanessa, Johanna and Nicole, who really encouraged and supported me continuously. Special thanks to my sister Anja and Benny for stimulating discussions, encouraging words and much patience.

## Table of Contents

Abstract.....	1
Acknowledgement .....	3
Table of Contents .....	4
The GeoPoNDD project .....	7
Motivation .....	8
Research approach .....	10
1 Introduction.....	11
2 Working area and geological setting.....	14
3 Methods.....	18
4 Lower Cretaceous stratigraphy .....	22
4.1 Biostratigraphy .....	22
4.1.1 Upper Jurassic.....	22
4.1.2 Upper Berriasian (Wealden-type) – Valanginian strata .....	23
4.1.3 Hauterivian - Barremian.....	23
4.1.4 Aptian – Lower Albian.....	24
4.1.5 Middle – Upper Albian .....	25
4.2 Palynostratigraphy .....	26
4.3 Sequence stratigraphy .....	27
4.3.1 Berriasian.....	28
4.4 Lithostratigraphy .....	31
4.4.1 Comparison of the Darß-Rügen-Usedom area and the Altmark-Prignitz Basin .....	33
4.5 Discussion.....	34
4.5.1 Influence of sea-level changes on sediment deposition .....	34
4.5.1.1 Polish Trough.....	35
4.5.2 Bio- and sequence-stratigraphic correlations.....	37
5 Structural controls on Lower Cretaceous strata .....	39
5.1 Unconformities in the Upper Jurassic – Lower Cretaceous successions.....	39
5.1.1 Base-Berriasian Unconformity.....	39
5.1.2 Base-Hauterivian Unconformity.....	39
5.1.3 Base-Albian Unconformity .....	40
5.2 West Western Pomeranian Fault and Graben System.....	42
5.2.1 Darß Graben.....	42
5.2.2 Samtens Graben System .....	44
5.2.3 Usedom Basin .....	45
5.3 Salt structures .....	47
5.4 Upper Jurassic–Lower Cretaceous syn-tectonic strata.....	48
5.4.1 Distribution and thickness .....	48
5.4.1.1 Upper Jurassic strata.....	48

5.4.1.2	Upper Berriasian (Wealden-type) – Valanginian strata .....	48
5.4.1.3	Hauterivian–Barremian strata.....	49
5.4.1.4	Aptian –Lower Albian strata .....	49
5.4.1.5	Middle – Upper Albian strata .....	50
5.5	Discussion.....	50
5.5.1	Unconformities.....	50
5.5.2	Basin differentiation of the North German Basin .....	52
5.5.3	Estimated erosion.....	53
6	Petrography, granulometry and diagenesis of Lower Cretaceous sandstones .....	55
6.1	QFL and Granulometry .....	55
6.1.1	Upper Jurassic - Kimmeridgian .....	56
6.1.2	Upper Berriasian (Wealden-type) – Valanginian strata .....	57
6.1.3	Hauterivian.....	62
6.1.4	Barremian .....	65
6.1.5	Aptian – Lower Abian .....	66
6.1.6	Middle – Upper Albian .....	67
6.2	Heavy minerals .....	69
6.2.1	Heavy mineral assemblage .....	69
6.2.2	Heavy mineral distribution .....	71
6.3	Diagenesis and geochemical characterisation of Lower Cretaceous strata.....	72
6.3.1	Upper Berriasian - lower Valanginian (Wealden-type) sandstones.....	72
6.3.2	Upper Hauterivian - lower Barremian glauconitic sandstones.....	73
6.4	Geochemical characterisation of Lower Cretaceous sediments.....	74
6.5	Discussion.....	75
6.5.1	Heavy minerals .....	75
6.5.2	Diagenesis .....	77
7	Lower Cretaceous Depositional environments.....	79
7.1	Upper Jurassic .....	79
7.2	Upper Berriasian (Wealden-type) – Valanginian strata.....	80
7.2.1	Sporomorph Ecogroup Model .....	84
7.3	Hauterivian – Barremian .....	87
7.4	Aptian – Lower Albian .....	88
7.5	Middle – Upper Albian.....	88
8	Geothermal Potential of Lower Cretaceous sandstones.....	90
8.1	Geothermal utilisation in the North German Basin.....	91
8.1.1	Hydrothermal doublet system.....	94
8.1.2	Aquifer thermal energy storage in porous sandstone aquifers.....	95
8.1.3	Hydrogen storage in porous sandstone aquifers.....	96
8.2	Characterisation of Lower Cretaceous Geothermal reservoirs.....	97
8.2.1	Petrophysical parameters.....	98



8.2.2	Berriasian sandstone reservoirs.....	99
8.2.3	Hauterivian – Barremian sandstone reservoirs.....	103
8.3	Exploration examples.....	108
8.3.1	Proposal 1: Wittstock/Dosse region .....	108
8.3.2	Proposal 2: Rheinsberg region.....	109
8.3.3	Proposal 3: Werle region .....	110
9	Conclusions.....	111
10	Further perspectives.....	113
	Curriculum vitae.....	114
	Bibliography.....	115
	Appendix.....	129

## The GeoPoNDD project

This doctoral thesis includes parts of the (R&D) GeoPoNDD project: Lower Cretaceous reservoirs, which aims the development of exploration methodologies by enabling high-resolution subsurface maps of deep geothermal reservoirs to minimise exploration risks and develop new reservoir exploration opportunities in the North German Basin. The GeoPoNDD project was led by Matthias Franz (University of Göttingen) and Markus Wolfgramm (GTN) and funded by the German Federal Ministry of Economics (Bundesministerium für Wirtschaft und Energie) in the years 2015–2019. This thesis deals with the application of the exploration strategy to Lower Cretaceous Reservoir Complexes (*Fig. 1*), and therefore unpublished results will be used. After implementing the project results into the web-based GeotIS, reservoir thickness maps of the Lower Cretaceous Reservoir Complexes will be available to project developers and the scientific community.

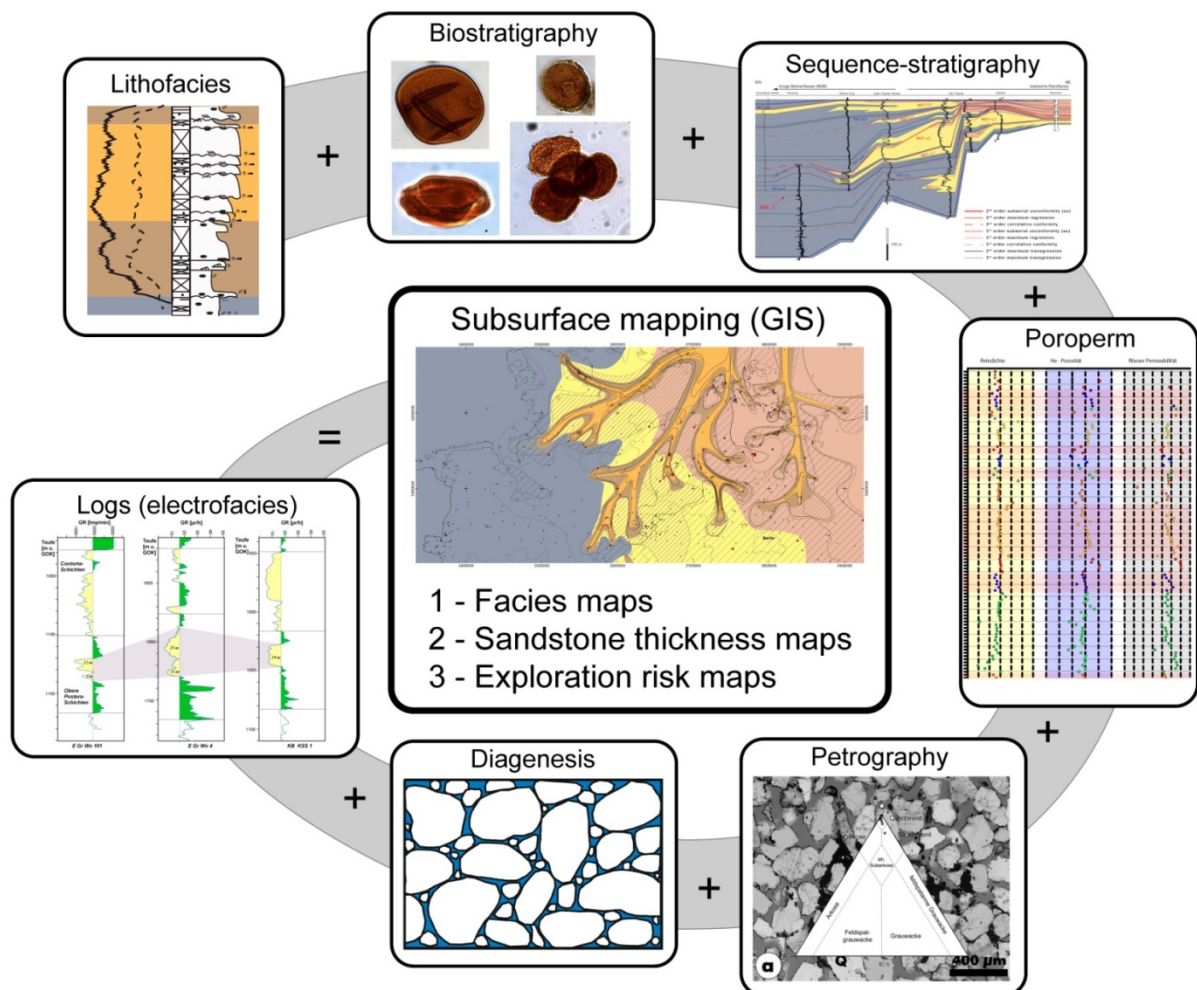


*Fig. 1: Workflow in the GeoPoNDD project show included data sources and the simplified exploration strategy applied to Mesozoic hydrothermal reservoirs.*

## Motivation

In 2010, the German government decided to reduce greenhouse gas emissions until 2050 by 80–95 % compared to 1990 levels. As an appropriate contribution to the Paris Agreement of achieving global greenhouse gas neutrality in the second half of this century, the Climate Action Plan 2050 represents a strategy for modernising the economy and finding possibilities for reducing greenhouse gas emissions for the present and near future. The energy sector is currently causing more than 80 % of the emissions in Germany.

In 2021, Germany's primary energy consumption amounted to 12,265 petajoules (PJ) or 418.5 million tons of coal equivalents. The most important energy carrier continued to be mineral oil, with a share of 32.3 % in 2021, followed by natural gas at 26.8 % and renewable energy at 15.9 % (AGEB, 2022). Deep geothermal energy, and environmental heat, including near-surface geothermal energy and solar thermal energy, continued to account for a share of about 5 % in the primary energy consumption in 2021. According to the German Federal Heat Pump Association (BWP), about 154,000 heat pumps for heating purposes as well as 23,500 hot water heat pumps, were newly installed in 2021 (AGEB, 2022). Consequently, the renewable environmental heat generated using heat pumps increased by 11 % to 68 PJ, including 4 PJ energy production from deep geothermal energy.

However, Germany is a considerable net importer of almost all fossil fuels (i.e. hard coals, mineral oil, and natural gas). In 2021, domestic primary energy consumption has been covered by imports which amounted to 95 % for mineral oil and 89 % for natural gas. One of the most important supplier countries for crude oil and natural gas continued to be Russia, with 34 % and 55 % (AGEB, 2022). Higher domestic production volumes generally reduce the dependence on imports. Developing renewables is a crucial step toward reaching this goal, not least because of climate change and political conflicts.

By 2030, 50 % of the heat supply will be produced on a climate-neutral basis. Therefore, the Climate Action Status report of January 2022 contains the specific target of developing a geothermal potential of 10 TWh by 2030 as far as possible. This means multiplying the amount of geothermal heat sources fed into heat networks by a factor of 10 (BMWK, 2022). To attain this goal, a concept providing eight specific measures was developed. This study contributes to the measures by collating existing data to provide a basis for identifying potentially promising areas for specific geothermal projects. By giving an exploration strategy, integrating palaeontological, sedimentological, petrophysical and hydraulic methods into a standard workflow, which was applied to a large data base of abundant well data in the North German Basin, this study contributes to the development of geothermal energy in Germany.

The North German Basin yields deep geothermal resources bound by Paleozoic petrothermal and Mesozoic hydrothermal (Fig. 2) reservoirs. These resources have been exploited in the past fifty years at several localities. Neustadt-Glewe, Neubrandenburg and Waren may serve as examples. Despite this long-term energy production and usage, the exploration risks remain high and necessitate a reliable prediction and targeting of subsurface geothermal reservoirs. Therefore, this study aims to improve the understanding of Lower Cretaceous geothermal sandstone reservoirs in the North German Basin.

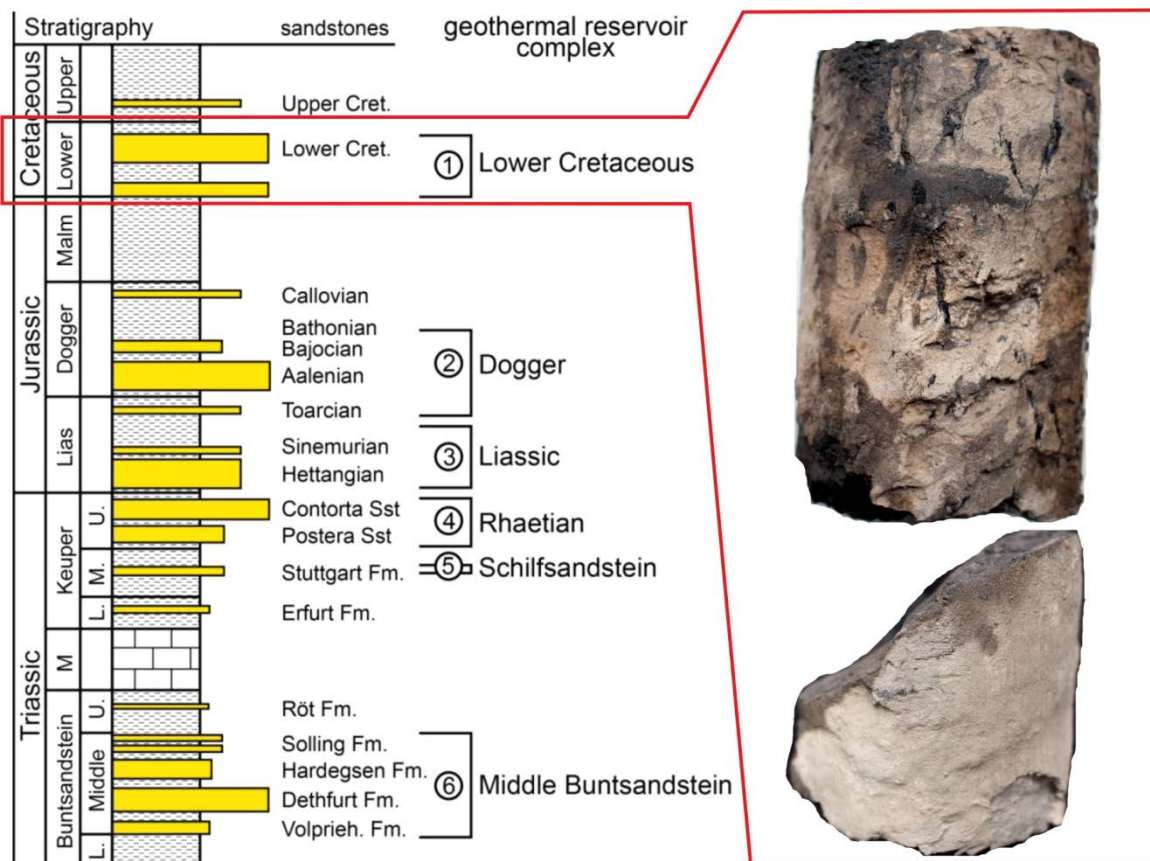


Fig. 2: Mesozoic hydrothermal reservoirs in the North German Basin. This study aims the characterisation of Lower Cretaceous reservoirs. Core material from well Darßer Ort serves to illustrate sandstone reservoirs in northeastern Germany.

## Research approach

This doctoral thesis is based on unpublished results of the preceding project work, which detail the development of the exploration strategy, including the improvement of the time-control on the Lower Cretaceous succession and the subsurface mapping development methodology and the evaluation of the remaining exploration opportunities. *Chapters 1 and 2* introduce the working area located in the eastern North German Basin according to previous research and the geological setting, as well as a description of the working area. *Chapter 3* summarises the applied analytical methods to characterise the Lower Cretaceous strata. By means of stratigraphy in *chapter 4*, structural controls in *chapter 5*, the petrography, granulometry and diagenesis in *chapter 6* and the depositional environments in *chapter 7*, the Berriasian – Albian strata were analysed and characterised in detail. Therefore, analysing structural geologic features, petrographic and litho-facies characterisation on a basin-wide scale enabled a correlation to the western North German Basin. Moreover, a detailed lithostratigraphic description of the previously unnamed stratigraphic units from the eastern North German Basin is proposed. *Chapter 8* gives a short overview of the utilisation of geothermal energy in Northeast Germany and the characterisation of the most promising Lower Cretaceous geothermal reservoirs, including the proposal of three potential exploration sites by evaluating detailed and site-specific well-, lithofacies- and petrography data.

## 1 Introduction

In Late Jurassic to Early Cretaceous times, the Upper Jurassic to Lower Cretaceous strata of the North German Basin were deposited during a phase of pronounced changes in the global sea-level and fundamental structural reorganisation of the Central European Basin System (CEB) (e.g. Haq et al., 1987; Nöldeke and Schwab, 1977; Vail, 1977; Ziegler, 1990; Sneider et al., 1995; Mutterlose and Bornemann, 2000; Kossow and Krawczyk, 2002; Scheck-Wenderoth et al., 2008; Haq, 2014). During Berriasian to Barremian times, the paleoclimate conditions were relatively cool, entering to full-greenhouse conditions during the Aptian (Voigt et al., 2008a), with the onset of maximum rates of oceanic crust formation and related tectonic CO<sub>2</sub>-production (Larson, 1991, Wilson et al., 2002; Voigt et al., 2008a). Global oceanic anoxic events are marked by the deposition of black shales during times of oceanic anoxic conditions (Schlanger and Jenkins, 1976) in the Early Aptian and latest Cenomanian witness major palaeoceanographic changes.

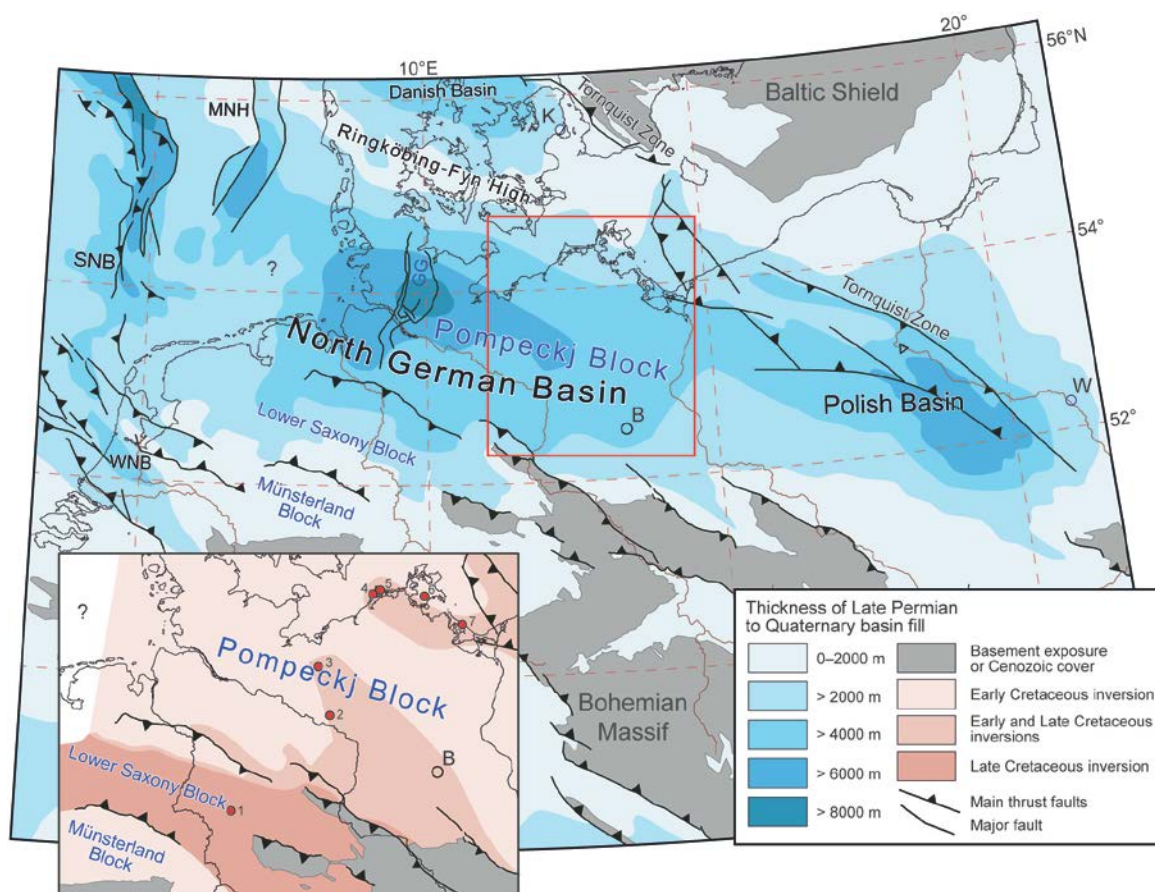


Fig. 3: Central European Basin System with subbasins, major fault systems and basement exposures, MNH – Mid North Sea High, SNB – South North Sea Basin, WNB – West Netherlands Basin; GG – Glückstadt Graben, modified after Kley and Voigt (2008). Thickness of the Later Permian–Quaternary basin fill according to Ziegler (1990). Red box shows working area; the inset schematically shows the Cretaceous inversion history of some Blocks of the North German Basin and standard sections shown in Fig. 10. 1 – Gt Groß Buchholz 1, 2 – E Gorlosen 12, 3 – Gt Schwerin 6, 4 – Kb Barth 10, 5 – Kb Darßer Ort 1/ E Prerow 1, 6 – Kb Garz 1/E Rügen 105, 7 – Kb Ückeritz 1/Kb Wolgast 1, 8 – Eulenflucht 1, 9 – Isterberg 1001.

The major drop of the global sea-level in the Tithonian and low stand in the Berriasian resulted in the progradation of terrestrial environments into the North German Basin and neighbouring subbasins of the CEB (e.g. Lott et al., 2010; Vejrbæk et al., 2010). Consequently, the exchange across western European basins was hampered, leading to faunal and floral endemism in Tethyan and Boreal provinces (Haq et al., 1987; Ziegler, 1990; Ruffell, 1991; Voigt et al., 2008; Haq, 2014). The following step-wise and pronounced sea-level rise culminated in the first-order highstand in the Turonian stage (Haq et al., 1987, 2014; Ziegler, 1982, 1990) and led to pelagic sedimentation in western European shelf basins (e.g. Einsele, 1992; Hay, 1995; Hay et al., 1999).

Contemporaneously, the structural reorganisation of the CEB resulted in the widespread erosion of Mesozoic strata in the North German Basin and the subsidence of several basin parts (TTZ, Prignitz Basin, Lower Saxony Basin). The Late Cimmerian Unconformity (e.g. Stille, 1924; Voigt, 1963; Heybroek et al., 1967; Hallam, 1971), which may be developed as individual unconformity or composite unconformity, represents a major bounding surface marking the transition from the basin fill stage to the basin differentiation stage and the inversion stage in the development of the North German Basin (e.g. Nöldeke and Schwab, 1977; Schwab, 1985; Ziegler, 1990; Kockel, 1998; Frisch and Kockel, 2004; Bachmann et al., 2008; Scheck-Wenderoth et al., 2008). In other subbasins of the CEB, for example, the northern North Sea Basin, the Late Cimmerian Unconformity is attributed to the transition from the syn-rift stage to the post-rift stage (e.g. Badley et al., 1988; Gabrielsen et al., 1990; Nøttvedt et al., 1995; Kyrkjebø et al., 2004).

The Pompeckj Block, the Permo–Jurassic depocenter of the North German Basin, was subsequently uplifted during Late Jurassic–Early Cretaceous times, resulting in erosion of Lower Cretaceous to Upper Triassic strata (Jaritz, 1969, 1980; Jaritz et al., 1991; Kossow et al., 2000; Kossow and Krawczyk, 2002; Beutler et al., 2012; Bruns et al., 2013; Sosnicka and Lüders 2020; Schnabel et al., 2021). Resulting from the complex interplay of uplift, erosion and deposition at the Pompeckj Block during these inversion phases, Albian post-uplift strata are disconformably overlying truncated Jurassic and Triassic strata (*Fig. 3*; e.g. Jaritz, 1969; Al Hseinat and Hübscher, 2017; Ahlrichs et al., 2020).

As the present-day occurrences of Upper Jurassic to Lower Cretaceous strata of the eastern extension of the Pompeckj Block, formerly known as 'Ostelbisches-Massiv' (Katzung and Ehmke, 1993), are limited to smaller subbasins, rim-synclines and grabens. These occurrences are commonly explained by the formation of isolated syn-depositional epeiric basins (e.g. Elstner and Mutterlose, 1996; Kockel, 1998; Voigt et al., 2008), but the assumption of isolated basins is not supported by petrography of sandy detritus, heavy minerals, facies, and correlatable sequences. In all remnant basins, marine influence is obvious, pointing to an extended depositional system eroded lately.

Previous research was mainly focused on the Lower Cretaceous in the western part of the North German Basin, in particular, the Lower Saxony Basin and western Pompeckj Block, and the southern margins of the North German Basin (e.g. Kölbel, 1944; Wolburg, 1949, 1959; Schott, 1967; Jaritz, 1969, 1980; Kemper, 1973; Dörhöfer, 1977; Pelzer and Wilde, 1987; Jaritz et al., 1991; Pelzer et al., 1992; Mutterlose, 1992, 1995; Kockel, 1998; Pelzer, 1998; Mutterlose and Bornemann, 2000; Baldschun et al., 2001; Voigt et al., 2007, 2008; Schneider, 2017; 2018; Malz et al., 2020). In the eastern part of the North German Basin, only a few studies investigated the late Jurassic–early Cretaceous strata in detail, for example, Diener (1968, 1974), Döring (1965a, b, 1966) and Wienholz (1967), who contributed much to the stratigraphic correlation. But the controls on depositional processes and environments in a subsequently flooded and tectonically influenced basin were not investigated in detail so far.

This work reports the results of a study on previously unpublished Lower Cretaceous well and seismic data from NE Germany (*Fig. 3 and Fig. 4*). New results from the application of palaeontological, sedimentological and sequence-stratigraphic methods are merged into a tectono-eustatic framework disentangling the controls on sedimentological processes and depositional environments of Berriasian–Albian syn-tectonic strata. The strongly varying and regional different subsidence and uplift rates as well as the sea-level changes, complicate the reconstruction of primary strata distribution and thickness.

The primary focus of this study was to enhance and update the geological knowledge of the Lower Cretaceous sandstone aquifer complexes. A lithofacies analysis and determination of depositional environments were required to enhance the understanding of sandbody architecture, sediment distribution and basin-scale configuration. Granulometric and petrophysical properties of lithofacies types and depositional environments were determined, correlations and dependencies were differentiated according to available data. This work will give a contribution in terms of reconstructing the primary basin extension in the eastern North German Basin and the basin history to predict the location, thickness and facies of Lower Cretaceous geothermal reservoirs. Thickness maps were developed and three potential exploration sites were proposed.



## 2 Working area and geological setting

The Central European Basin (CEB) is a large epicontinental sag basin (c.f. Bally and Snellson, 1980) composed of several subbasins usually referred to as basins, for example, the North German Basin (e.g. Nöldecke and Schwab, 1977; Ziegler, 1990; Bachmann et al., 2008, 2010). The CEB started to form in the latest Carboniferous after the Variscan Orogeny and was subsiding up to recent times (Sirocko et al. 2008). During this long basin history, first, a thick volcano-sedimentary basin fill accumulated, followed by a poorly sedimentary sequence with the greatest thickness of more than 8000 m in the North German Basin (Glückstadt Graben, Pompeckj Block; *Fig. 3*). The complex basin history is commonly subdivided into three major phases of basin evolution: 1) basin initiation stage (Latest Carboniferous to Middle Permian), 2) basin fill stage (Middle Permian to Middle Jurassic) 3) basin differentiation stage (Late Jurassic to Early Cretaceous) 4) inversion stage (Late Cretaceous to recent) (e.g. Nöldecke and Schwab, 1977; Schwab, 1985; Ziegler, 1990; Breitzkreuz et al., 2008; Bachmann et al., Stollhofen et. al., 2008). The major phases of basin evolution are bounded by pronounced and geographically wide-spread unconformities, the Middle Permian “Altmark I” unconformity (Hoffmann et al., 1989), the base-Cretaceous Unconformity (*Fig. 10*) also referred to as “Late Cimmerian Unconformity” (Stille, 1924; Ziegler, 1990), the Subhercynian unconformity.

In Cretaceous times, the CEB was situated in the NW peri-Tethyan realm at around 30°N (e.g. Stampfli and Borel, 2002). The North German Basin was connected with neighbouring basins, such as the Danish-Polish Basin, and the North Sea Basin, which were linked with the Tethys and Boreal Oceans (*Fig. 4*). Accordingly, transgressions and faunal migrations via these subbasins are documented in the North German Basin (Bartenstein and Brand, 1951, Bartenstein, 1962, Marek and Raczynska, 1979, Marek, 1988, Strauss et al., 2003, Mutterlose and Bornemann, 2000).

As the North German Basin was well connected with Tethyan and Boreal waters, the global sea-level primarily controlled late Jurassic–early Cretaceous depositional environments. Thickness was controlled by rapid subsidence of the Lower Saxony basin and the uplift of neighbouring areas (northern Rhenish Massif-Münsterland, Pompeckj-Block) and reached more than 5 km (Senglaub et al, 2005; Munoz, 2006). As a consequence of the low global sea-level during the Tithonian–Berriasian stages (Haq, 2014), evaporitic to fluvio-deltaic depositional environments of the Münders Formation and the Bückeberg Group are wide-spread in the western North German Basin (Diener, 1974, 2004, Kemper, 1973, 1979). Due to post-depositional erosion, the strata in the eastern NGB show a limited present-day distribution. The subsequent rise of the global sea-level throughout the Cretaceous contributed to the formation of a large shelf sea in the CEB. During the Valanginian–Albian

stages, this shelf sea was dominated by siliciclastic depositional environments of the Minden-Braunschweig Group (Kemper, 1973, 1979, Mutterlose and Bornemann, 2000). Later, in the Albian and Cenomanian, increasing carbonate sedimentation triggered the transformation into a pelagic shelf sea dominated by carbonate depositional environments of the Plänerkalk and Schreibkreide Groups (Wilmsen, 2003; Wilmsen et al., 2005; Voigt, S. et al., 2008a, b) accompanied by an enormous sea-level rise during the early late Cretaceous.

The investigated Lower Cretaceous strata were deposited during the basin differentiation, which was dominated by uplift, extension and probably strike-slip tectonics before the late Cretaceous inversion (Scheck-Wenderoth et al., 2008; Senglaub et al., 2005). In this c. 50 Ma long interval ranging from the Kimmeridgian to the early Albian, the Pompeckj Block, a Permian– early middle Jurassic depocenter of the northeastern North German Basin, was uplifted and considerable parts of the Mesozoic succession were eroded (e.g. Jaritz, 1969; Diener, 1974; Ziegler, 1990; Kossow et al. 2000; Kossow and Krawczyk et al., 2002; Beutler et al., 2012; Bruns et al., 2013; Sosnicka and Lüders, 2020; Schnabel et al., 2021). Consequently, Lower Albian to Cenomanian strata disconformably cover Jurassic and even Triassic strata, representing a significant geological time gap related to a single unconformity or the amalgamation of several unconformities (*Fig. 4*; Beutler et al., 2012). In the western North German Basin, for example, the German North Sea sector, the base-Cretaceous Unconformity exhumed the so-called Mid-Cimmerian Unconformity associated with doming in the North Sea area (Hallam and Sellwood, 1976; Ziegler, 1990; Underhill and Partington, 1993).

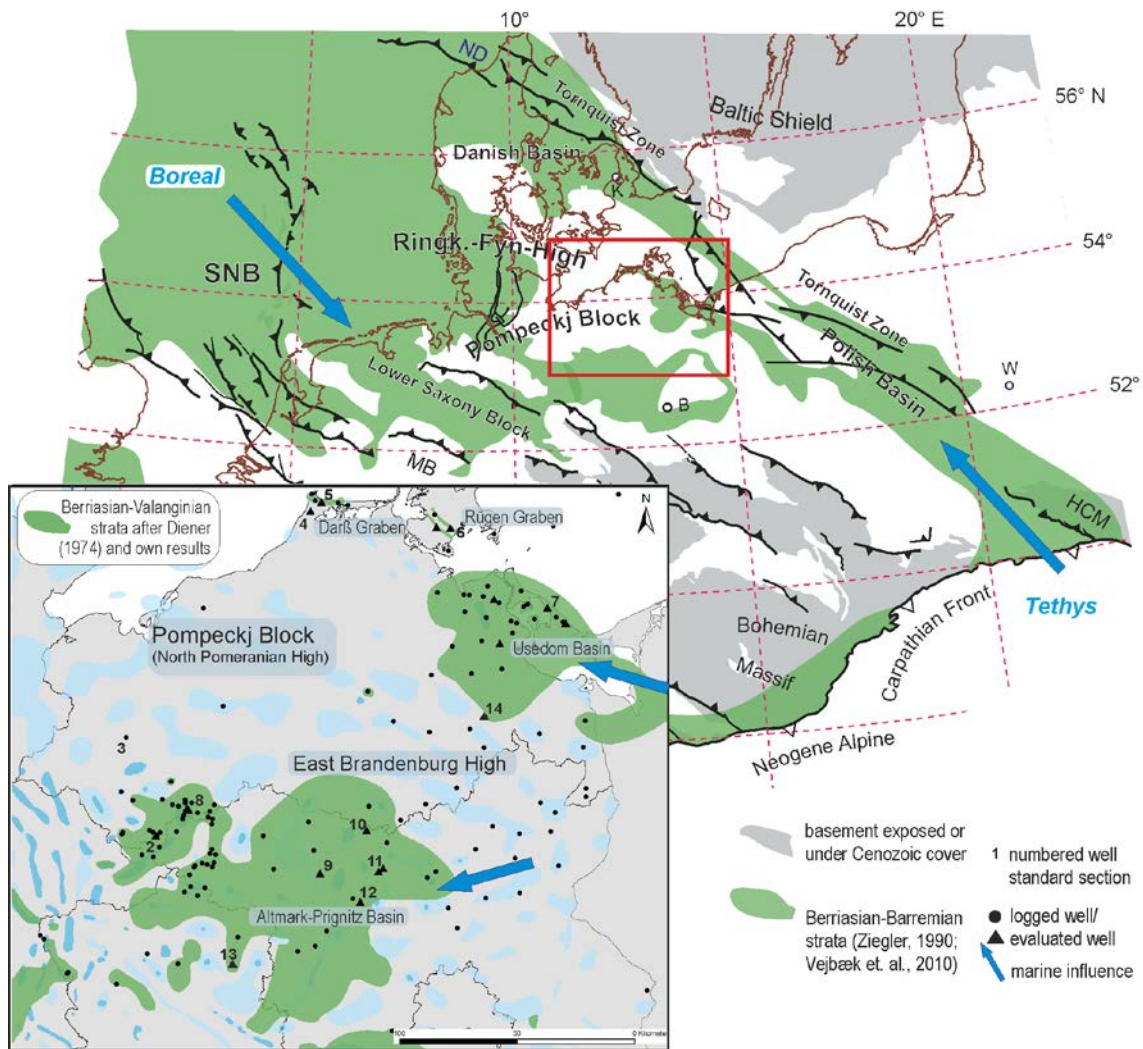


Fig. 4: Present-day distribution of Lower Cretaceous strata in the Central European Basin. Transgressions and faunal migrations via the Danish Basin (Eltner 1993; Mutterlose 1992a) and Polish Basin (Leszczynski, 1997; Vejbaek et al., 2010) continued into the North German Basin. The brackish-marine influence on Wealden-type environments in the eastern NGB is linked to the Polish Basin (this study). Overview map compiled from Ziegler (1990) and Vejbaek et al. (2010); detailed map compiled from Diener (1968) and own data; standard sections shown in Fig. 10 and Fig. 11: 2 – E Gorlosen 12, 3 – Gt Schwerin 6, 4 – Kb Barth 10, 5 – Kb Darßer Ort 1/ E Prerow 1, 6 – Kb Garz 1/E Rügen 105, 7 – Kb Uckeritz 1/Kb Wolgast 1, 8 – Werle 19/20, 9 – Teetz 1, 10 – Zechlinerhütte 1, 11 – Gransee 2, Zippelsförde 1, 12 – Neuruppin 2, 13 – Sanne 1, 14 – JomB 3.

Resulting from uplift and erosion during the basin differentiation in the following late Cretaceous inversion stage, the present-day occurrence of Upper Jurassic–Lower Cretaceous strata at the Pompeckj Block is limited to smaller sub-basins, rim-synclines and grabens. In smaller sub-basins, the preserved successions and thicknesses of strata differ notably. In the Prignitz-Altmark Basin, an almost complete Lower Cretaceous succession rests unconformably on Middle Jurassic strata. In contrast, in the Usedom Basin, an incomplete Upper Jurassic–Lower Cretaceous succession is preserved, showing internal unconformities (Fig. 10). The partly elevated thicknesses of Upper Jurassic–Lower Cretaceous in grabens and rim-synclines point to the syn-sedimentary formation of these structures (Diener, 1974, 2004; Kossow et al., 2000; Kossow and Krawczyk, 2002). Despite the formation of salt structures at the Pompeckj Block starting already in the late Triassic, the

initiation of several salt structures began in the late Jurassic–early Cretaceous interval (Jaritz, 1974, 1987). A particularly good example is the rim-syncline between the Conow, Rambow and Werle salt plugs, where an approximately 600 m thick succession of Tithonian–Albian strata rests unconformably on Middle Jurassic strata (Diener, 1974).

The Lower Saxony Basin formed during the late Jurassic and early Cretaceous. The neighbouring Pompeckj Block, the Münsterland Block together with the Rhenic Block represent uplifted blocks that were active at the same time. Indicated by a stratigraphically complete Upper Jurassic–Lower Cretaceous succession of an enormous thickness (e.g. well Groß Buchholz 1 (*Fig. 10*), the Lower Saxony Block was unaffected during the late differentiation and early inversion stage. But strongly enhanced thicknesses, particularly at the Lower Saxony Block, demonstrate the syn-sedimentary increase of subsidence rates (Betz et al., 1987; Petmecky et al., 1999; Senglaub, 2005, Bruns et al., 2013).

After a tectonically quiet period from the late Albian to Turonian the North German Basin was subject to a subsequent phase of uplift and erosion during the inversion stage. Some authors argue that mild basin inversion started already in the Late Cenomanian (Voigt et al., 2021) and culminated in the Santonian-Campanian. The most prominent features of Late Cretaceous inversion are exhumed basement blocks, such as the Harz Mountains or the Flechtingen High (Kockel, 1998; Eynatten et al., 2006, 2019; Voigt, T. et al, 2008; Malz et al., 2020). Moreover, the Lower Saxony Block, the Grimmen Swell but also larger parts of the South German Basin were uplifted and more than 4,000 m of pre-inversion strata were eroded (Petmecky et. al, 1999; Senglaub et. al, 2005; Bruns et. al, 2013). A particularly good example of Upper Cretaceous syn-inversion deposits was described from the Subhercyn Basin north of the Harz Mountains (e.g. Köbel, 1944, 1967; Voigt et al. 2006, 2008). The phase of Late Cretaceous inversion tectonics ceased in the late Campanian (Voigt et al., 2008, 2021), as is shown by the transgression of Maastrichtian sediments on the uplifted Gradelegen and Prignitz blocks.

At the larger Pompeckj Block, the Upper Cretaceous strata show, in general, no evidence of syn-sedimentary tectonics (Diener, 1967, 1968; Diener et al, 2004). Only individual parts of the eastern North German Basin, for example, the Prignitz-Altmark Basin, also referred to as Prignitz-Lausitz Swell or Block (e.g. Lange et al., 2008; Voigt, 2015; Malz et al., 2020), and the Grimmen Swell (e.g. Diener et al., 2004), were affected by Late Cretaceous inversion tectonics as indicated by some 200 m of Coniacian–Santonian strata missing below upper Campanian post-inversion strata (e.g. Diener et al., 2004; Voigt et al., 2008). In individual parts of the North German Basin, the Subhercynian Unconformities, or base-Campanian Unconformity, were exhumed by the base-Palaeocene Unconformity resulting from an Early Paleogene inversion phase.

### 3 Methods

Although the history of the Lower Saxony Basin is already well understood, the eastern and northeastern basin parts affected by late Jurassic-early Cretaceous basin differentiation are still under discussion. The working area is situated in NE Germany including the Darß Peninsula and the islands of Rügen and Usedom (*Fig. 3 and Fig. 5*). Today, the occurrences of Lower Cretaceous strata are limited to the Usedom Basin and to fault-bounded graben structures at the Darß Peninsula (Köhler and König, 1965; Fritzsche and Doß, 1980) and the Rügen Island (Krauss and Mayer, 2004). The Lower Cretaceous strata in the Usedom Basin are connected to contemporaneous strata in the Polish Basin regarding stratigraphy and fossils pointing to a former connection of the North German Basin with the Polish and the Danish Basins (*Fig. 4*; Diener, 1967, 1974).

The working area was chosen for two reasons: 1) salt tectonics were limited due to the low thickness of Zechstein-salt, and 2) abundant well and seismic data are available from previous drilling campaigns. The aim is to characterise the lithofacies, structural patterns and sedimentary petrography of Lower Cretaceous strata concerning suitability as potential geothermal reservoirs.

The limited vertical migration of Permian salt resulted in only a few small and immature salt pillows (*Fig. 5*). Immature salt pillows represent an incipient stage of salt movement and are characterised by low-amplitudes of vertical uplift, shallow flanks and narrow rim synclines (e.g. Trusheim, 1960; Kossow et al., 2000; Ahlrichs et al., 2020). Accordingly, the influence of these salt pillows on depositional processes and environments was strongly reduced compared to the large salt plugs and walls of the western Pompeckj Block (e.g. Jaritz 1974, 1987; Diener et al., 2004).

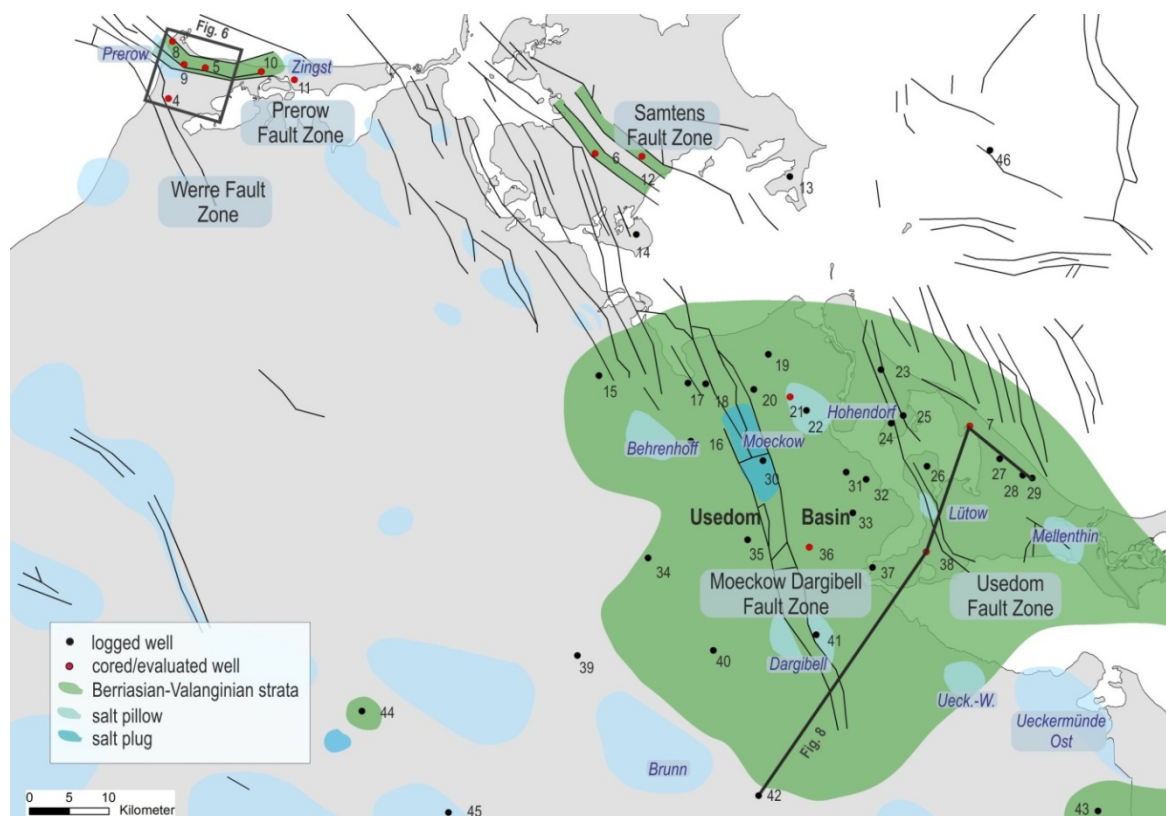


Fig. 5: Detailed map of the working area showing the distribution of Berriasian–Valanginian strata, fault zones of the Western Pomeranian Fault and Graben System, salt structures and investigated wells. Distribution of Berriasian–Valanginian strata according to Diener (1974) and own results.

In the northeastern North German Basin, salt pillows are present in the subsurface of the Darß and Usedom regions but not in the subsurface of Rügen (Fig. 5). The timing of the formation of the Prerow and Zingst salt pillows (Darß Peninsula) is still under discussion. Zöllner et al. (2008), Hübscher et al. (2010), Ahrichs et al. (2020) argue for the initiation in the late Triassic followed by a second phase of salt movement in the latest Cretaceous to Paleogene (Kossow and Krawczyk, 2002). The same refers to the salt pillows Behrenhoff, Dargibell, Hohendorf, Lütow, Mellenthin and Moeckow (Deutschmann, pers. comm.). However, Kossow et al. (2000) reconstructed the initiation of salt pillows in the northeastern part of the North German Basin in the late Jurassic–early Cretaceous interval.

The Lower Cretaceous in NE Germany was studied based on seismic data and well data. Pre-interpreted, unpublished 2D seismic lines from the Darß area (Köhler and König, 1965; Fritzsche and Doß, 1980) were evaluated and combined with well data to reconstruct the Darß Graben. The Lower Cretaceous succession was studied on 18 cored and logged wells of the Darß and Rügen Graben structures and the Usedom Basin (Fig. 5). For comparison, another five cored and logged wells were investigated in neighbouring areas of the North German Basin (Fig. 3). Together, about 1200 m of Lower Cretaceous cores were logged in detail for lithology, bedding structures, palaeosols, sedimentary cyclicities and macro fossils. In addition, the sections were sampled to enable analyses on petrography, granulometry, heavy mineral assemblages, bulk rock geochemistry and palynology.

The petrography of fine- to coarse-grained clastics and limestones was studied on thin sections. Sixty regular-sized thin sections were examined employing standard microscopic methods. Transmitted light microscopy was used for detrital mineralogy of fine- to coarse-grained clastics and qualitative petrographic analysis of limestones. For quantitative detrital mineralogy of sandstones, 300 grains in each thin section were counted, and the step size was adapted to the grain sizes of individual samples. Resulting from point counting analysis, the sandstones were classified according to Mc Bride (1963). Furthermore, petrographical analysis was supported by scanning electron microscopy (SEM) and cathodoluminescence microscopy (CL). For scanning electron microscopy, a SEM-EDX Zeiss-Evo MA 10 equipped with a tungsten filament and an EDAX element (resolution 3 nm at 30 kV) was used at the Geological Institute of the University of Greifswald. For cathodoluminescence microscopy, a high-power HC3-LM- Simon-Neuser CL microscope (Neuser et al., 1995) with a coupled Peltier-cooled Kappa PS 40C-285 camera system equipped with an Olympus BH-2 microscope was used at the Geoscience Centre of the University of Göttingen. The electron gun with an electron beam diameter of ca. 4 mm was operated at a voltage of 14 keV under a high vacuum ( $10^{-4}$  bar) with a filament current of 0.18 mA.

The granulometry and heavy mineral assemblage were analysed on 19 samples of the Anklam 1 well. After mechanical disintegration by gently mortar grinding using a wooden pestle, the samples were inspected under a binocular microscope. The disintegrated samples were drily sieved with standard mesh sieves according to DIN 4022 standard and results were classified following Wentworth (1922). Granulometric values of mean grain size, sorting and skewness were calculated according to Folk & Ward (1957).

The heavy minerals of the 65–300  $\mu\text{m}$  fraction were separated from light minerals using Lithiumpolytungstate (LST) at the density of 2,95  $\text{g}/\text{cm}^3$ . After drying, magnetic heavy minerals were separated by a magnet separator and non-magnetic heavy minerals were mounted on slides with epoxy resin and polished down to a thickness of about 30  $\mu\text{m}$ . The quantitative and qualitative heavy mineral composition was determined by the pointcounting of 200 grains in each thin section. The results were compared to results from other localities published in the literature or provided in unpublished well reports.

For bulk rock geochemistry, 66 samples of the Ückeritz 1 well were taken at regular sample steps. The samples were processed at ALS Laboratories Galway, Ireland. Carbon and sulphur were determined by combustion furnace and acid digestion, major trace elements and base metals by ICP-AES ( $\text{LiBO}_2$  fusion, four acid digestion), and trace elements and REE's by ICP-MS ( $\text{LiBO}_2$  fusion).

Samples for palynology and micropalaeontology were taken from wells Darßer Ort 1 and Ückeritz 1 at sample steps of 5–10 meters. In total, 72 samples were processed and slides

## *Methods*

were prepared following the procedure described by Heunisch in Kustatscher et al. (2012a, 2012b). For palynofacies analysis, the Sporomorph Eco Group method (SEG) established by Abbink (1998) and Abbink et al. (2004a, 2004b) for Lower Cretaceous palynomorph assemblages was applied. If possible, 200 palynomorphs were counted for each slide. The results were assigned to the following Sporomorph Eco Groups: aquatic marine (AM); restricted marine = aquatic, lagoonal, brackish (ALB); aquatic, brackish, fluvial (ABF); pioneer (PI); coastal (CO); lowland, wet (LW); lowland, dry (LD); river (RI) or hinterland (HL) habitats. For calcareous nannofossil analysis, sample preparation established by Hay (1965) was applied to eight samples.



## 4 Lower Cretaceous stratigraphy

In the Polish trough, biostratigraphical control of Berriasian–Albian strata is provided by ammonite zones (e.g. Marek, 1967, 1997; Marek and Raczynska, 1979; Leszczynski, 1997). Likewise, biostratigraphic age control of Valanginian–Albian strata in the western North German Basin is based on ammonites (e.g. Mutterlose and Bornemann, 2000). In contrast to these neighbouring sub-basins, the biostratigraphic control of the Lower Cretaceous succession in the eastern North German Basin relies on zonation schemes based on bivalves, ostracods and palynomorphs (*Fig. 6*).

For the Wealden-type strata of the western North German Basin, ranging from the Middle Berriasian to the Berriasian-Valanginian transition, Wolburg (1949, 1959) established a zonation based on the phylogenetic succession of ostracods. The ostracod zones 1–6 are also valid in the Altmark-Prignitz Basin but not in the Darß and Rügen Grabens and the Usedom Basin. There, Döring (1965a) established a zonation based on sporomorphs (Wealden A-G), which was correlated with the ostracod zonation of Wolburg (1949, 1959) on the example of the Werle standard section (*Fig. 6*). The base Valanginian is marked by the first occurrence of the ammonite *Platylenticeras* (Mutterlose et al., 2014) in the western North German Basin. To the East, brackish-marine environments prevailed and therefore, the biostratigraphic control in the Prignitz-Altmark-Basin relies on ostracod and foraminifera marker species (*Fig. 6*), described by Wolburg (1959), Bartenstein and Brandt (1951) and Bartenstein (1962). Further to the North and East, for example, in the Darß und Usedom area, the presence of Valanginian strata may be indicated by the sporomorph *Trubasporites* sp. (Eiermann, 1965). According to Rusbült and Döring (1962), Eiermann (1965), Sparfeld and Dreyer (1970), and Diener et al. (2004), biostratigraphic control on Hauterivian–Albian strata in the eastern North German Basin is provided by ostracod, foraminifera and dinocyst marker species (*Fig. 6*).

### 4.1 Biostratigraphy

#### 4.1.1 Upper Jurassic

This section is concluded with the northwest German Münden Formation, based on the biozones joOM1 to joOM6. In the Usedom area, the Upper Oxfordian was testified by well Zinnowitz, where samples yield the ostracod species *schuleridea triebeli* (Petzka et al., 1964). The Lower to Middle Kimmeridgian of well Hanshagen 18 provide the ostracod species *Macrodentina wicheri*, *M. lineata* and *Klieana alata*. Upper Jurassic succession of well Heringsdorf 4 (Rusbült, 1964) includes the Upper Oxfordian, the Lower to Middle Kimmeridgian and the Upper Tithonian. The Oxfordian succession is lacking microfossils and provides only macrofossil remains and ooids, whereas the Middle Kimmeridgian is testified

by the ostracod species *Protocythere sigmoidea*, *P. rodewaldensis* and *Orthonotacythere interrupta*. The Upper Tithonian Serpulite of well Heringsdorf 4 could i.a. be testified by the ostracod species *Ilyocypris jurassica spinosa* and *Cypridea carniata*. The occurrence of the spore species *Hughesisporites galeriticus*, known from the fluvial-terrestrial Wealden facies, suggests that these facies was established already during the Tithonian. The Kimmeridgian and Tithonian strata from the Rügen area show faunal similarities to NW-Germany and the Altmark-Prignitz Basin. Furthermore, the Kimmeridgian to Tithonian dated silty claystone successions drilled in the Danish well Øresund 1A (Christensen, 1965; Döring et al., 1970) are correlatable to the Rügen area. In contrast, the strata drilled in well Heringsdorf 4 were correlatable to the Danish-Polish Trough (Döring et al., 1970).

#### 4.1.2 Upper Berriasian (Wealden-type) – Valanginian strata

In the Altmark-Prignitz Basin, the ostracod *Cypridea fasciculata* marks the transition from the brackish-marine Tithonian Münden Formation, to the brackish-marine Berriasian strata of the Bückeberg group, informal called 'Wealden' facies. Dinoflagellate species *Broomea gochti* characterise Wealden zones 1 and 2 (Fig. 6). Marked by short-time marine incursions, typical Wealden zone 2 species are *Macrodentina mediostricta*, *Fabanella polita* and *Cypridea altissima* as an indication of an increased saltwater influence. *Valencythere* (*Protocythere pseudopropria*) *emslandensis* marks the middle part of the Wealden-facies (2–4) (Dreyer and Sparfeld, 1970).

The foraminifera *Citharina sparsicostata* (Bartenstein and Brandt, 1951) marks the direct transition from Wealden-type facies to the Valanginian open marine facies. A former connection to the Tethyan realm (Jurassic of Switzerland) is testified by the marine ostracod species *Protocythere*, *Orthonotacythere*, *Schuleridea*, *Dolocysteridea* and foraminifer species *Lenticulina* and *Citharina* analysed in core material from wells Brome 2, Bismarck Ost 1, Sanne 1 and Nettgau 3 (Sparfeld, 1970; Dreyer 1971). Diener (1967) and Mutterlose and Bornemann (2000) mentioned, that Valanginian strata is defined by fully marine species like ammonites *platylenticeras*, brachiopods and Echinodermata remains. Common Upper Valanginian species are the ostracod *Protocythere praetriplicata*, as well as foraminifer species *Lenticulina* (*Vaginulinopsis*) *humilis*, *Dolocysteridea hilseana*, *Schuleridea thoerensis*. According to Sparfeld and Dreyer (1970), the Valangian species are attributed to shallow, quiet and eurline waters.

#### 4.1.3 Hauterivian - Barremian

According to Diener (1974) and Haupt (1962), Hauterivian strata in Western Pomerania are indicated by the brackish-marine ostracod species e.g. *Protocythere triplicata*,

*Cytherelloidea ex. gr. ovata* and the foraminifer species *Epistomina caracolla* and *Citharina harpa* (Eiermann, 1965; Diener et al., 2004). The dinocyst *Coronifera oceanica*, analysed in well Darßer Ort 1, is attributed to the Upper Hauterivian (Bornemann and Heunisch, 2017). Typical macrofossil species analysed from core material are i.a. bivalvia species like *Isognomon mullet* and *Panopea schroederi*, as well as cephalopods like *Speetonicerias sp.* remains (Tröger, 1966). The ostracod species *Protocythere triplicate* is attributed to the Lower Hauterivian strata in the Altmark-Prignitz Basin, whereas the Upper Hauterivian is characterised by species like *Epistomina ornata* and foraminifera species *Vaginulina flexa* (Sparfeld and Dreyer, 1970).

The belemnite species *Aulacothoeuthis ascendens* marks the transition to Barremian strata (Tröger, 1966) and according to Tröger (1966), the following macrofossil species suggest a Barremian age: *Pecten crassitesta*, *Cyprina protensa* and *Lima sp.* The Barremian in Western Pomerania is lacking microfossil marker species (Diener, 1974). However, foraminifera species like *Citharina harpa* and *Vaginulina weigelti* (Eiermann, 1965; Diener et al., 2004) are quite common. Diener et al. (2004) mentioned that foraminifer species like i.a. *Epistomina chapmani*, *Gavelinella barremiana* (Fig. 6) are common in the Altmark-Prignitz Basin. During Hauterivian and Barremian times, the Usedom sub-basin also represented a part of the Danish Polish Trough (Diener, 1974; Mutterlose and Bornemann, 2000), characterised by mainly sandy shallow marine deposits. According to evaluated well reports, a macrofaunal influence of the Polish Trough during Hauterivian and Barremian times is not yet testified. The faunal spectrum of the Altmark Prignitz Basin includes marine foraminifer species like i.a. *Gavelinella barremiana*, *Citharina acuminata*, *Gaudryinella sherlocki* (Diener et al., 2004).

#### 4.1.4 Aptian – Lower Albian

According to Diener (1974) and evaluated well reports, the few core material from Western Pomerania lacking microfossil marker species witnessing Lower Aptian dated strata. However, the occurrence of the foraminifer species *Globigerina*, *Gavelinella*, *Lenticulina*, fish remains and claystone remains ('Blättertön') are characteristic. A macrofossil species indicating a Lower Aptian age is *Neohibolites ewaldi* (Diener, 1974). Typical Upper Aptian foraminifer species are *Gaudryina dividens*, *Gavelinella barremiana*, *Lenticulina gaultina* and the ostracod *Protocythere tricostata*. Lower Albian strata are marked by the occurrence of the foraminifer species *Spiroplectinata lata*, *Lenticulina spinosa* and the ostracod species *Protocythere nodigera* (Sparfeld and Dreyer, 1970; Diener, 1974). Resulting of the general lack of microfossils and core material, the transition from Upper Aptian to Lower Albian strata is not definable (Diener, 1974).

#### 4.1.5 Middle – Upper Albian

The transgressive onset of the Middle Albian strata is characterised by a rich microfauna (Diener, 1974). Middle Albian strata provide the foraminifer species *Spiroplectinata complanata*, *Sp. annectens*, ostracods *Platycythereis excavate* and *Cythereis glabarella* (Fig. 1 and Fig. 6, Eiermann, 1965; Diener et al., 2004). Well Darßer Ort 1 revealed the marker species *Physocythere steghausi*, associated with the steghausi-events in the upper Upper-Albian (Diener, 1974). Upper Albian marker species are represented by *Eiffellithus turriseiffelii*, *Tranolithus orionatus* and *Gartnerago praeobliquum* (Bornemann and Heunisch, 2017).

Stage	Lithostratigraphy		Lithostratigraphy W NGB		Biostratigraphy		M= macrofossils		Lithostratigraphy E NGB	
	Cent. Low. Saxony	NE Lower Saxony	W NGB (LSB) Biozones (Mutterlose and Bornemann, 2000)	Altmark Prignitz Basin	E NGB Pomerania	Altmark Prignitz Basin	Pomerania	own results and Diener, 1974		
Albian	upper	Peine Fm. Kirchrode Sfm.	<i>Stoliczkaia dispar</i>	<i>Spiroplectinata annectens</i>	<i>Eiffellithus turriseiffelii</i> <sup>3</sup> , <i>Tranolithus orionatus</i> <sup>3</sup> ; <i>Gartnerago praeobliquum</i> <sup>3</sup>	unnamed unit fine-grained glauconitic sandstones,  Marlstones (reddish „Flammgerel“)	unnamed unit			
	mid.		<i>Mortoniceras inflatum</i>	<i>Platycythereis spp.</i> <sup>5</sup>	<i>Gavellina intermedia</i> <sup>2</sup>					
lower	<i>Diploceras cristatum</i>		<i>Physocythere steghausi</i> <sup>5</sup>	<i>Platycythereis gaultina</i> <sup>2,5</sup>						
	<i>Euhoplites lautus</i>		<i>Rehacythereis reticulata</i> <sup>5</sup>	<i>Spiroplectinata annectens</i>						
	<i>Euhoplites loricatus</i>		<i>Spiroplectinata annectens</i>	<i>Rehacythereis glabrella</i>						
	<i>Hoplites dentatus</i>		<i>Rehacythereis glabrella</i>	<i>Isocythereis fortninodis reticulata</i>						
	<i>Douvilleiceras mammillatum</i>		<i>Saxocythere nodigera</i> <sup>5</sup>	<i>Textularia bettenstaedti</i> <sup>5</sup>						
	<i>Leymeriella regularis</i>		<i>Protocythere nodigera</i> <sup>5</sup>							
	<i>Leymeriella tardefurcata</i>									
	<i>Proleymeriella schrammeni</i>									
Aptian	upper	Sarsstedt Sfm.	<i>Hypacanthoplites jacobi</i>	<i>Gaudryina dividens</i> <sup>5</sup>	<i>Gaudryina dividens</i> <sup>2,5</sup>	silty, biogenic glauconitic and fine-grained sandstone layers  organic-rich, silty calcareous claystones,	unnamed unit			
	lower		<i>Acanthoplites nolani</i>	<i>Conorotalites aptiensis</i> <sup>5</sup>	<i>Gavelinella cf. barremiana</i> <sup>5</sup>					
<i>Parahoplites nutfieldensis</i>			<i>Spiroplectinata lata</i> <sup>5</sup>	<i>Hedbergella infracretacea</i> <sup>5</sup>						
<i>Epicheloniceras tschemyschewi</i>			<i>Gavelinella cf. barremiana</i> <sup>5</sup>	<i>Protocythere tricostata</i> <sup>5</sup>						
<i>Tropaeum drewi</i>			<i>Saraceneria spinosa</i> <sup>5</sup>							
<i>Tropaeum bowerbanki</i>			<i>M Oxyteuthis depressus</i> <sup>5</sup>							
<i>Deshayesites deshayesi</i>			<i>Lenticulinen</i> <sup>5</sup>							
<i>Prodeshayesites tenuicostatus</i>			<i>Hedbergellen</i> <sup>5</sup> ,							
<i>Prodeshayesites tenuicostatus</i>			<i>Gavelinellen</i> <sup>5</sup>							
Barremian	upper		Hoheneggelsen Fm. Wesendorf Fm.	<i>Parancyloceras bidentatum</i>	<i>Epistomina chapmani</i> <sup>5</sup>			<i>Citharina harpa</i>	unnamed unit fine-grained sandstones, locally medium- to coarse-grained layers, partly glauconitic and calcite cement,  organic-rich, silty claystones	unnamed unit
	lower	<i>Simancyloceras stolley</i>		<i>Gavelinella barremiana</i> <sup>5</sup>	<i>Coronatalites sigmoicostata</i>					
<i>Ancyloceras innexum</i>		<i>Citharina acuminata</i> <sup>5</sup>		<i>Vaginulina weigelti</i> <sup>5</sup>						
<i>Paracrioceras denckmanni</i>		<i>Conorotalites bartensteini</i> <sup>5</sup>								
<i>Paracrioceras elegans</i>		<i>Gaudryinella sherlocki</i> <sup>5</sup>								
<i>Hoplocrioceras fissicostatum</i>		<i>Ammobaculites reophacoides</i> <sup>5</sup>								
<i>Hoplocrioceras rarocinctum</i>				<i>M Aulacothoeuthis assendens</i> <sup>5</sup>						
<i>Simbirskites (Cr.) discofalcatus</i>		<i>Vaginulina flexa</i>		<i>Epistomina caracolla</i> <sup>1,5</sup>						
<i>Simbirskites (Cr.) gottschei</i>		<i>Marsonella kummi</i> <sup>5</sup>		<i>Lagena haut. hauteriviana</i> <sup>1</sup>						
<i>Simbirskites (M.) staffi</i>	<i>Haplophragmium aequale</i> <sup>5</sup>	<i>Citharina harpa</i>								
Hauterivian	upper	Stadthagen Fm.	<i>Epistomina ornata</i>	<i>Epistomina ornata</i> <sup>5</sup>	<i>Cytherelloidea ex gr. ovata</i> <sup>1,5</sup>	unnamed unit fine- to medium-grained calcareous greensandstones and siltstones,  calcareous, biogenic claystones, marlstones	unnamed unit			
	lower		<i>Aegioceras spp.</i>	<i>Protocythere triplicata</i>	<i>Protocythere triplicata</i>					
<i>Endemoceras regale</i>			<i>Rehacythereis senckenbergi</i>	<i>Rehacythereis senckenbergi</i> <sup>5</sup>						
<i>Endemoceras noricum</i>										
<i>Endemoceras ambygonium</i>										
<i>Eleniceras paucinodum</i>										
<i>Dicostella tuberculata</i>			<i>Protocythere frankei</i>	3						
<i>Prodicotomites ivanovi</i>			<i>Lenticulina (Vaginulinopsis) humilis</i>	+4						
<i>Dichotomites bidichotomoides</i>			<i>Dolocythereida hilseana</i>	2b						
<i>Dichotomites triptychoides</i>			+c							
<i>Dichotomites crassus</i>	<i>Schuleridea thoerenensis</i>	2								
<i>Prodicotomites polytomus</i>	<i>Protocythere praetriplicata</i>	1								
<i>Prodicotomites hollwedensis</i>	<i>Protomarsionella kummi</i>	2								
<i>Polyptychites sphaeroidalis</i>	<i>Dentalina sp., Frondicularia sp.</i>									
<i>Polyptychites clarkii</i>										
<i>Polyptychites multicoastatus</i>										
<i>Polyptychites pavlowi</i>										
<i>Platylenticeras involutum</i>										
<i>Platylenticeras heteropleurum</i>										
<i>Platylenticeras robustum</i>	<i>M ammonite remains (Platylenticeras?)</i>									
<i>Platylenticeras robustum</i>										
<i>Platylenticeras robustum</i>										
Valanginian	upper	Nienhagen Fm.	<i>Protocythere frankei</i>			unnamed unit fine-grained calcareous, bioclastic sandstones, marl-, lime- and claystones	unnamed unit			
	lower		<i>Lenticulina (Vaginulinopsis) humilis</i>							
<i>Dolocythereida hilseana</i>										
<i>Schuleridea thoerenensis</i>										
<i>Protocythere praetriplicata</i>										
<i>Protomarsionella kummi</i>										
<i>Dentalina sp., Frondicularia sp.</i>										
<i>M ammonite remains (Platylenticeras?)</i>										
<i>M ammonite remains (Platylenticeras?)</i>										
<i>M ammonite remains (Platylenticeras?)</i>										
<i>M ammonite remains (Platylenticeras?)</i>										
Berriasian	upper	Fuhse-Fm. Wealden-type (Cy. recta) Isterberg Fm. (Deister Fm.) Wealden-type Bückeberg Group	<i>Pachycytheridea trapezoides</i>	<i>Sternbergella benthemensis</i>	<i>Gradisporites gradibus</i> <sup>2,4,5</sup>	marine influenced fine-grained sandstones, coarse-grained layers, calcite and chalcidone cements, carbonaceous claystones	unnamed unit Wealden-type Low. Valanginian was not yet biostrat. testified	unnamed unit Wealden-type Low. Valanginian was not biostrat. testified but presumed in the Usedom basin		
	lower		<i>Pachycytheridea rotundata</i>	<i>Cypridea valdensis</i>	<i>Gleicheniidites triplex</i> <sup>2,3,5</sup>					
<i>Cypridea parallela</i>			<i>Valencythere emslandensis; Macrodentina mediostricta transfuga</i>	<i>Parvisaccites radiates</i> <sup>2,5</sup>						
<i>Cypridea setina angulata</i>			<i>Cypridea altissima</i>	<i>Deltoidospora spp.</i> <sup>2,4,5</sup>						
<i>Cypridea rectidorsata</i>			<i>Fabanelia polita</i>	<i>Classopollis spp.</i> <sup>2,4,5</sup>						
<i>Cypridea bispinosa</i>			<i>Cypridea fasciculata</i>	<i>Cerebropollenites spp.</i> <sup>2,4,5</sup>						
<i>Cypridea altissima</i>				<i>Perinopollenites elatoides</i> <sup>2,3,4,5</sup>						
<i>Cypridea fasciculata</i>				<i>Citricosisporites spp.</i> <sup>2,4,5</sup>						
				<i>Trilobosporites spp.</i> <sup>2,5</sup>						
			<i>Densoisporites spp.</i> <sup>2,5</sup>							

Fig. 6: Bio- and Lithostratigraphy of the Lower Cretaceous in the North German Basin from the western Lower Saxony Basin to the Prignitz Altmark area and northeast Germany.

### 4.2 Palynostratigraphy

Döring (1965a) established a sporomorph zonation A-G (Fig. 6) calibrated on the Werle standard section of southwest-Mecklenburg-Vorpommern, correlatable to the Berriasian Wealden-type strata of the Darß, Rügen and Usedom area of NE-Germany. Despite the

differences regarding range and distribution of the single spore and pollen species, the western Western Pomeranian zonation after Döring is well correlatable to the Hils area (Dörhöfer, 1977) and to the Polish lowlands (Mamczar, 1968; Dörhöfer, 1977).

According to Döring (1966a), bisaccate pollen marker taxa from Wealden zones B-G could be identified from samples of well Darßer Ort 1 and partly correlated to the Werle standard section. In this study, a second biostratigraphic evaluation of samples from well Darßer Ort 1 validated (Heunisch, 2019) marker taxa from Wealden zones B-F (Appendix A). According to Eiermann et al. (1969/70, 1970) marker taxa from Wealden zones A-G could be validated in biostratigraphic samples from wells Rügen 105 and Garz 1/1a. In the Usedom area, the main taxa from Wealden F and taxa that suggest a Valanginian age could be validated in the wells Usedom 1 (Döring, 1963) and Ückeritz 1 (Heunisch and Bornemann, 2017). Döring (1963) argues that the individuals found in core material of well Usedom 1 are well correlatable to taxa found in Valanginian strata south of Berlin in well Schünow 1 and Dabendorf 1 as well as in the Polish region of Tomaszów.

### 4.3 Sequence stratigraphy

The progradation of terrestrial-dominated environments in the North German Basin and neighbouring basins was a consequence of the major global sea-level drop (*Fig. 9*) in the Tithonian and the global lowstand during Berriasian times (Haq et al., 1987; Haq, 2014; Ziegler, 1977; e.g. Lott et al., 2010; Vejbæk et al., 2010). According to Haq (2014), the long-term sea-level curve throughout the Cretaceous propose a 75-250 m higher sea-level than the present-day sea-level (Haq, 2014). The sea-level (*Fig. 9*) reached a trough in mid-Valanginian (~ 75 m above present-day sea-level) and a high point in early Barremian with ~160 – 170 m above present-day sea-level (Haq, 2014). The curve also displays a high and stable sea-level from Aptian through early Albian. A global estimation of third-order events was done by averaging the eurybatic data from widely distributed time-synchronous events. Most of these short-term events have been documented in several basins and vary from ~ 20 m to a maximum of over 100 m with a duration between 0.5 and 3 Myr (Haq, 2014).

Despite basin extension and a relative rise in long-term sea-level, the overlying Valanginian to Aptian successions is only preserved fragmentarily in the northeastern and eastern North German Basin. Generally, the most complete stratigraphical sections were found within Berriasian strata, not least because of the relatively thicker deposits, enabling a basin-wide well correlation. Thicker Hauterivian and Barremian successions locally allowed the preservation of microfossils but rarely marker species. Aptian to Lower Albian strata is strongly reduced in thickness or completely missing. Following the mid-Albian transgression, Cretaceous strata are geographically widespread in the North German Basin. Additionally, salt movement strongly influenced the Lower Cretaceous thickness (*chapter 5.3*).

### 4.3.1 Berriasian

According to Haq et al., (1988) and Hardenbol et al., (1998), the 3<sup>rd</sup>-order Berriasian event KBe3 has been identified in western European basins and on the Russian platform (Sahagian et al., 1996) and by oxygen isotopic data (Haq, 2014). The event KBe4 was also documented in the e.g. western European basins, on the Russian platform and the Arabian Platform (Haq and Al-Qahtani, 2005). Events KBe2 through KBe4 are also associated with 4<sup>th</sup>-order (400 Kyr) cyclicity in the European basins (Hardenbol et al, 1998).

Drawing a link from the adjacent western Lower Saxony Block to the Northeast German Basin, five wells were correlated, as shown in *Fig. 7*. They represent distal brackish-marine basin parts of the neighbouring Lower Saxony Block, as drilled in well Isterberg 1001, shallow marine and dominantly fluvial-deltaic influenced areas drilled in the wells Eulenflucht 1. Representing the Altmark-Prignitz Basin, the wells Werle 13 and Rhinow 2/5 are to be considered. As the westernmost extension of the Polish Trough, well Usedom 1 provides evidence of Tethyan freshwater influence, testified by dinocysts and marine foraminifera (this study, see *chapter 4.1.2*).

The middle Berriasian (Wealden 2) regressive trend on the western Saxony Block is introduced by limestone layers and in the eastern shallow basin areas and the Altmark-Prignitz Basin by sandy, horizontal laminated calcareous sandstones, pedogenic mudstones and paleosols, providing ferric and calcareous concretions. Recognisable by sharp-based and decreased gamma ray values, the maximum regressive surface Mrs 1 is marked by progradating horizontal laminated to low-angle cross-bedded sandy lithologies.

Following, a transgressive trend is recognisable by dark claystone lithologies, displayed by increased gamma ray values, and the increasing dinocyst abundance, accompanied by ostracods and bivalve occurrences (Strauss et al., 1993; Schneider, 2017). The maximum flooding surface MfsBe3 on the transition from Wealden 2/3 is marked by dominant mudstones, a maximum in dinocyst occurrence, ostracods and bivalves and, in the Altmark-Prignitz Basin, by the occurrence of calcareous sandstones. Becoming less pronounced towards the northeastern basin part, this event could be correlated to the transgressive event TE1, referring to Strauss et al., (1993) and Schneider (2017).

The following regressive trend during Wealden 3 is introduced by dominantly sandy lithologies and deltaic fining upward sequences in the eastern Lower Saxony Basin, the Altmark Prignitz and Usedom Basin. Supported by the absence of dinoflagellate cysts, the transition towards deltaic settings is also suggested by phytoplankton assemblages composed of *Botryococcus* (Schneider et al, 2017) in well Eulenflucht 1. In the neighbouring Altmark-Prignitz Basin, sandy and horizontal laminated calcareous sandstones, pedogenic mudstones and paleosols provide ferric and calcareous concretions and plant remains, as

shown in well logs from Werle and Rhinow. The maximum regressive surface (Mrs 2) is marked by strongly decreased gamma ray values and prograding horizontal laminated to low-angle cross-bedded sandy lithologies with root trace fossils, followed by clayey paleosols or pedogenic horizons.

Persisting through Wealden 3 and 4, regressive conditions slightly turned into transgressive conditions during Wealden 5 and 6. This transgressive trend established dominantly clayey and marly lithologies, recognised by sharp-based and strongly increased gamma values. These lithologies provide evidence for marine incursions into the deltaic-dominated basin parts. The marine microplankton sampled from these clayey horizons yield ostracod species of Wealden 4 and are therefore considered to be associated with the Maximum flooding surface mfsBe4.



Lower Cretaceous stratigraphy

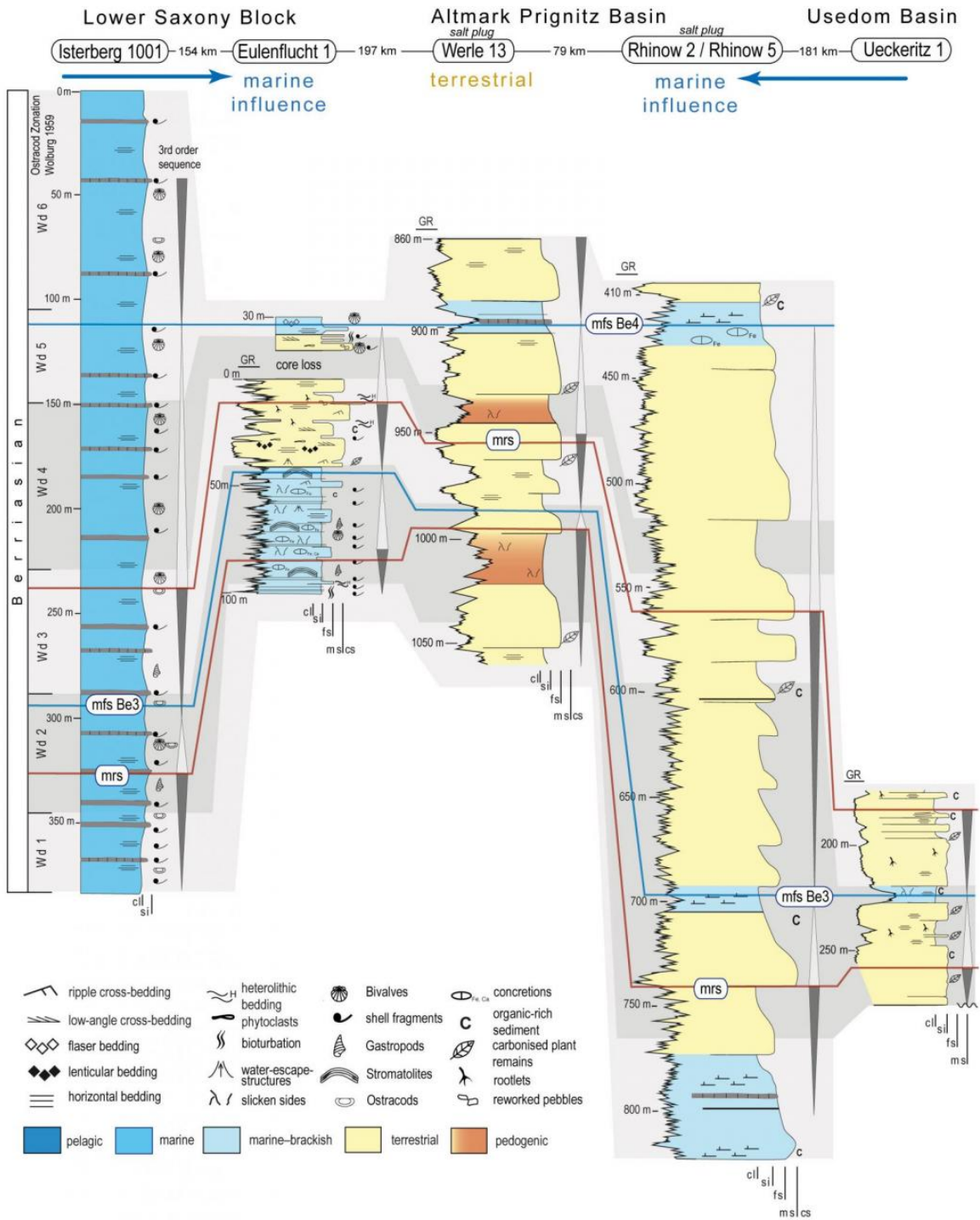


Fig. 7: Well correlation from the Lower Saxony Block to the Prignitz Altmark and the Usedom Basin across the North-German Basin show the facies correlation of two transgressive (mfsBe3, mfsBe4) and two regressive (mrs1 and 2) surfaces.

#### **4.4 Lithostratigraphy**

The Berriasian to Albian strata of NE Germany awaits formal lithostratigraphic classification. Because traditionally used informal stratigraphic terms (“Wealden”) or terms concerning chronostratigraphic stages (“Hauterive”) are not applicable, the Lower Cretaceous strata are referred to as “unnamed units” of the Bückeberg and Minden-Braunschweig Groups in the lithostratigraphic scheme of the German Stratigraphic Commission (STD 2016, Hiss et al. 2018). The upper Berriasian Wealden-type strata of NE Germany are correlative equivalents of the Wealden-type Fuhse and Deister Formations of the Bückeberg Group of NW Germany (*Fig. 6*). The Valanginian–Albian strata of NE Germany correlate with the Nienhagen to Peine Formations of the Minden-Braunschweig Group in NW Germany. For more detailed information about Lower Cretaceous lithostratigraphy, the reader is referred to Ehrbacher et al. (2014) and Hiss et al. (2018). Detailed litho-logs from evaluated wells are provided in Appendix B.

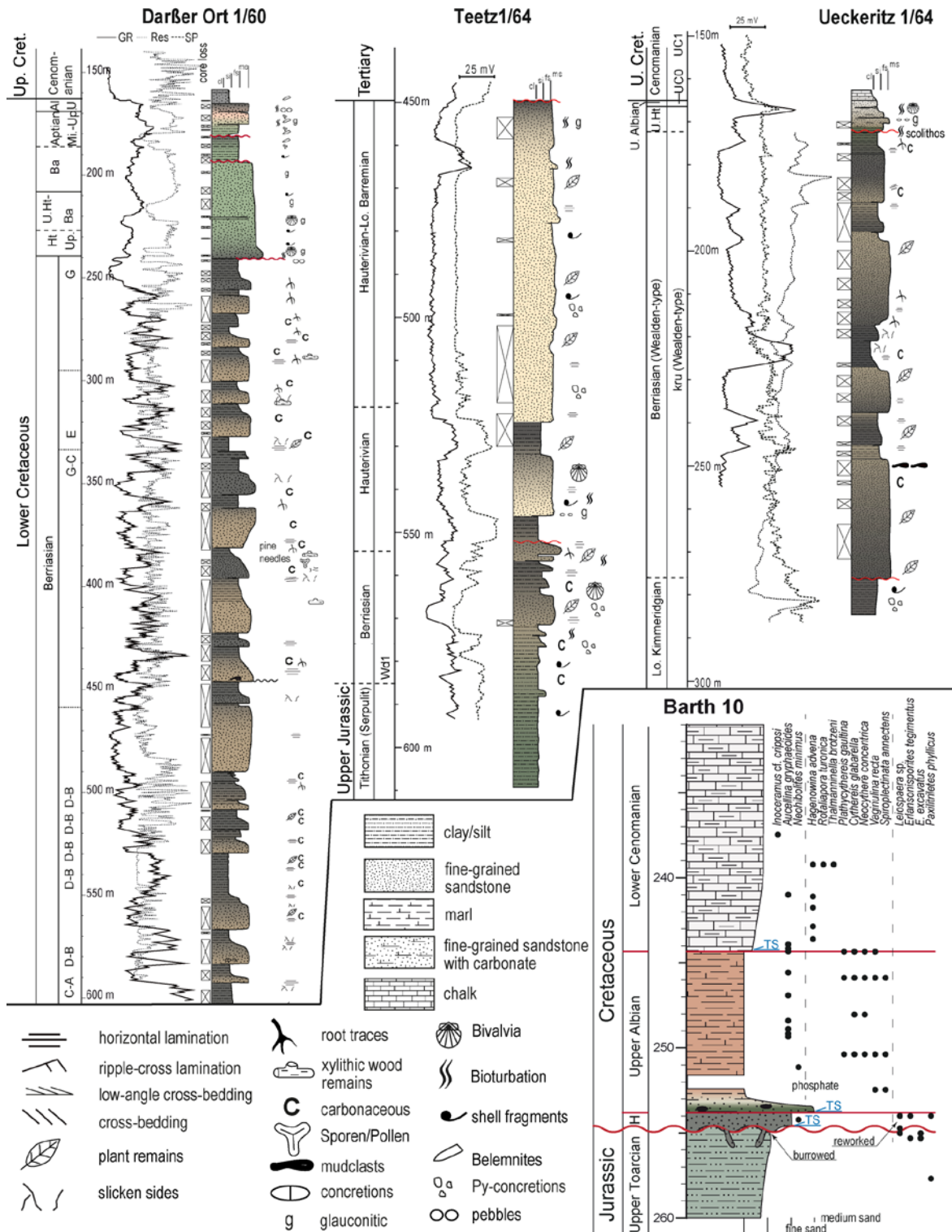


Fig. 8: Different lithostratigraphic profiles from the eastern North German Basin. Well Darßer Ort and Barth 10 from the Darß graben area and well Usedom 1, located in the Usedom Basin and the well Tetz 1, located in the Altmark-Prignitz Basin.

#### 4.4.1 Comparison of the Darß-Rügen-Usedom area and the Altmark-Prignitz Basin

According to the lithostratigraphic unit description of the Bückeberg and Minden-Braunschweig group (Kemper, 1973, Erbacher et al., 2014) of the Lower Cretaceous successions in the western basin part, this work focuses on the northeastern part of the Lower Cretaceous depositional area, the Altmark-Prignitz Basin of Brandenburg and southwest Western Pomerania. A detailed description of the NE-german lithostratigraphic units of Western Pomerania and the Altmark-Prignitz Basin is given in *chapters 4 - 6.4*. A stratigraphic classification into the Darß-Werle Formation and Altmark-Prignitz-East Brandenburg Formation is proposed. A comparison of these two depositional areas is shown in *Table 1*. Considering litho- and biostratigraphic data resulted in the declaration of the two formations, according to the Bückeberg Group descriptions after Erbacher et al. (2014), known from neighbouring basin parts such as the Lower Saxony Basin.

*Table 1: Lithostratigraphic comparison of the northeastern Western Pomeranian and the Altmark Prignitz sub-basins.*

Stage	Western Pomerania-Darß-Werle Fm.	Altmark Prignitz-East-Brandenburg Fm.
<b>Berriasian</b>	Brackish-marine, fluvio-deltaic fine-grained sandstones from upper delta plain, less compacted, horizontal to low-angle bedded, siltstones and claystones, xylithic plant remains, heterolithic bedding, calcisols and histosols; slicken sides, carbonaceous and ferritic concretions, fining-upward cycles. 40 m thick sandstone units, crevasse-splays and deltaic channel sediments, Lower and upper delta plain	Brackish-marine fluvio-deltaic fine-grained sandstones from upper and lower delta-plain, horizontal to low-angle bedded, medium to coarse-grained layers, siltstones and claystones, xylithic plant remains, slicken sides, intercalated by marlstone or calcareous sand-, silt- and claystone units with up to 10 m thickness, quartzose and calcitic cemented sandstone layers, chalcedony cements → marine ingressions, shell fragments layers, weakly bioturbated porifera spicules, near shore and shoreface sediments
<b>Valanginian</b>	Not yet biostratigraphical testified no core material and well reports are available	fine-to partly coarse-grained calcareous or dolomitic sandstones and siltstones, bioturbated, pyrite, carboniferous layers and lenticules, fine-gravel layers, glauconite-rich lime- and marlstones, shell fragments, interlayered by claystone and marly fine-grained sandstones, mica and glauconite-bearing, and iron ooides.
<b>Hauterivian</b>	fine-grained clayey, bioturbated greensandstones and siltstones, homogenous, mottled, partly glauconitic and calcareous, shell fragments and pyrite nodules, Xylithic plant remains, glauconite grains in a glauconitic and clayey matrix, less	Lower Hauterivian: basal calcareous sandstone, superimposed by a glauconitic and sandy claystone, silty marlstones Upper Hauterivian: clayey marlstones, interlayered by glauconite-rich fine-grained sandstone and silty layers, which yield pyrite,

	consolidated, calcite, dolomite, siderite cementation	partly calcareous cement, ooids
<b>Barremian</b>	organic-rich fine-grained, calcareous, glauconitic sandstones, less consolidated, biotite and muscovite, calcite and dolomite/ankerite cement, pyrite nodules, shell fragments of bivalves	silty and sandy claystone and marlstones, mica, partly calcareous cemented layers, fine-grained sandstones, thin clayey layers
<b>Aptian</b>	Basal chalky, fine-grained glauconitic and clayey, calcareous sandstones, glauconite, biogenic components like foraminifers and shale fragments, sparitic calcite and siderite-ankerite cement, layers of glauconitic matrix, pyrite; calcareous silt- and claystones Upper Aptian: sandy, calcareous and glauconitic siltstones	Lower Aptian: claystones, partly silty and calcareous layers, marlstones (Hoth, 1993). Upper Aptian: silty, marlstones, partly glauconite-bearing, pyrite.
<b>Albian</b>	Middle Albian: glauconite-rich fine-grained sandstones, glauconite, pyrite and magnetite, ankerite-dolomite and siderite pore-filling and rhombic cements Upper Albian: marlstones, 'Flammenmergel,' glauconite; basal transgressive marlstone shows layers of fine-grained and glauconite	Lower Albian: basal fine-grained sandstones, layers of fine-gravel pebbles and iron oxide nodules; clayey, fossil-rich marlstones, calcareous claystone, pyrite Middle to Upper Albian: marlstones, claystone

## 4.5 Discussion

### 4.5.1 Influence of sea-level changes on sediment deposition

The interplay of sediment deposition, fluctuating sea-levels and tectonic activity caused a complex geological situation, dominated by regional varying subsidence or uplift and multiphase erosion and deposition (*Fig. 10 and Fig. 11*) and reduced sediment thickness in the northeastern North German Basin (*Fig. 9*). The fluvio-deltaic and later shallow and brackish-marine conditions forced the deposition of widespread sandy lithologies and hampered the preservation of microfossils. Despite the Berriasian and early Valanginian regressive eustatic conditions (Haq, 2014), several hundred meters of sediment were preserved from erosion, for example, in the Darß and Rügen grabens. Brackish-marine conditions prevailed and are testified by ostracods (*Fig. 6*). However, well correlation from the Lower Saxony Basin via the Altmark-Prignitz Basin to the Usedom area shows a link between the neighbouring sub-basins using bio- and sequence stratigraphy. During the lower Valanginian, the Lower Cretaceous long-term sea-level lowstand (Haq, 2014) was reached, which impacted the poor distribution of Valanginian strata, for example, in the northeastern Darß Rügen Usedom area. During Upper Valanginian, open marine conditions are testified

by marine foraminifera in the Altmark-Prignitz Basin. A slightly transgressive trend led to the Upper Hauterivian transgression and highstand (Haq, 2014), typified by the deposition of reworked pebbles on the Hauterivian base during the transgressive systems tract. Whereas fully marine conditions prevailed in the adjacent Lower Saxony Basin, brackish-marine conditions prevailed in the eastern North German Basin, which is testified by ostracods. Despite transgressive conditions, Hauterivian strata are widely missing or could not be testified due to sandy lithologies (Fig. 9). The slightly Barremian sea level drop is displayed by the patchy present-day distribution of the deposits in NE-Germany and a smaller basin extent contrasting to Hauterivian times (Diener, 1974). Despite a relative sea level rise from Barremian to the Lower Albian (Haq, 2014), the Darß Rügen Usedom area and the south-(eastern) Altmark-Prignitz Basin are characterised by swell regions and consequently missing strata.

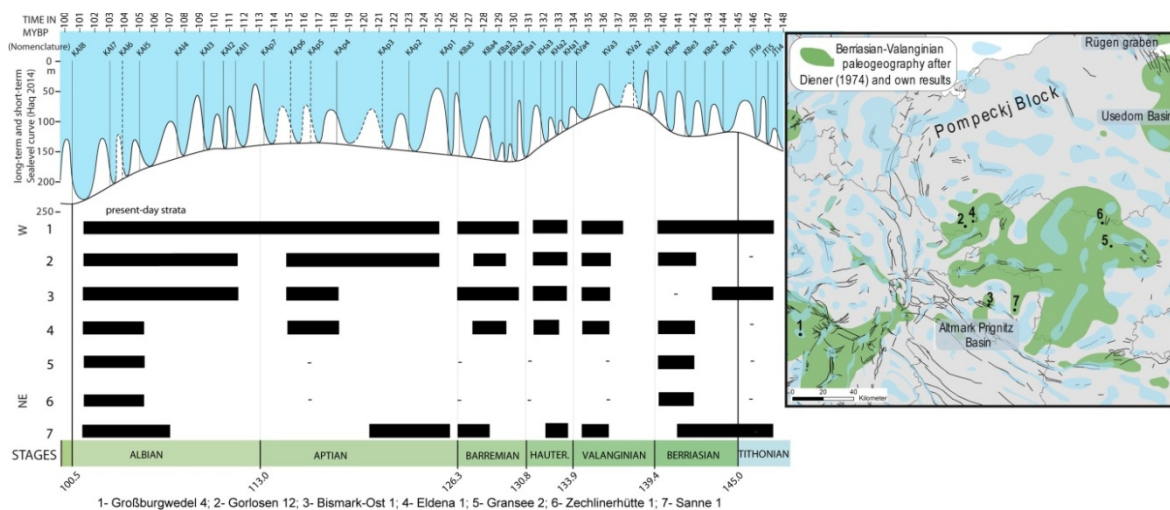


Fig. 9: Stratigraphy vs sea level (Haq et al., 2014) show erosional gaps from stratigraphic records of the numbered wells (map on the right side) and 3<sup>rd</sup>/4<sup>th</sup> order cycles. Stratigraphic data taken from unpublished core reports.

#### 4.5.1.1 Polish Trough

The Lower Cretaceous successions of the NW-SE striking Mid-Polish Trough reach a thickness of 650 m (Marek, 1988, 1997). According to Raczynska (1979) and Marek and Raczynska (1979), lithostratigraphic units were established for the correlation of the marginal basin parts, where fossils are lacking and only well logs and well cores are available, whereas the biostratigraphic subdivision of the Lower Cretaceous is based on ammonites (e.g. Marek, 1967, 1997; Marek and Raczynska, 1979) largely from Western Pomerania and Kujawy. In the earliest Berriasian, ostracods play an important role, while the Barremian, Aptian and Lower Albian deposits do not yield any stratigraphically important fossils. Their chronostratigraphic affiliation is based on correlations with transgressive-regressive events observed in the adjacent German, Danish and Russian epicontinental basins (Raczynska,

1979). The middle to late Berriasian in the adjacent Polish Trough is characterised by transgressive shallow marine shelf deposits of the Zarkrewo-Member, shifting upwards into deeper marine shelf shale deposits of the Opoczki Member (Leszczynski, 1997). The overlying late Early Valanginian (Opoczki Member) is like in the northeastern North German Basin, considered to be a regressive phase expressed by a progradation of shallow marine shelf deposits, prograding deltas or fresh-water environments like swampy-lacustrine and fluvial deposits. Döring (1963) argued that the spore and pollen individuals found in core material of well Usedom 1 are well correlatable to taxa found in Valanginian strata south of Berlin in well Schünow 1 and Dabendorf 1 as well as in the central Polish region of Tomaszow. These results support the suggestion that the Usedom area and the eastern Altmark-Prignitz Basin were directly linked to the Polish Trough. This is also supported by Diener (1974), who argued that the shallow-marine strata in the Usedom Basin could also be of a Valanginian age, deposited in a former extensional bay of the Polish Trough. So far, this could not be testified by microfossils. Leszczynski (1997, 1998) also suggested the Usedom sub-basin as the northwestern extension of the Polish Trough and identified a roughly 100 m thick Early Valanginian succession in NW-Poland near the present-day German border. The Late Valanginian Transgression forced a basin extension by the deposition of silty and clayey sediments. In contrast, the overlying upper part is characterised by shallowing and the deposition of mainly shelf sandstones in the marginal areas (Leszczynski, 1997). The central basin parts shifted to a carbonate shelf system. The Upper Valanginian siliciclastic shelf deposits contain, amongst others, marine ammonites, which were found in the northwestern area of the Polish Trough near the Usedom Basin (Leszczynski, 1998). Sparfeld (1970) described core material from well Sanne 1 in the Altmark-Prignitz Basin as Upper Valanginian deposits. The Early Hauterivian transgression in the marginal parts of the Polish Trough is characterised by erosional surfaces and breaks in sedimentation as known from the wells of this study (e.g. wells Darßer Ort 1, Teetz 1, Ueckeritz 1, see *chapter 4.4, Fig. 8*). The overlying cycle from Early Hauterivian to early Late Hauterivian begins with silty-clayey deposits which rapidly change up into dark-coloured claystones followed by a regressive coarsening upward sequence reflecting a shallow shelf siliciclastic shelf progradation. This sequence could be drilled in well Ueckeritz 1, which is, so far, according to Dreyer (1969), classified as Berriasian (Wealden-type) based on lithostratigraphic features. Leszczynski (1998) mentioned the distribution of Hauterivian deposits in the northwestern Polish Trough through the adjacent Usedom Basin. The marginal parts are characterised by deltaic and even fluvial sedimentation, lacking lithological records due to erosion. The Upper Hauterivian represents a maximum transgressive stage and the sandy-muddy deposits mark a considerable deepening of the sea, whereas the upper part (Barremian, Zychlin Member) is composed of sandy sequences, in central basin parts characterised by shallow shelf deposits

or prograding delta deposits. This corresponds to the maximum regressive stage (*Fig. 9*) (Haq, 2014) and the sequence yields no faunal fossils (Leszczynski, 1997). These sandy sequences were drilled in the Altmark-Prignitz Basin (e.g. well Teetz 1) and the Darß area (well Darßer Ort 1). Aptian deposits (Goplo Member) are characterised by dark grey to black shales and siltstones from a deep shelf, as they were drilled in the Altmark-Prignitz Basin e.g. by wells Gorlosen 12, Eldena 1. Despite a prevailing relatively high sea-level from Aptian to Lower Albian times, these deposits are missing or strongly reduced in the Darß Rügen and Usedom area. The overlying strata are grading up into alternating clay- to siltstone and sandstone shallow shelf deposits in the Lower to Middle Albian, a characteristic 3-5 m thick sandy and glauconitic horizon in the northeastern North German Basin. This reflects the progressively expanding middle Albian basin resulting in the overall late Albian to Cenomanian carbonate shelf deposits.

#### 4.5.2 Bio- and sequence-stratigraphic correlations

The Berriasian spore taxa *Gleicheniidites triplex* found in well Darßer Ort 1 and Ückeritz 1 is correlating to the sporomorph zone 'Hils 4b' (Dörhöfer, 1977c) from the Lower Saxony Basin and according to Lindström and Erlström (2011) to the Berriasian/Valanginian boundary. Bornemann and Heunisch (2017) mentioned that the wide range of this spore taxa conclude in a minor stratigraphic relevance. Based on the ostracod zonation established by Wolburg (1949, 1959), several brackish-marine ostracod taxa from the Lower Saxony Basin could be correlated to the eastern Altmark-Prignitz Basin e.g. well Sanne 1. Strauss et al. (1993) and Schneider (2017, 2018) considered two maximum regressive surfaces (mrs 1 and 2) and two maximum transgressive surfaces transgressive events TE1 and TE2 could be figured out within the Middle to Upper Berriasian strata, which are correlatable to the Boreal of southern England and southern Sweden. Terrestrial spores and pollen, as well as brackish-marine palynomarkers can be used for intra- and interbasinal correlation (Schneider, 2017). In correlation to the adjacent Lower Saxony Basin and the biostratigraphic record, these transgressive events were considered mfsBe3 and mfsBe4 (*Fig. 9*), according to Haq (2014). The Upper Valanginian siliciclastic shelf deposits contain, amongst others, marine ammonites like *Dichotomites* and *Saynoceras* beds, which were found in the northwestern area of the Polish Trough, near the Usedom Basin (Leszczynski, 1998). Sparfeld (1970) described undefined ammonite remains found in core material from well Sanne 1 in the Altmark-Prignitz Basin. Moreover, the Upper Valanginian age was testified by microfossils there (*Fig. 6*). Early to middle Hauterivian clayey to silty deposits of the marginal Polish Trough could also be drilled in well Ueckeritz 1 in the core section from 175 m to 225 m, where the Upper Hauterivian (Prössl, 1990) dinocyst taxa *Coronifera oceanica* was testified in a depth of 224.5 m (this study, Bornemann and Heunisch, 2017). So far, this



*Lower Cretaceous stratigraphy*

sequence is, according to Dreyer (1969), classified as Berriasian (Wealden-type) based on lithostratigraphic features and without biostratigraphic evidence.

## 5 Structural controls on Lower Cretaceous strata

The base-Cretaceous Unconformity (Kossow et al., 2000; Beutler et al., 2012), the disconformable contact of Lower Cretaceous strata to truncated Jurassic–Triassic strata, is the dominating feature in the Mesozoic succession of the Pompeckj Block (*Fig. 10*) and the Altmark-Prignitz Basin (*Fig. 11*). A typical example from the eastern Pompeckj Block is the disconformable contact of greyish to reddish Upper Albian marls and shales to greyish Upper Pliensbachian silts and shales as drilled in the Schwerin 6 well (*Fig. 10*) or the disconformable contact of Hauterivian sandstones to Upper Toarcian silty shales (*Fig. 8*) as drilled in well Barth 10. More complete successions, including Upper Jurassic–Lower Cretaceous strata, are associated with graben structures of the West Western Pomeranian Fault and Graben System, the Usedom Basin (*Fig. 4 and Fig. 5*), as well as the rim synclines of salt structures in the Altmark-Prignitz Basin. The analysis of these successions and their comparison to the disconformable successions at the eastern Pompeckj Block enables the timing of uplift phases and estimation of erosion rates. As shown in *Fig. 10 and Fig. 11*, the evaluation of well data revealed that the recorded unconformities occur single or amalgamated.

### 5.1 Unconformities in the Upper Jurassic – Lower Cretaceous successions

#### 5.1.1 Base-Berriasian Unconformity

This unconformity is characterised by Berriasian strata in disconformable contact with Upper, Middle, or Lower Jurassic strata. Especially in the Darß graben, Berriasian strata disconformably overlie the Rhaetian (Döring, 1966a) or Lower Jurassic strata. In the Rügen graben and the Usedom basin, several gaps within the Upper and Middle Jurassic strata indicate erosion of the Aalenian to Bajocian and Oxfordian to Kimmeridgian-dated succession. In the successions of well JOmb 3, the Middle and Upper Jurassic to Berriasian is missing. The analysis of well data from the Altmark-Prignitz Basin revealed missing Upper to Middle Jurassic from the Aalenian to Lower Berriasian strata in well Gorlosen 12 as well as missing Upper Jurassic Kimmeridgian to Tithonian-dated strata in well Zechlinerhütte 1.

#### 5.1.2 Base-Hauterivian Unconformity

This unconformity is characterised by the disconformable contact of Hauterivian and rarely Valanginian strata to the Berriasian. Except in the western and southernmost Altmark-Prignitz Basin, where mostly the Upper Valanginian was preserved, nearly the whole working area lacks Valanginian-dated strata. There, Hauterivian strata lie disconformably on Lower to Middle Berriasian strata. On the easternmost Pompeckj Block, the amalgamation of the base-Berriasian and base-Hauterivian unconformity occurs widely distributed and formed a large stratigraphic gap from Lower Hauterivian down to the Toarcian (*Fig. 11*) as drilled in

well Barth 10. In contrast, in the Rügen Graben, Hauterivian is generally missing and in the Usedom Basin, where only Upper Hauterivian deposits could be dated. In the Altmark-Prignitz Basin, the amalgamation of both unconformities occurs widely distributed

### 5.1.3 Base-Albian Unconformity

A further significant gap within Lower Cretaceous successions is given by the base-Albian Unconformity, characterised by the disconformable contact of Upper and Lower Albian strata to Hauterivian strata. Locally, parts of Barremian to Aptian strata were preserved, as shown by the wells Darßer Ort 1 and Sanne 1. This unconformity is distributed all over the eastern Pompeckj Block and the Altmark-Prignitz Basin, except in the western part, where complete successions were drilled in well Gorlosen 12. The amalgamation of all three unconformities was recorded in nearly all basin parts and could be differentiated by the fragmentarily preserved strata in between.

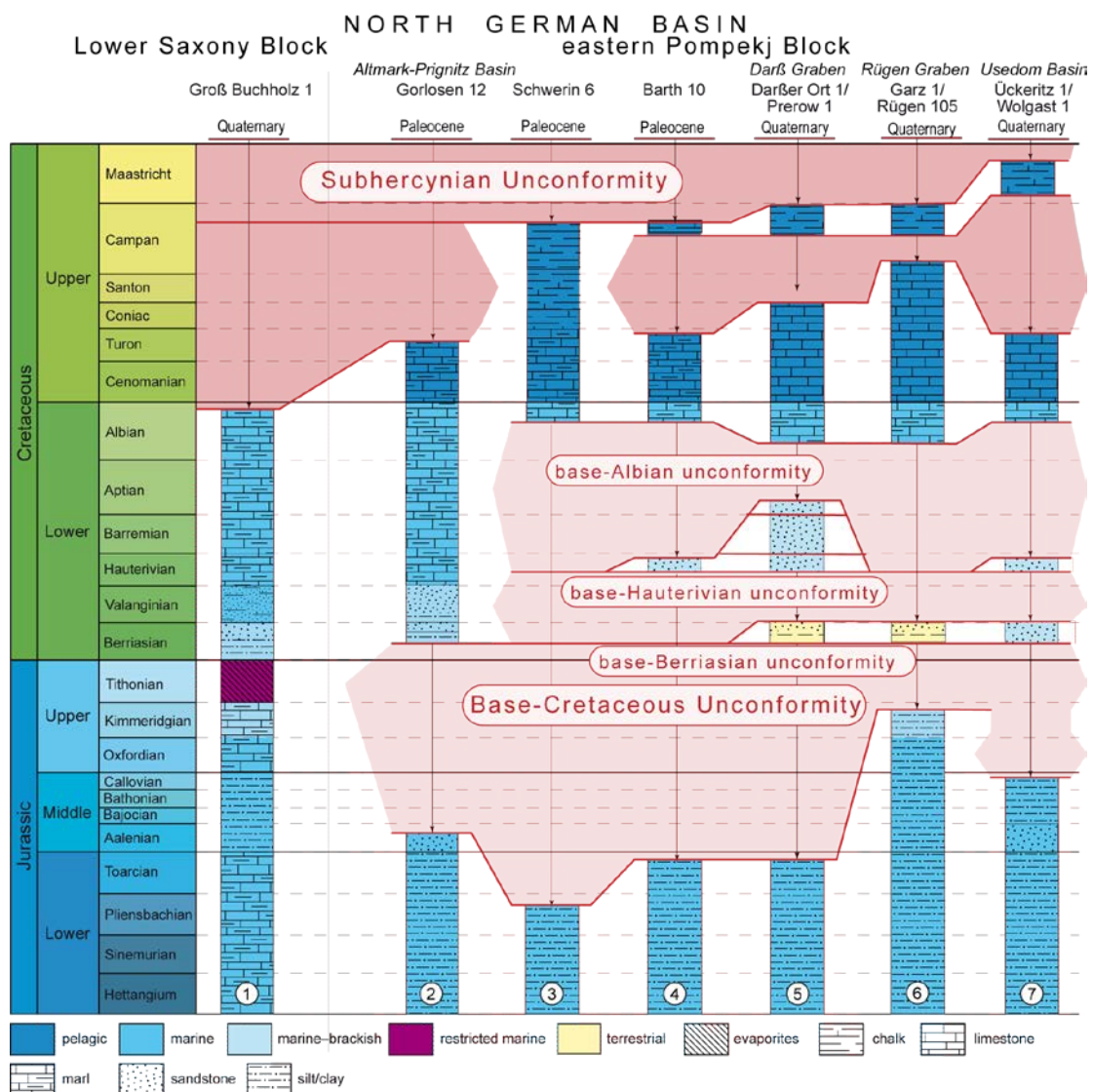


Fig. 10: Unconformities contribute to significant gaps within the Jurassic–Cretaceous succession of the North German Basin based on well data and biostratigraphical data. Low sea-level and repeated uplift of the Pompeckj Block during the late Jurassic–early Cretaceous phase resulted in several unconformities. Their amalgamation contributed to a substantial gap at the base of the Cretaceous strata (base-Cretaceous Unconformity). Late Cretaceous–Palaeogene uplift phases affected the Lower Saxony Block and the Pompeckj Block resulting in the Subhercynian Unconformity. Encircled numbers refer to localities shown in Fig. 3 and Fig. 4, Groß Buchholz 1 well according to (Schäfer et al., 2012), other wells according to unpublished core reports.

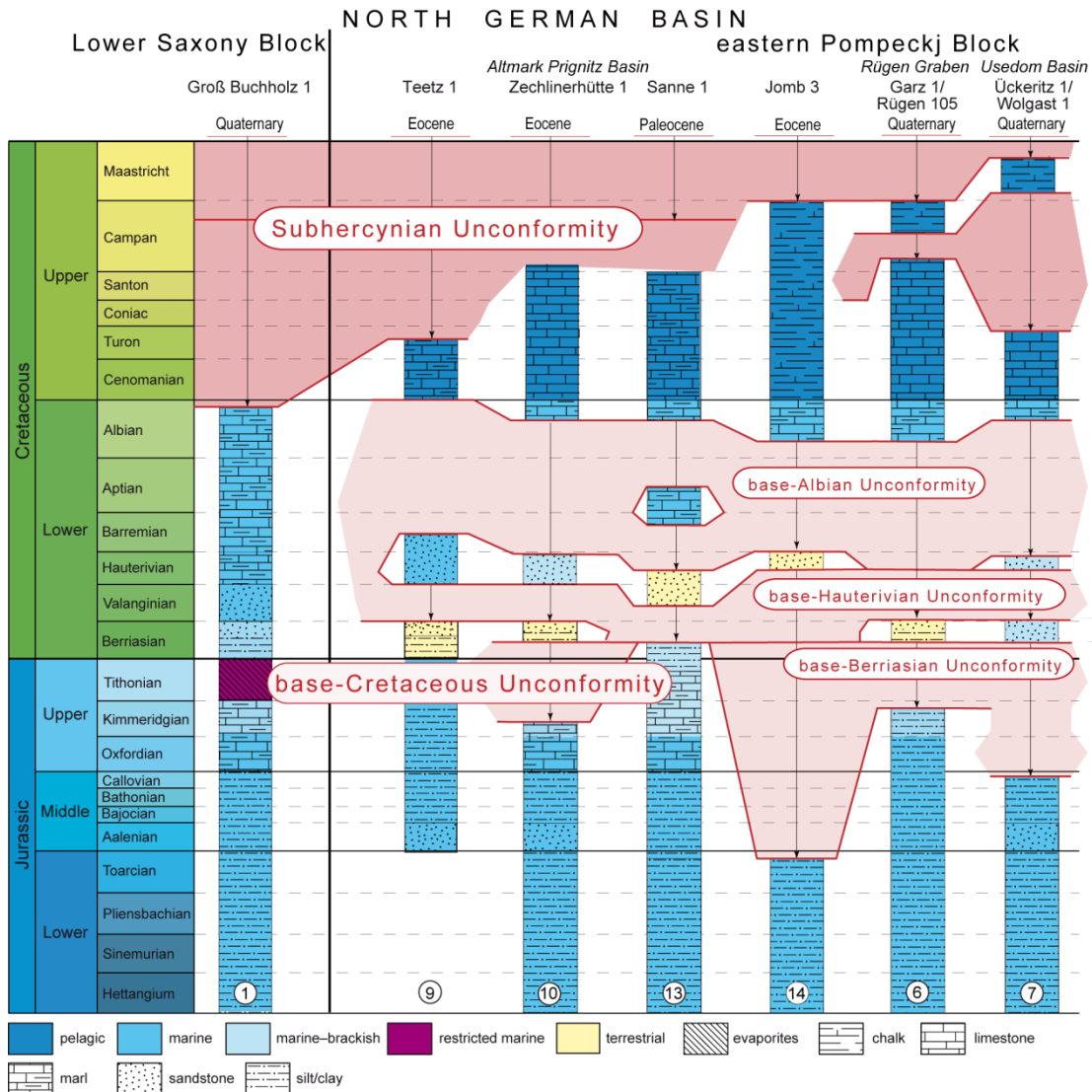


Fig. 11: Unconformities contribute to significant gaps within the Jurassic–Cretaceous succession in the Altmark-Prignitz Basin based on well data and biostratigraphical data from unpublished core reports. Encircled numbers refer to the well locations described in Fig. 4.

## 5.2 Western Pomeranian Fault and Graben System

The Western Pomeranian Fault System (WPFS) is a WNW-ESE orientated fault system within Permian to Mesozoic successions, extending from the southern Falster Block, located in the southern Baltic Sea to the Darß peninsula and the southern Rügen island to the Usedom island (Krauss and Mayer, 2004, Deutschmann et al., 2018). The formation of the WPFS is linked to the Early Cimmerian (Late Triassic) stress field that caused the reactivation of pre-existing faults in the pre-Permian, Variscian and Caledonian basement. These WNW-ESE-orientated basement faults caused the detachment of the sedimentary cover along the Zechstein salt layer resulting in an NNW-SSE-orientated system of pull-apart grabens in the supra salt successions (Krauss and Mayer, 2004). The extensional structures further evolved during Late Cimmerian to early Cretaceous time and the extent and internal structure are clearly influenced by the superordinate Trans European Fault (Krauss and Mayer, 2004).

### 5.2.1 Darß Graben

The mainly WNW-ESE-oriented Darß Graben is situated in the northern Darß peninsula, from where it continues into the Baltic Sea (Deutschmann et al., 2018). The 0.8–2.4 km wide and 1.1–1.8 km deep y-shaped graben structure is internally composed of three narrow blocks, which are bounded by 60–70° dipping normal faults of the Prerow Fault Zone (Köhler and König, 1965; Fritzsche and Doß, 1980), which is partly propagating into the pre-Zechstein strata (*Fig. 12*; Krauss and Mayer, 2004). The Mesozoic graben fill shows an 500–600 m offset (Köhler and König, 1965). The Darß Graben is partly flanked by low-amplitude salt structures: the Prerow salt pillow to the Southwest and the Zingst salt pillow to the East (*Fig. 5*). According to seismic data, the Prerow salt pillow represents a passive salt structure, which was formed due to the migration of Zechstein salt into the southern graben shoulder (*Fig. 12*). The structural relation of the Darß Graben and the Zingst salt pillow is unclear as the continuation of the graben across the salt pillow is not proven so far.

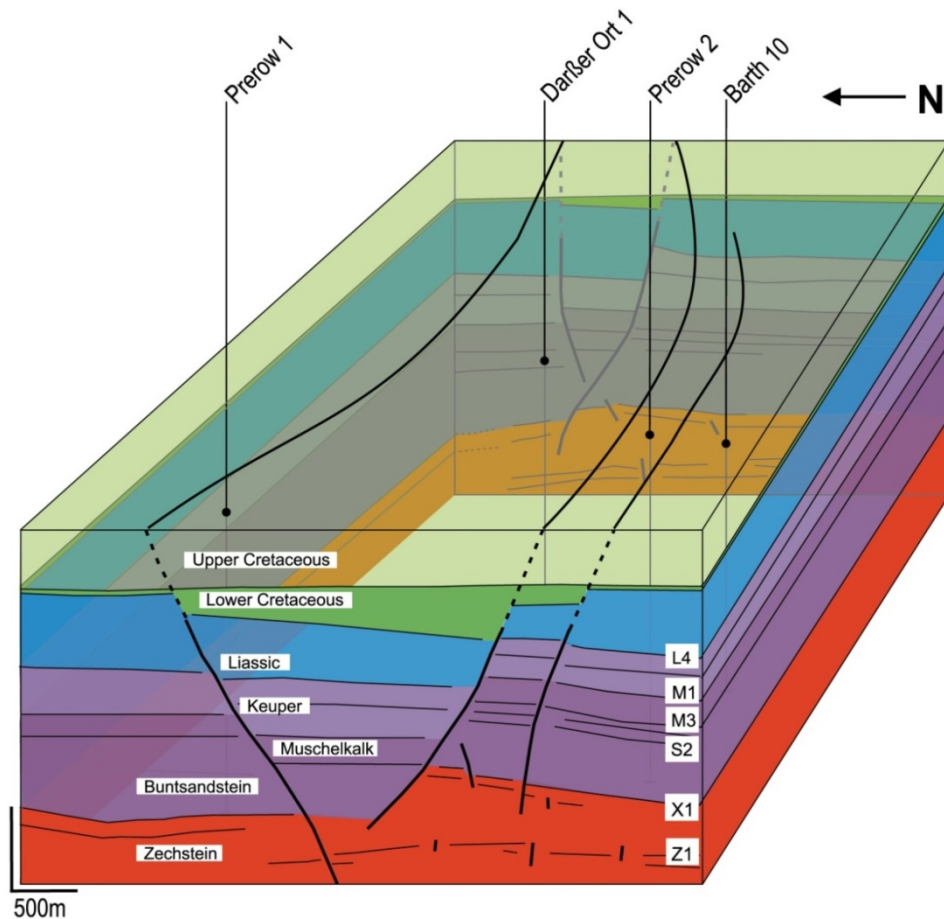


Fig. 12: Block model of the Darß Graben based on ten 2D seismic lines running parallel and normal to the ENE-WSW oriented graben (modified from TWT-seismic line after Fritzsche and Doß, 1980). For detailed stratigraphic patterns, see Fig. 13.

2D seismic and well data show that the Darß Graben evolved in the early Cretaceous as a post-cursor structure of a former basin-internal swell. The repeated activity of the swell in the Triassic–Jurassic is indicated by reduced thicknesses of individual stratigraphic intervals and several gaps, such as the Early Cimmerian Unconformity (Beutler, 2012; Stollhofen et al., 2008). The uplift of the Pompeckj Block in the Late Jurassic to Early Cretaceous resulted in the superimposition of the swell and wide-spread erosion of Tithonian–Rhaetian strata in the Darß area. Associated with the base-Cretaceous Unconformity, Wealden-type strata unconformably overlay Toarcian to Rhaetian strata in the Darß Graben. Outside the graben, the gap is even more pronounced as Hauterivian strata or Albian strata overlay Liassic strata resulting from amalgamation of several unconformities (Fig. 10). The Darß Graben comprises an up to 430 m thick Lower Cretaceous succession, which was cored in the Darßer Ort 1 well. The discontinuous succession is biostratigraphically dated as Upper Berriasian (Wealden-type) and Upper Hauterivian–Lower Aptian strata followed by Upper Albian strata (Fig. 13). The thick Lower Cretaceous graben fill is in remarkable contrast to the limited thickness of the Lower Cretaceous strata at the graben shoulders, where an approximately 10 m thick succession is dated as Upper Albian to Hauterivian strata in the Barth 10 well.

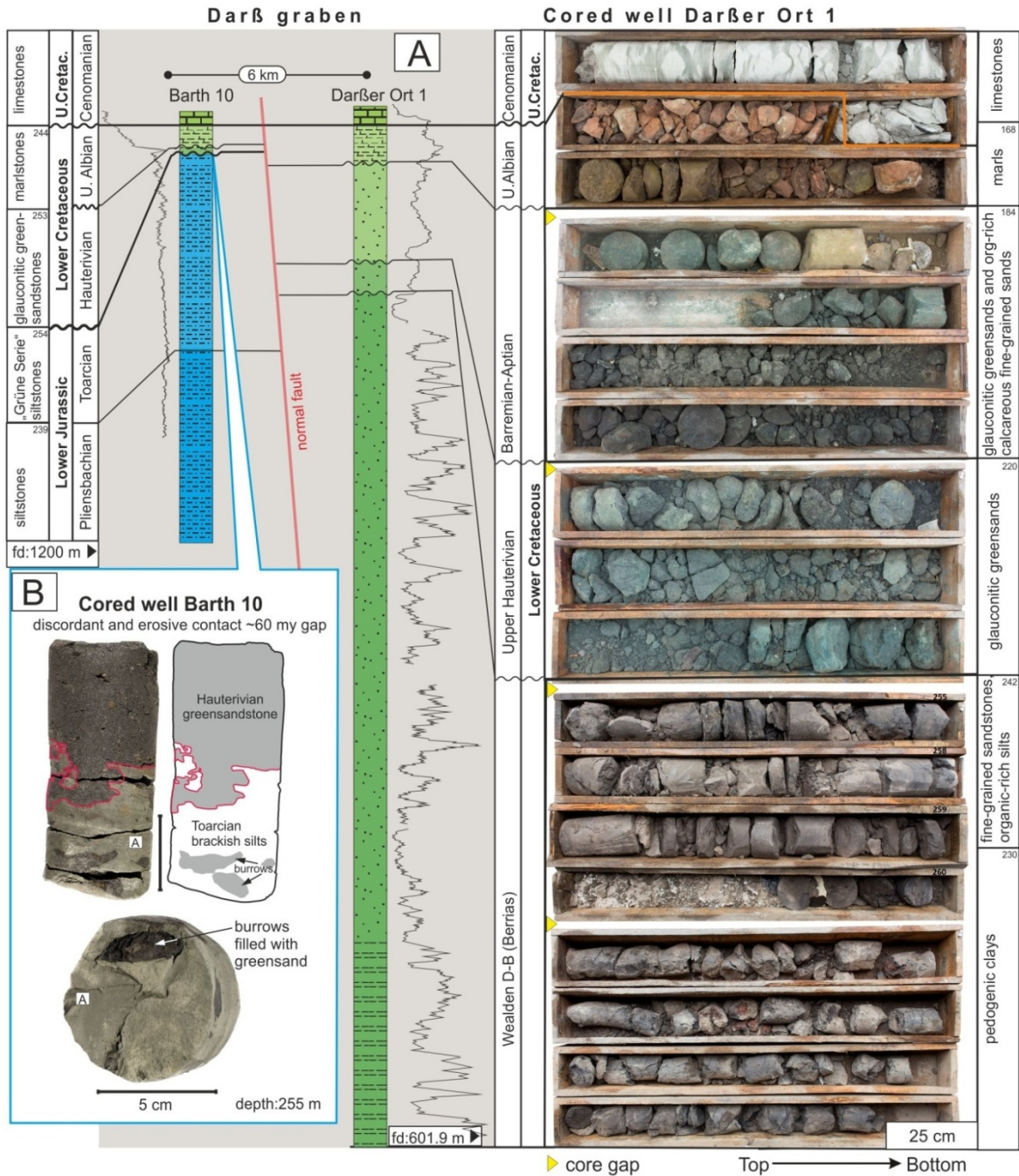


Fig. 13: Detailed stratigraphic model of the Darß Graben, showed by well darßer Ort 1. The graben shoulder is shown by well Barth 10. The model is based on biostratigraphic and well data (Haupt and Heppner, 1962; Döring, 1966).

### 5.2.2 Samtens Graben System

The NW-SE-oriented Samtens Graben System is named after the small village of Samtens located in the southern part of the Rügen island (Fig. 5). The subsurface of the Rügen island represents a basement high, which is composed of several blocks bounded by NW-SE oriented basement faults. This basement high controlled facies pattern and depositional environments during Permian–Mesozoic times and contributed to generally limited thicknesses of the Rotliegend to Jurassic basin fill. Resulting of the strongly reduced

thickness of the Zechstein, salt structures are absent in the subsurface of Rügen (Krauss and Mayer, 2004).

Seismic and well data were interpreted as (I) two narrow NW-SE oriented graben structures with an up to 280 m thick discontinuous Middle Jurassic–Early Cretaceous graben fill (Fitzsche and Doß, 1980). The parallel grabens are c. 1–1.8 km wide and 2 km deep and bounded by 70–80° dipping basement faults of the Samtens Fault Zone, which propagate to the Zechstein or partly across the (Döring et al., 1970) Zechstein base. Other authors argued that there is a (II) 3.5 km wide single graben structure (Linke and Krauss, 1966). The Samtens Graben System evolved already in the Middle Jurassic with offsets up to 350 m (Kubon, 1966) and was active up to the Early Cretaceous. The Garz 1 and Rügen 105 wells recovered an almost 80 m thick successions of Middle Jurassic strata, biostratigraphically dated as Aalenian, Upper Bathonian and Lower Callovian, followed by an about 100 m thick succession of Upper Jurassic strata, dated as Middle–Upper Kimmeridgian and Upper Malm. The Lower Cretaceous succession is c. 150 m thick and identified as Upper Berriasian (Wealden-type) and Middle–Upper Albian (Döring et al., 1970). Outside the graben system, the Middle–Upper Albian and thin Hauterivian strata disconformably overlay truncated Liassic strata resulting in a pronounced base-Cretaceous Unconformity.

### **5.2.3 Usedom Basin**

During Lower Cretaceous times, the Usedom Basin was supposed to be the western extension of the Polish Trough (Leszczynski, 1998). The Usedom basin is dominated by two main tectonic structures: the Moeckow - Dargibell Graben and the Usedom Fault Zone. The NW-SE to NNW-SSE orientated Moeckow Dargibell graben fault zone (*Fig. 5*) is bounded by 80° - 85° dipping bounding faults and adjoining single normal faults (Krauss and Mayer, 2004) and is a main fault within the Western Pomeranian Fault System (Beutler, 2012). Graben internal faults show different directions and single normal faults, which continues to the Zechstein (Diener et al., 1989). Due to halocinetic movement of the salt plug Moeckow, complex tectonic conditions make it impossible to trace graben internal faults in the seismic sections. Split into two parts by the southern fault zone, the salt structure Dargibell (*Fig. 5*) shows a horizontal offset. The first movements of salt plug Moeckow during the Keuper are attested by differences in strata thickness, whereas Buntsandstein and Muschelkalk strata provide constant thickness. Due to post-Malm graben activity, recovered by well Hanshagen 18, 166 m of Middle Jurassic strata, dated as Bajocian to Callovian and 16 m thick Upper Jurassic strata, dated as Oxfordian to Tithonian, could be preserved.

Seismic and well data show an NW-SE to NNW-ESE striking Usedom fault zone, which continues to the Zechstein (Diener et al., 1989). The fault zone consists of parallel multiple 80° - 90° steep normal faults (Petzka et al., 1964), dipping to SW. According to seismic data,



the main fault offset is up to 650 m, decreasing in the southeastern direction to 150 m. The easternmost faults show an offset in Mesozoic strata of 50 m. The main activity of this fault is dated from Jurassic to Upper Cretaceous times (Diener et al., 1989). An NW-SE striking axis, representing the former basin axis and the extension of the Danish Polish Trough, provides the highest thickness of Berriasian strata (Petzka et al., 1964). Ranging from several meters in the northern part of Usedom Basin in the area of Lubmin, the thickness of Berriasian strata is constantly increasing in the southeastern direction up to 100 m in the vicinity of the Polish Trough. The influence of salt structures in the Usedom basin is given by different Zechstein salt pillows, such as Hohendorf, Behrenhoff, Neetzow and Dargibell. In the salt structure Hohendorf for example, seismic data revealed a range in salt thickness from 350–900 m (Petzka et al., 1964). Towards the margins of the Usedom Basin, to the east and west of the Moeckow Dargibell fault zone, salt thickness decrease to a minimum of 250 m. Maximum salt thickness is provided by the salt structure Neetzow with more than 1000 m. The Dogger base shows a smoothing in the shape of the underlying salt structures.

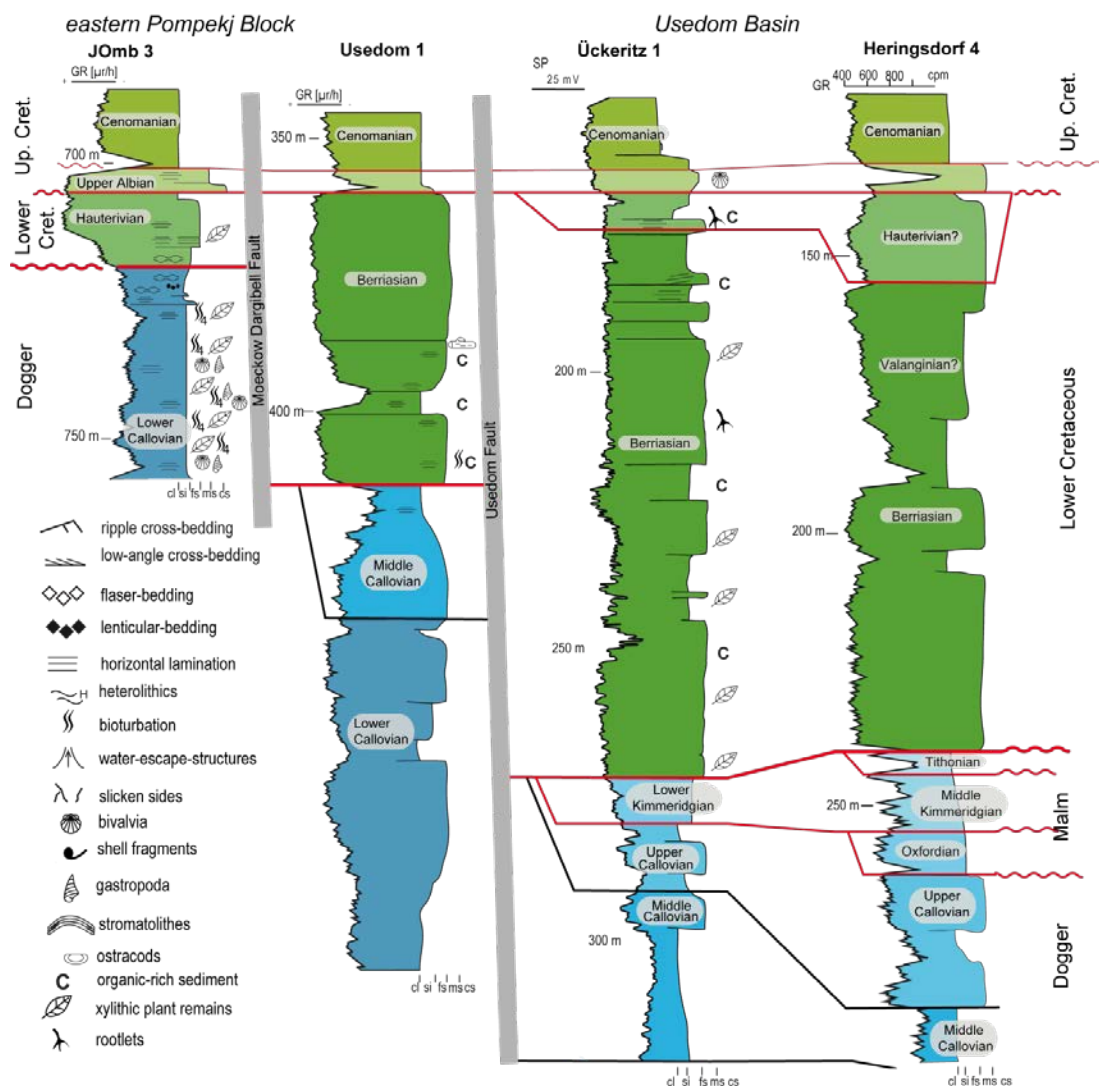


Fig. 14: Cross section from the eastern Pompeckj Block to the Usedom basin demonstrates the influence of Pompeckj Block uplift, represented by decreasing the thickness of Lower Cretaceous strata thickness. Section line is shown in Fig. 5. Based on biostratigraphic and well data from unpublished core reports.

### 5.3 Salt structures

According to Kossow et al. (2000), salt diapir structures are almost entirely absent in the northern part of the Northeast German Basin, whereas it hosts a large number of Zechstein salt pillows. During late Permian and Early Triassic, evaporates and clastics were deposited. Salt movement was initiated after the deposition of the Middle Triassic Muschelkalk (Zöllner et al., 2008). Salt pillows are responsible for the creation of smaller subsidence centers. In fact, the Lower Cretaceous strata in the Darß-Rügen-Usedom area were less affected by salt pillow activity than by fault zones and the formation of syn-sedimentary graben structures. Subsidence in the salt plug rim-synclines caused thicker sandstone reservoirs in increased depths providing present-day temperatures  $> 40^{\circ}\text{C}$  e.g. salt plugs Werle, Neuruppin, Pritzwalk and Wittstock. The sandstone reservoirs are located in depths ranging from 900 m to 1900 m. In contrast to the stratigraphic profiles drilled between the salt plugs, the ones located in the rimsynclines e.g. Werle, Pritzwalk, include nearly complete stratigraphic successions.

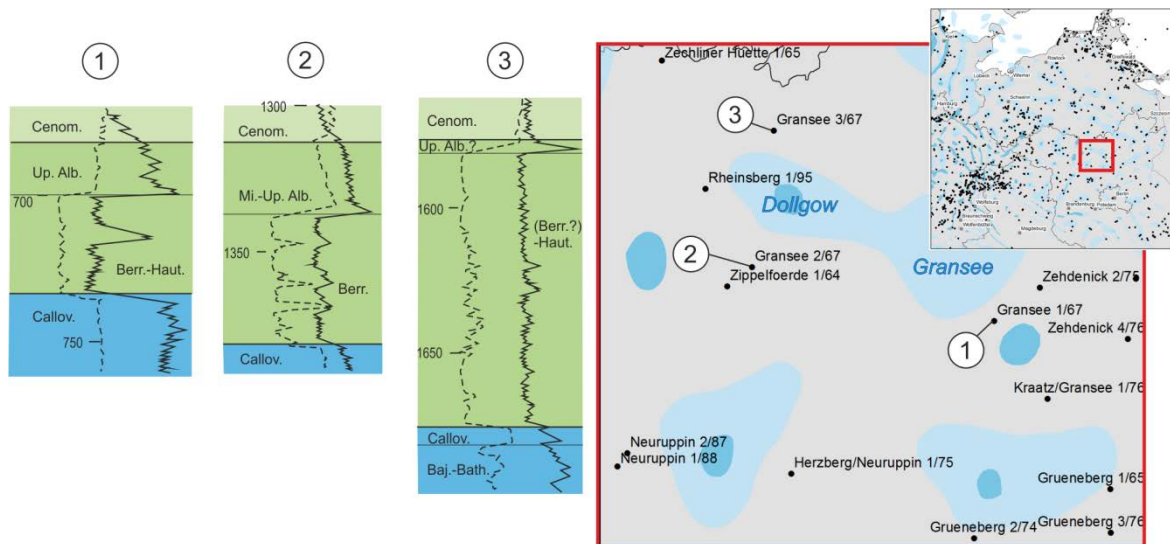


Fig. 15: Stratigraphic succession of well Gransee 1, 2, and 3 are located (small map, top right) surrounding the salt plugs Dollgow and Gransee. Despite deep subsidence of up to 1650 m, large parts of the Berriasian – Albian strata were eroded. Based on biostratigraphic and well data from unpublished core reports.

However, despite the tectonically protected position within a marginal syncline, the stratigraphic profiles also include erosional gaps, as shown by the example of the wells Gransee 1, 2, and 3 (Fig. 15). Berriasian, Hauterivian and Albian strata was preserved with reduced thickness and subsided to variable depths up to  $\sim 1700$  m. Varying strata thickness might also be influenced by dipping towards the marginal syncline and/or thickening caused by subsidence. Nevertheless, substantial parts of Berriasian, Valanginian, partly Hauterivian, Barremian – Aptian and Lower – Middle Albian are missing.

## 5.4 Upper Jurassic–Lower Cretaceous syn-tectonic strata

### 5.4.1 Distribution and thickness

#### 5.4.1.1 Upper Jurassic strata

The Upper Jurassic drilled successions of northeast Germany include the Upper Oxfordian, informally called 'Korallenoolith', the Lower to Middle Kimmeridgian and the Middle to Upper Tithonian, informally called 'Münder Mergel' and 'Serpulite'. Due to uplift and erosion combined with low sea level, the Upper Jurassic is strongly decreased in thickness compared to the Lower Saxony Basin and the Gifhorn Trough. Its distribution is limited to graben structures in the Rügen and the Usedom area. In the Rügen Graben, 35 m thick, calcareous and glauconitic fine-grained sandstones, silt- and claystones were drilled by well Garz 1 and dated to the Kimmeridgian and Upper Tithonian (Döring et al., 1970). Furthermore, a 76 m thick succession of clayey marlstones, lime-, silt- and sandstones, dated to the Middle to Upper Kimmeridgian, was drilled in well Rügen 105. The underlying strata, dated to the Callovian, imply the local erosion of Oxfordian strata within the Rügen Graben. This could neither lithostratigraphically nor biostratigraphically be testified (Döring et al., 1970). Largely eroded in the Usedom Basin, here, the Upper Jurassic strata provide thicknesses from 16 m to 23 m, drilled in well Heringsdorf 4 and dated to the Kimmeridgian. Well Hanshagen 18 provides 16 m of Middle Kimmeridgian to Upper Oxfordian dated limestones and oolitic marlstones. In contrast to the previously described graben structures, the Darß Graben provides no strata which could be biostratigraphically dated to the Upper Jurassic.

The Upper Jurassic marlstones and clayey marlstones of the Altmark-Prignitz Basin were drilled in well Teetz 1, 30 m dated to the Tithonian, 15 m Kimmeridgian 40 thick Oxfordian. Well Sanne 1 drilled a succession from less than 10 m thick Oxfordian, 30 m Kimmeridgian to 50 m Tithonian (Münder Mergel and Serpulite) dated marlstones, silt- and claystones.

#### 5.4.1.2 Upper Berriasian (Wealden-type)–Valanginian strata

Whereas subsidence rates in the Lower Saxony basin were higher than in the neighbouring eastern sub-basins, the easternmost extension of the Pompeckj Block, the North Western Pomeranian High (*Fig. 4*), represents an early Cretaceous swell region (Kemper, 1973; Diener, 1974). Decreased thicknesses of Lower Cretaceous strata and erosional gaps imply that these swell kept less affected by transgressions, most of the time. However, it was temporarily flooded pre-Lower Albian and completely flooded during basin extension and the rising sea-level during the Middle to Upper Albian. The present-day distribution of the Northeast German Berriasian succession is limited to the Darß and Rügen Graben and the Usedom sub-basin. In the Darß Graben successions, thickness ranges from

360 m to 60 m on the graben flanks and 150 m on the Rügen graben. The Usedom sub-basin provides up to 10 m to 110 m thick strata of Berriasian (Wealden-facies), increasing NW to E towards the Polish Trough. Smaller isolated deposits of up to 40 m thickness exist in the southern direction from the Usedom basin and suggest a former connection to the Altmark-Prignitz Basin and, therefore, a wide-spread sedimentary cover. Evidence of marine Valanginian-aged strata is only suggested by Diener (1974) in the Usedom basin as an extension of the Polish Trough but could not be testified by microfossils. Leszczynski (1998) also suggest the Usedom sub basin as the northwestern extension of the Polish Trough and identified a roughly 100 m thick Early Valanginian succession in NW-Poland in the vicinity of the Usedom Basin.

Widespread distributed in the Altmark-Prignitz Basin, thicknesses of Berriasian strata are widely influenced by salt structures activity, the accumulation in rim synclines, ranging from roughly 400 m in Rhinow 2 to 30 m in well Teetz 1. The Middle to Upper Valanginian dated strata are mainly distributed in the southeastern part of the Altmark-Prignitz Basin and was drilled with up to 50 m thickness in well Bismarck-Ost 1.

#### 5.4.1.3 Hauterivian–Barremian strata

Due to the existence of the North Western Pomeranian High as the eastern part of the Pompeckj Block, the thickness of Hauterivian to Barremian strata is strongly decreased and partly eroded in pre-Albian times (Diener, 1974). In the Darß area, Hauterivian fine-grained, glauconitic sandstones reach a thickness of 2 m to 25 m and transgressively cover Liassic clay- and siltstones, informally called 'Grüne Serie'. The Rügen Graben provides 15 m to 35 m thick successions. As a former extensional bay of the Polish Trough (Diener, 1974; Leszczynski, 1998), the Usedom Basin provides present-day thicknesses of roughly 20 m; 10 m were drilled in well Ueckeritz 1. However, Diener (1974) assumed a primary Hauterivian thickness of 80 m to 100 m. In the Altmark-Prignitz Basin, Hauterivian strata were drilled with up to 50 m thickness. The distribution of Barremian strata is limited to the Darß Graben with thicknesses up to 30 m, whereas the Altmark-Prignitz Basin provides Hauterivian dated strata thickness ranging from less than 20 m (Teetz 1) and up to 90 m drilled in well Bismarck Ost 1. The Lower Barremian dated strata is missing within drilled cored material. Middle to Upper Barremian dated and dominantly sandy shallow-marine (Sparfeld, 1972) strata were drilled with up to 50 m thickness in e.g. well Waddekath 35.

#### 5.4.1.4 Aptian–Lower Albian strata

During the Aptian and Lower Albian, more and more marginal swell areas are affected by regression. A stronger trend to differentiation into subbasins and swells is assumed (Diener, 1974). The present-day distribution of Aptian strata in the northeastern Northgerman Basin is very limited to the Darß Graben, while the Lower Albian strata are missing. Influenced by

pre-mid-Albian erosion, thicknesses are strongly decreased compared, for example, to the Prignitz Altmark region (Diener 1974). These strongly reduced thicknesses are caused by the swell position and subsequent pre-Albian erosion (Diener, 1974; Raczynska, 1967).

Consequently, the area lacks a biostratigraphic classification by marker species, dominantly caused by core loss and the sandy lithologies of Aptian strata. In the Darß Graben, the Aptian strata compile 15 to 20 m thickness. The Usedom Basin was still a western extension of the Polish Trough and drilled core material provides no Upper Aptian to Lower Albian dated strata. In contrast, in the Altmark-Prignitz Basin, Lower Aptian black shales strata, informally called “Blättertonmergel”, were drilled in well Waddekath 35. However, Upper Aptian dated strata is more widely distributed with a maximum 20 m thickness in the Westprignitz or Rambow area and calcareous sandstones were drilled in well Waddekath 35 with 10 m thickness.

#### 5.4.1.5 Middle–Upper Albian strata

The Middle Albian deposits transgressively cover Berriasian to Aptian strata with a 5 to 10 m thick clayey, glauconitic, calcareous sandstone and are superimposed by Upper Albian marlstones. The Upper Albian base is characterised by a sandy marlstone onset. These strata type is distributed all over the working area, except the Grimmen Swell (Diener, 1974). The total thicknesses of Middle to Upper Albian strata range from 5 to 25 m in the Darß Graben, 5 to 15 m in the Usedom Basin and 10 to 15 m in the Samtens Graben on the Rügen island.

## 5.5 Discussion

### 5.5.1 Unconformities

According to Bachmann (2008) and Beutler et al. (2012), the c. 40 Mio years lasting late Cimmerian Cycle (DC 7) includes the Upper Middle Jurassic to the Valanginian/Hauterivian. Within this cycle, the depositional conditions change from marine during the late Middle Jurassic to Upper Kimmeridgian into a brackish-marine trend, lasting to the Berriasian. Several pulses of uplift interrupted the long-term subsidence trend of the northeast German Basin at this time (Kossow and Krawczyk, 2002). The Valanginian transgression starts a new cycle. Beutler et al. (2012) described a pre-Berriasian Unconformity, which is the disconformable contact of Berriasian to Liassic or Triassic strata, observed in the Altmark, Prignitz and the Wendland. This unconformity was also observed within data from this study, as described in *chapter 5.1.1*. The authors refer to diapiric piercing of salt plugs from this time e.g. Wustrow, Gorleben-Rambow, Lübtheen, to the late Cimmerian activation of faults and, therefore, to the pre-Berriasian Unconformity. They also mentioned the influence of

tectonic block activity, separated by faults on sediment thickness and preservation and established a structural map (Fig. 16.) based on seismic-, biostratigraphy- and well data.

According to Beutler et al. (2012), the pre-Hauterivian Unconformity is limited to Berriasian –Hauterivian strata. They mentioned a former wide-spread sedimentary cover by Hauterivian strata, witnessed by the analysis of present-day erosional remnants, which could be validated by this study. Tectonic activity had a strong influence on the West Western Pomeranian Fault and Graben system, which resulted in strongly decreased thicknesses, for instance, on the Barth-Block. There, Berriasian sediment thickness not exceeds 50 m. This is in accordance with results from this study, except in Darß Graben, as shown in Fig. 13 and the Rügen Graben. Most prominent within this unconformity is the missing Lower Valanginian, or in the case of the eastern Pompeckj Block, the Valanginian in total, followed by the missing Lower Hauterivian.

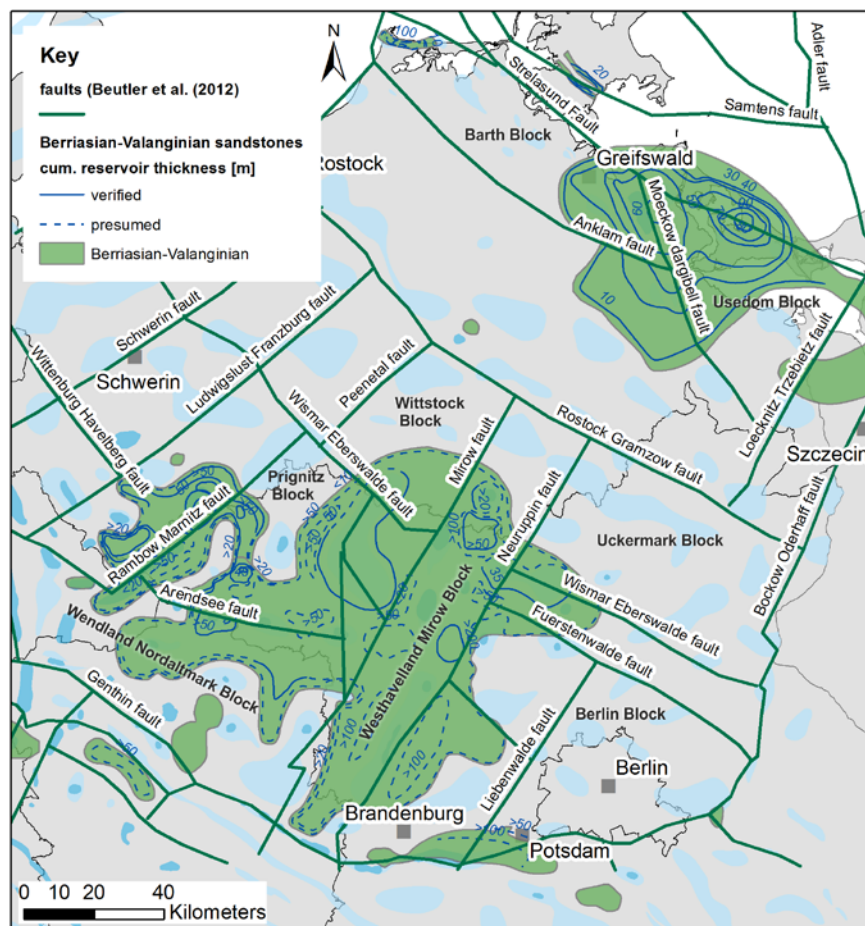


Fig. 16: Faults and blocks according to Beutler et al. (2012) in the eastern North German Basin. Fault and block activity influenced the sediment deposition and thickness during Lower Cretaceous times.

Another c. 30 myr lasting marine cycle (DC 8a) starting in the Valanginian/Hauterivian and lasting to Middle/Upper Albian could be figured out by Beutler et al. (2012). Intensive uplift and erosion combined with sea-level fluctuations are characteristic forming features. Due to post-Hauterivian regressive conditions, the deposition of Barremian to Aptian strata is

concentrated on the Altmark and Prignitz area and the Darß Graben, which could be validated by results from this study. Whereas the Altmark-Prignitz Basin was connected to the Lower Saxony Basin, Beutler et al. (2012) considered the Darß area a former extension of the Danish Basin. Large parts of the Barremian and Aptian, as well as the Lower Albian strata, were eroded due to the base-Albian unconformity.

### **5.5.2 Basin differentiation of the North German Basin**

The pronounced gaps and noticeable thickness contrast point to differential vertical movements of individual blocks in the northeastern North German Basin, visible in the syn-tectonic Darß and Rügen Graben fill. Following uplift and erosion in the Tithonian, downfaulting of graben blocks in the Darß graben, sea-level fluctuations and syn-tectonic sedimentation in the Berriasian–Albian was interrupted by uplift and erosion during Valanginian–Lower Hauterivian, Lower Barremian, Lower Aptian and Lower Albian. Sediment accumulation was obviously more pronounced in the Berriasian, indicated by the up to 358 m thick Wealden-type succession drilled in well Darßer Ort 1, and subsequently slowly decreasing as shown by limited thicknesses of the Upper Hauterivian (25 m), and the Upper Barremian (30 m) and Middle to Upper Aptian (18 m). Outside the graben, Berriasian, Valanginian and Upper Barremian–Lower Aptian strata are missing and the thickness of Upper Hauterivian greensandstones is limited (1,5 m), indicating starved sedimentation (condensation). The overlying post-uplift Upper Albian thickness (10 m) is also very limited (*Fig. 13*).

The northeastern sub-basin was temporarily separated from the southern Altmark Prignitz sub-Basin by the eastern Pompeckj Block, also referred to East Holstein - North Mecklenburg swell (Meinhold et al., 1960; Diener, 1974). Changing by the Middle to Upper Albian, the swell was permanently flooded through the Upper Cretaceous. As a former extension of the Lower Saxony Basin, the Altmark Prignitz sub-basin was less deeply subsided. This subsidence trend decreased in the eastern direction. Hence, the differences in the depositional evolution and a strong differentiation caused the development of smaller sub-basins and sub-swells, starting during the Berriasian. Enhanced by salt movement, strong variations in thickness developed, especially increased within the rim synclines of salt plugs, for instance the 600 m thick (excluding Middle to Upper Albian part) Lower Cretaceous successions of Gorlosen and Werle. Maximum thicknesses of up to 900 m (Friesack 1) are observed, whereas swell regions witness thicknesses ranging from 10 to 200 m (Diener, 1974, this study). Uplift is implied by the widespread and partly complete erosion of the Valanginian (Diener, 1974), Barremian, Aptian and Lower Albian. Bounded by a swell in the East, considered as East Brandenburg High, the Altmark-Prignitz Basin was temporarily separated from the Polish Trough (*Fig. 4*). However, a former connection is assumed by the

strongly reduced Hauterivian and Albian successions drilled by the wells Polssen 1, Gt Prenzlau 1 and JomB 10, northeast of Berlin. The Flechtingen swell is referred to be the southwestern bounding high. The Middle to Upper Albian transgression decreased the basin differentiation intensity in the eastern North German Basin.

Starting in the Cenomanian (Voigt et al., 2021), the following Late Cretaceous inversion caused inverted graben structures, newly formed marginal troughs and basement uplifts as the main expressions of crustal shortening (Kley and Voigt, 2008). The area of basement uplift includes prominent fault-bounded blocks composed of crystalline basement rocks and pre-Permian rocks such as the Bohemian Massif and the Harz Mountains (von Eynatten et al., 2020). Inverted sedimentary basins are basins that have been inverted along former extensional faults and occur partly between and within these blocks (Cooper, 1989). Syntectonic basins formed along the margins of inverting subbasins and uplifting basin blocks (Voigt, 1963; Krzywiec, 2002; Voigt et al., 2004; von Eynatten et al., 2008). The area of contraction closely coincides with the previous extension tectonics, even though not all major thrust faults are reactivated normal faults (Voigt et al., 2009). South of the main inversion axis extending from the North Sea Basins to the Polish Trough, contraction attenuates abruptly or gradually. For instance, shortening structures of small magnitude are widespread in the German uplands (von Eynatten et al., 2020). So far, the previously mentioned features were not observed to this extent within the Lower Cretaceous successions in the eastern North German Basin. However, Kossow and Krawczyk (2002) mentioned the determination of less than 1 km possible contraction for the Northeast German Basin at the Jurassic/Cretaceous boundary.

### **5.5.3 Estimated erosion**

Due to fluctuating sea-level and basin differentiation caused by salt movement and syn-tectonic activity, the determination of sedimentation rates and estimation of erosion is difficult. Therefore, the observed present-day thickness can not be compared to a standard thickness and is described by an assumed value range of eroded sediment thickness. For a detailed reconstruction of thermal history, the evaluation of thermochronological data like e.g. apatite and zircon fission track or fluid inclusions, would be necessary.

Berriasian thickness range from 400 m in the Rhinow rim syncline and 360 m in the Darß graben fill to < 50 m between several salt structures in the eastern Altmark-Prignitz Basin or was partly eroded e.g. well Gransee 1, 2, 3 (*Fig. 15*). Diener (1974) mentioned an average thickness of around 200 to 300 m. Beutler et al. (2012) mentioned a maximum 200 m erosional gap on the Barth-Block, resulting in a decrease of Berriasian strata < 50 m. In contrast, the Valanginian is widely eroded except in the southernmost basin parts and the vicinity of the Lower Saxony Basin and the Gifhorn Trough, where thickness ranges from 60



to 100 m in the Werle-Gorlosen-Rambow region. In terrestrial-dominated areas, the present-day existence of the (Lower) Valanginian is possibly still undiscovered due to similar lithostratigraphy of the underlying Berriasian and lacking microfossil record (Diener, 1974). However, regressive conditions (Haq et al., 2014) inhibited sediment deposition. Nevertheless, large parts (> 50 m) of the (Upper) Valanginian successions must have been eroded concerning ongoing basin extension and sea-level rise during the Valanginian transgression and the fully marine depositional environment (Diener, 1974; this study). Increased subsidence in the western Altmark-Prignitz Basin during Hauterivian is suggested by 220 m thick strata in well Gorlosen 2 to 33 m in the eastern Altmark Prignitz area and less than 35 m in the Rügen and Usedom area, linked to the activity of the Darß and Rügen Graben. Based on 50 m present-day thickness, primary thicknesses of 50 to 100 m in the Usedom Basin are assumed by Diener (1974). Minimum thickness of >10 m was observed on the Pompeckj Block. The Barremian – Lower Albian maximum thickness of 500 m was observed in the eastern Altmark-Prignitz Basin, whereas thickness was decreased in the swell areas due to pre- mid-Albian erosion (Diener, 1974, this study). There, <50 m sediment erosion is assumed.

Compared to the western Lower Saxony Basin, Berriasian strata are referred to as the Bückeberg Group and yield up to 800 m thick claystones successions (Kemper, 1973), deposited in a distal brackish marine basin. With up to 380 m thick Berriasian successions, well Isterberg 1001 recovered a fairly complete section of the Bückeberg Group (Strauss et al., 1993) in the western non-salt-influenced basin part, referred to as the Isterberg Formation. Influenced by a strong subsidence trend and salt movement during the Lower Cretaceous, the eastern Lower Saxony Basin (gas field Thönse) provides up to 1400 m of Lower Cretaceous strata recovered by well Großburgwedel 4. Situated at the salt structure Thönse, 325 m of these Lower Cretaceous successions are referred to as the Berriasian (Elstner, 1991). Hauterivian strata, drilled in well Großburgwedel 4, comprise 330 m thickness, Barremian strata are up to 220 m thick, Aptian strata reach thicknesses of 210–450 m and the Albian is up to 210 m thick.

## 6 Petrography, granulometry and diagenesis of Lower Cretaceous sandstones

### 6.1 QFL and Granulometry

Detrital grain classification of quartz, feldspar and lithoclasts after McBride (1963) are shown in Fig. 17 for western Pomerania, NE Germany and the Altmark-Prignitz Basin. Taken from seven different wells, the sandstone samples are classified as highly mature quartzarenites and a few samples are classified as subarkoses. Regarding the QFL distribution, monocrystalline and undulose quartz dominates with amounts of 93–98 % (Fig. 17), followed by feldspars like potash feldspar, microcline and plagioclase with up to 8% and magmatic and metamorphic rock fragments less than 1 %. Detailed amounts are given in the stratigraphic sections. According to Dickinson et al. (1983), the source area for Kimmeridgian and Lower Cretaceous sandstones in the North German Basin is a craton interior, such as the Fennoscandian High, which is also suggested by the ultrastable metamorphic heavy mineral assemblage (see chapter 6.2, Fig. 25 and Fig. 26).

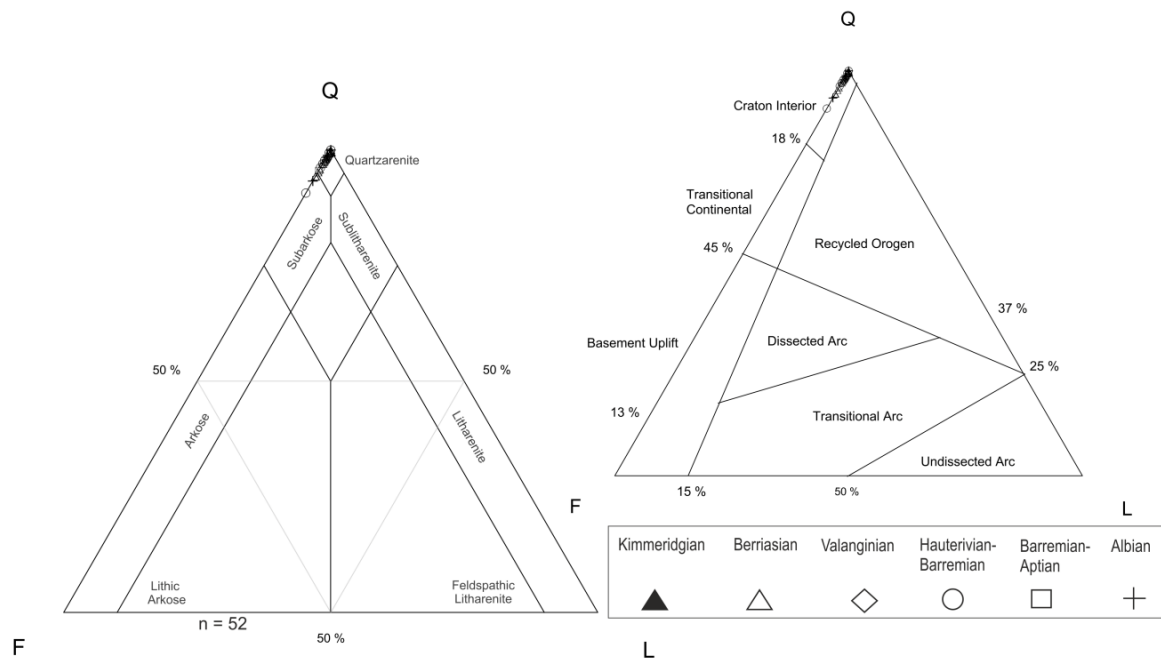


Fig. 17: Petrographic classification, left: mainly quartzarenites and subarkoses (McBride, 1963); right: sediment source is represented by an interior craton (Dickinson et al., 1983).

Grain size was analysed from Berriasian sandstones of the well Anklam 1. In addition, data from the grain size reports of the wells Darßert Ort 1, Werle 7 and Garz 1 were used (Fig. 18). All samples are dominated by fine-grained sand, while the samples of well Darßer Ort tend to be more silt-dominated than samples from well Werle 7, which tend to be more medium-grained sand. Well Anklam 1 revealed fine-grained sandstones to siltstones (Fig. 18).

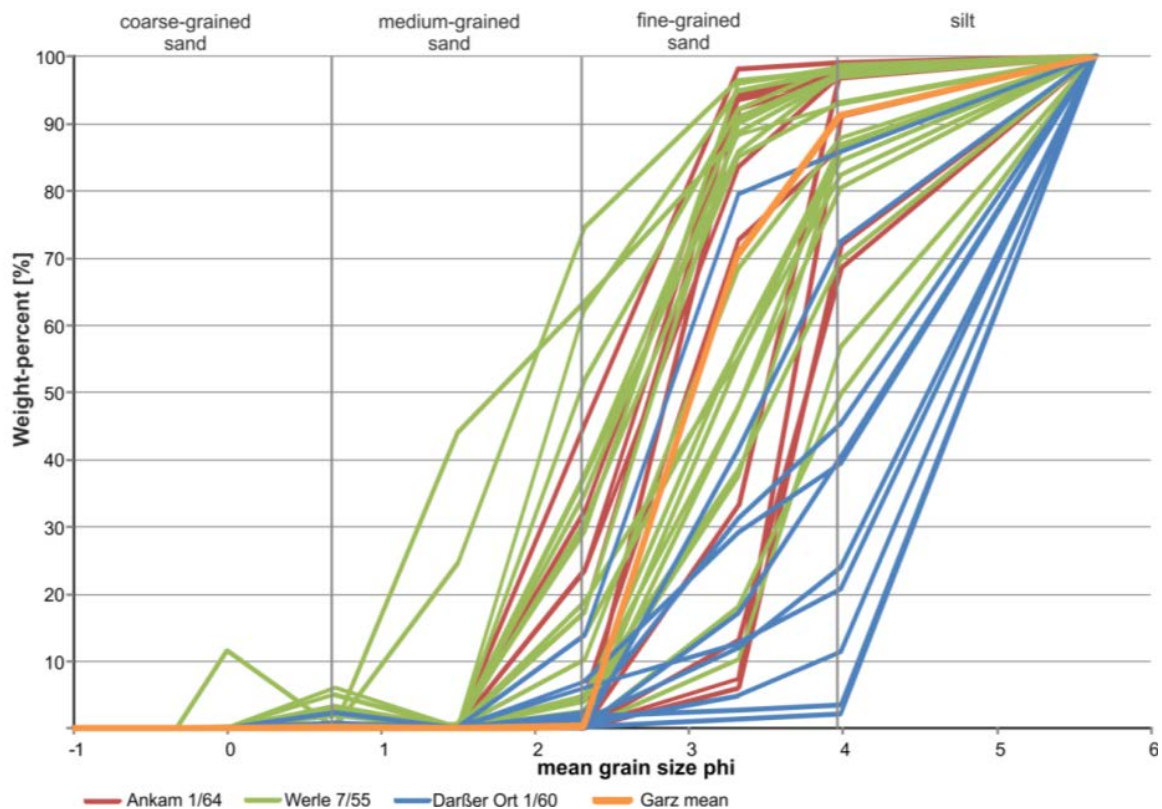


Fig. 18: Mean grain size of Berriasian samples taken from four wells from NE-Germany. Data of well Werle 7 according to Ludwig (1956); Darßer Ort 1 according to Haupt and Heppner (1962); Garz 1 according to Rudolph (1962), Anklam 1 according to results from this study.

### 6.1.1 Upper Jurassic - Kimmeridgian

Well Garz 1a provides biogenic calcareous, partly glauconitic, greenish-grey quartzose sandstone with up to 25 % detrital glauconite grains and up to 2.6 % shell fragments (Fig. 19, no. 3, 4). Heavy minerals like disthene occur in grain sizes up to 100  $\mu\text{m}$  (Fig. 19, no. 2). Authigenic components are pyrite, carbonate cement (19 %), such as rhombohedral siderites (15 %) and iron oxides. Kimmeridgian quartzarenites provide muddy silt- and fine-grained sandstones with a clayey matrix composed of subrounded to well-rounded quartz grains, less feldspar, occasional biogenic components and xylithic plant remains. Well Ückeritz 1 (Fig. 19, no. 1) shows a poorly sorted porous, light greyish biosparitic and calcareous fine- to medium-grained sandstone, composed of quartz, peloids, clayey matrix, plant remains and biogenic components like shell fragments with intergranular porosity up to 10 %. All mentioned components are bound by an irregular grain coating and, at grain contacts, developed drusy sparitic carbonate cement and locally poikilotopic calcite cement. The greyish-green, calcareous siltstone comprises fine-grained sand and shell fragment layers. According to core reports from well Teetz 1 and Zechlinerhütte 1, the Tithonian–Upper Kimmeridgian strata show dark greenish claystones and marlstones, interlayered by fossil detritus and thin oolitic layers. Tithonian evaporitic claystones are common in the eastern Altmark-Prignitz Basin known from reports of Werle 19.

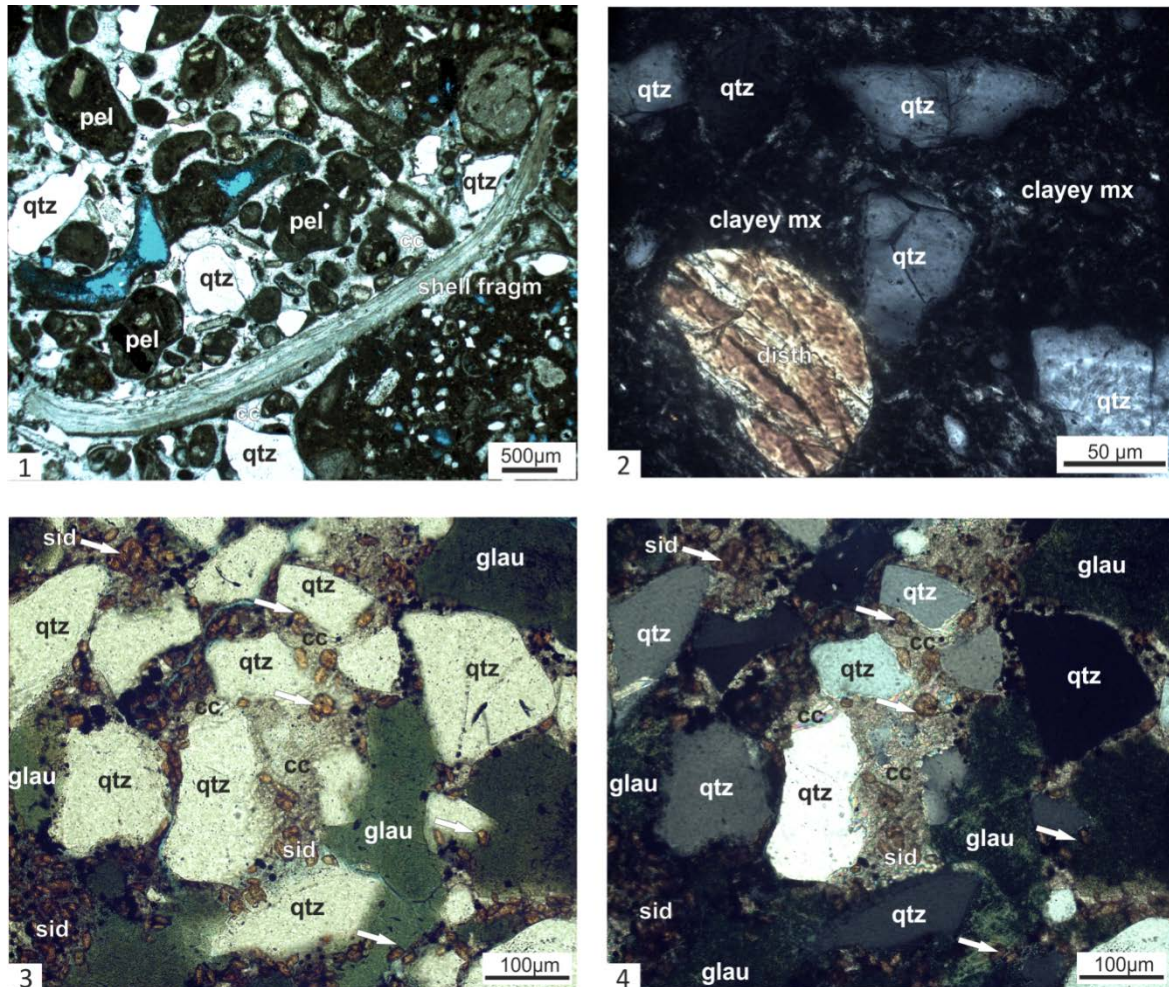


Fig. 19: Kimmeridgian sediments, samples from well Garz 1a and Uck 1a. 1: biosparitic calcareous sandstone with shell fragments (shell fragm) and peloids (pel); 2: quartzose (qtz) and disthene grains embedded in clayey matrix (mx); 3, 4: quartzose (qtz), glauconitic (glau) sandstone with calcite (cc) and siderite (sid) cements.

### 6.1.2 Upper Berriasian (Wealden-type) – Valanginian strata

In particular, Berriasian strata in Western Pomerania provide fine-grained sandstones (Fig. 20, Fig. 21), silt- and claystones with xylithic plant remains and heterolithic bedding. The detrital composition revealed high mature quartzarenites (see chapter 6.1) with nearly 98 % quartz, dominantly undulose and non-undulose mono-quartz, polyquartz and less chert. A maximum feldspar content of about 8 % is represented by plagioclase, alkali feldspar and microcline (Fig. 21, no. 1). Lithoclasts rarely make up less than 1 %. Furthermore, clayey matrix, muscovite and plant remaining up to 400 µm are common. Authigenic features (Fig. 21, no. 3) are remnants of pore-filling calcite cement (Fig. 21, no. 5), iron hydroxide grain coatings (Fig. 21, no. 3), pyrite framboids, muscovite, illite and chlorite (Fig. 21, 6). The amount of heavy minerals is approximately 1 % and is dominated by the ultrastable Zircon-Tourmaline-Rutile-group but also by intermediate fraction minerals like epidote, garnet and staurolite, as well as Rutile, epidote and zircon (Fig. 25). Silt- and claystones often show heterolithic bedding of millimetre thick laminae. In combination, xylithic plant remains of 100–300 µm size (Fig. 21, no. 2), and thin laminae or lenses of fine-grained sand, they can also

occur as single less compacted silt- or claystones (*Fig. 20, no. 8*). Pyrite, kaolinite, muscovite and iron oxides are common. The values of intergranular porosity range from 2.4 % in matrix-rich sandstones to 33 % in sandstones containing less matrix.

Berriasian samples from the Altmark-Prignitz Basin provide dominantly fine-grained, partly medium- to coarse-grained quartzarenites and subarcoses (*Fig. 22*), siltstones and claystones. Samples from well Neuruppin 2 and Zippelsförde 1 yield maximum 20 cm thick quartzitic sandstone layers. The detrital components are subrounded to well-rounded polyquartz, monoquartz and a few chert grains (*Fig. 22*). Further detrital components (1–3%) are potash feldspar, microcline, plagioclase, as well as small amounts of magmatic and metamorphic perthitic feldspar lithoclasts (<1%), as documented in the wells Neuruppin 2, Zippelsförde 1 and Teetz 1. The less compacted sandstones provide porosity values ranging from 26 %–30 % (*Fig. 24, no. 6*). The metamorphic heavy mineral assemblage drilled in wells Teetz 1 and Zippelsförde 1 consists of staurolite (sieve-structured) and disthene (*Fig. 22, no. 5*) in the same grain size as the other detrital grains. Furthermore, epidote, zircon, rutile, disthene, tourmaline and garnet are common. Authigenic calcite cement, as drilled in well Neuruppin 2, occasionally appears as blocky pore-filling cement (*Fig. 22, no. 3, 4*), remnants of such or calcite remains in the open pore volume and pore throats (*Fig. 22, no. 3, 4*) which can cause decreased intergranular porosities up to 5.4 %. The quartzitic layers provide chalcedony cements which occur as (I) chalcedonic overlays or fibrous fringe of equal thickness (*Fig. 22, no. 1, 2, 5, 6*) and (II) pore-filling spherulitic fan-forming chalcedony (*Fig. 22, no. 1, 2*). Siltstones are composed of nearly the same detrital composition, with lenticular bedded or interbedded layers with clayey matrix and staurolite or disthene in detrital grain size. Berriasian claystones are mostly iron oxide-bearing and often provide sideritic rhombohedral embedded in a calcitic-clayey matrix. Additionally, layers of interbedded quartzose silt grains are common. Well Gorlosen 12 drilled dark-grey, silty and dolomitic or calcareous claystones and marlstones with intercalated fine-grained sandstone layers and iron-rich nodules. Light grey brownish fine-grained sandstones contain thin coal layers and xylithic plant remains and iron-rich nodules occur occasionally (Hübner and Rasch, 1971). An intercalation of fossil-rich marl- and limestones and clayey fine-grained, partly glauconitic and non-calcareous sandstones was drilled by well Sanne 1. The fine-grained sandstones provide heterolithic bedding, xylithic plant remains, fossil-rich layers, clayey parts provide slicken sides. Especially in the Wealden 1 dated part, calcareous fine-grained sandstones layers are common (Ross, 1964). Well Eldena 1 drilled an intercalation of claystones and fine-grained sandstones (Hoth et al., 1993).

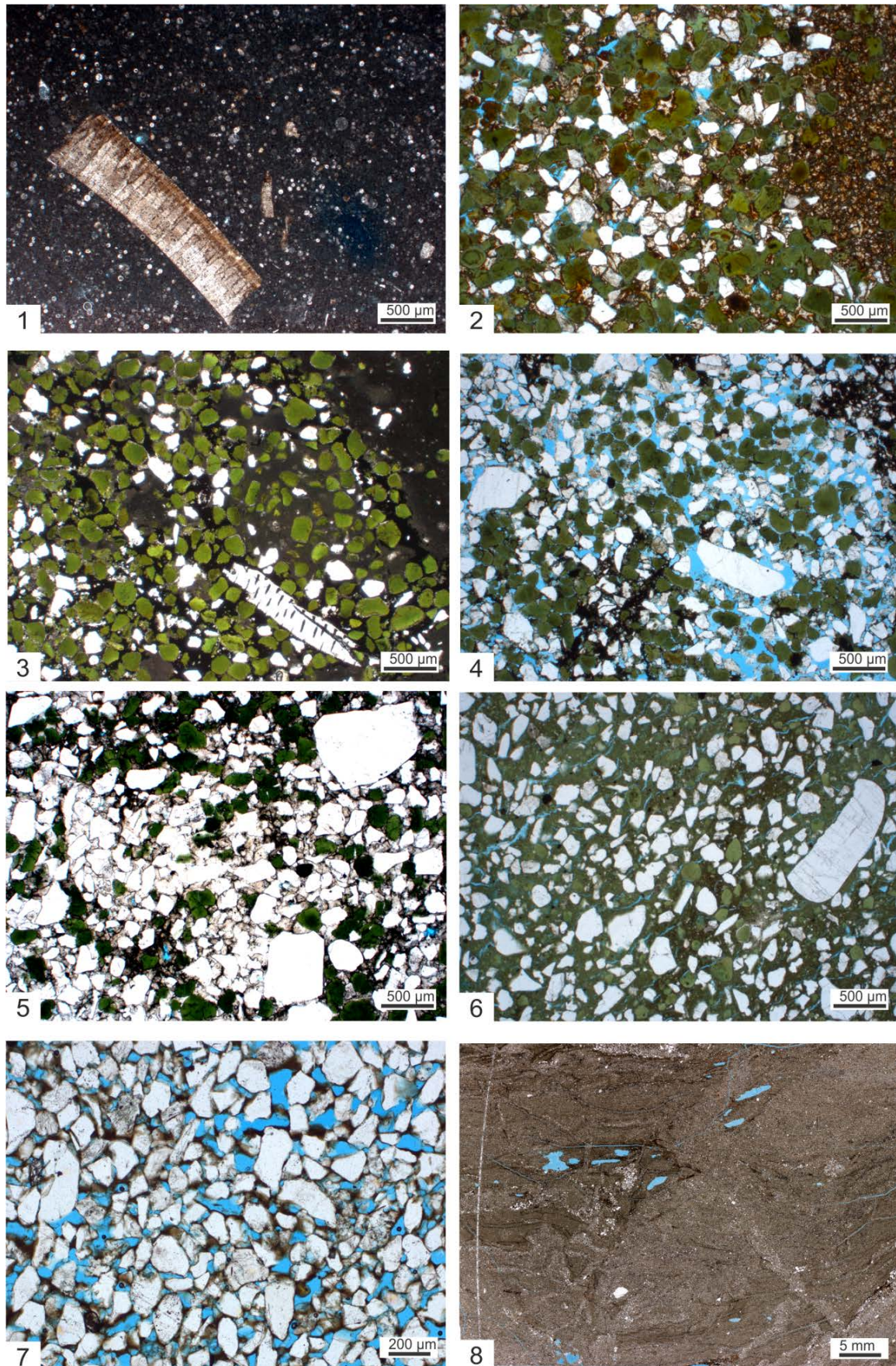


Fig. 20: Lower Cretaceous deposits from the northeastern NGB, samples from well Darßer Ort 1 under transmitted light. 1: Cenomanian limestone; 2: Albian glauconitic calcareous sandstone; 3: Aptian glauconitic sandstone; 4: Barremian-Aptian glauconitic sandstone; 5: Hauterivian-Barremian glauconitic sandstone; 6: Upper Hauterivian greensandstone; 7: Berriasian (Wealden-type) sandstone; 8: Berriasian silty claystone.

Valanginian strata of the Altmark-Prignitz Basin comprise quartzarenitic, calcareous and fine-grained sandstones (Diener, 1968; own results) consisting of felspar minerals like microcline, plagioclase, alkaline feldspar, perthitic feldspar as well as biogenic components, shell fragments, mica, muscovite, and glaucony grains. The poorly sorted detrital components are often embedded in a clayey matrix, providing decreased values of up to 5 % intergranular porosity. Silty claystones and iron-rich claystones often show siderite-rhombohedral structures. The heavy mineral assemblage comprises zircon, tourmaline, staurolite with sieve structures, and disthene. Authigenic components are a glauconitic-clayey matrix, calcite cement and thin chalcedony rims. Furthermore, carbonatic claystones with fine laminae of fine-grained sandstones composed of subrounded quartz-grains are common. Well Gorlosen 12 revealed fine- to coarse-grained dark grey calcareous or dolomitic sandstones and siltstones, containing pyrite, carboniferous layers and lenticules (Hübner and Rasch, 1971). Well Sanne 1 shows glauconite-rich grey-greenish limestones and marlstones, containing layers of shell fragments. Interlayered by claystones and marly fine-grained sandstones, which are mica and glauconite-bearing. These bioturbated, calcareous fine-grained sandstones contain thin fine-gravel layers and iron oolites (Ross, 1964). Well Eldena drilled sandstones interlayered by claystones and calcareous sandstones (Hoth et al., 1993).

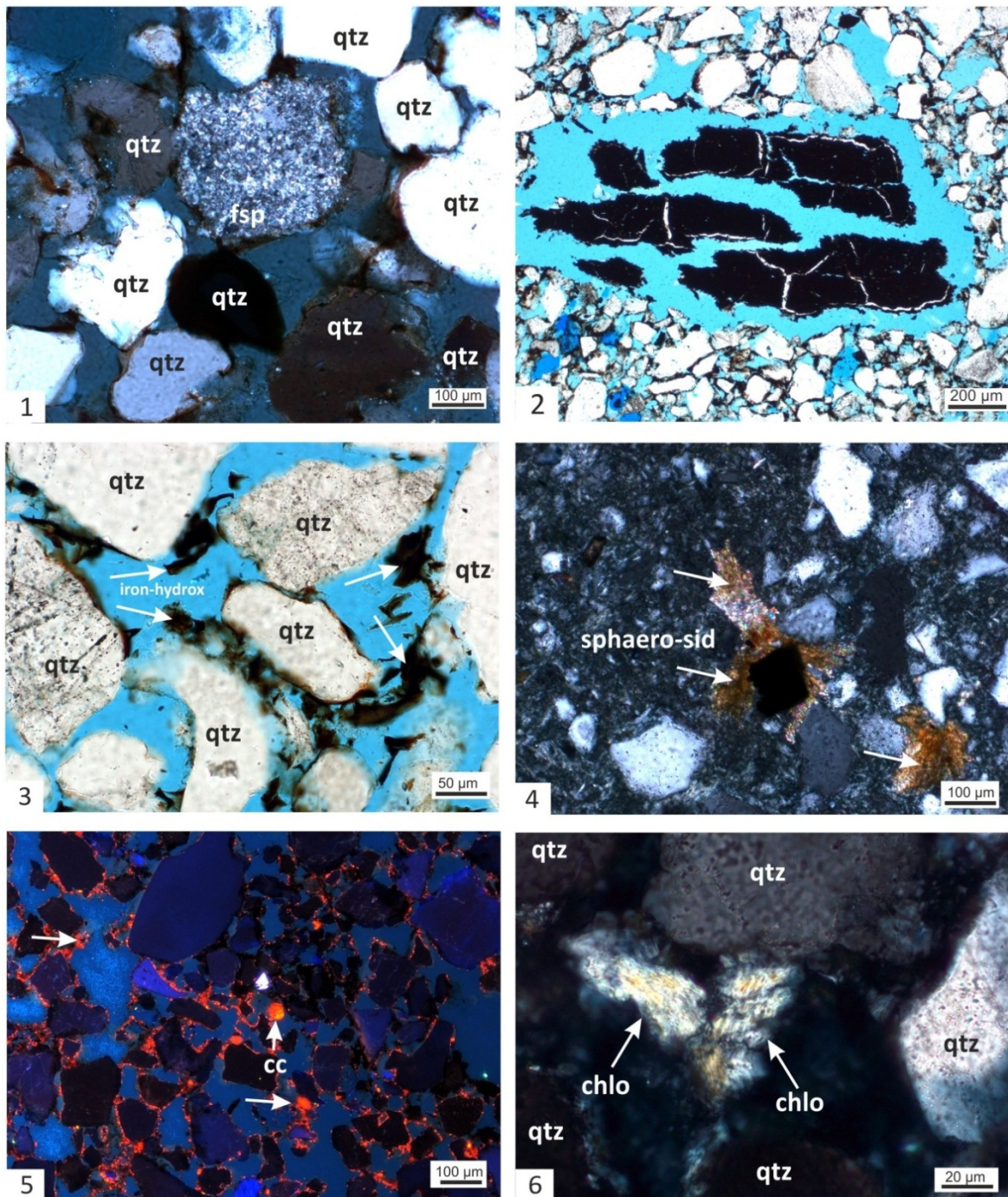


Fig. 21: Berriasian fine-grained sandstones from well Darßer Ort1 and Garz 1/a. 1-3 show the detrital composition of the quartzarenites under crossed polars (1) and transmitted light (2, 3). 4-6 show authigenic components under crossed polars (4, 6) and cathodoluminescence (5) show remains of early carbonate calcite cementation, sampled from well Ückeritz 1.



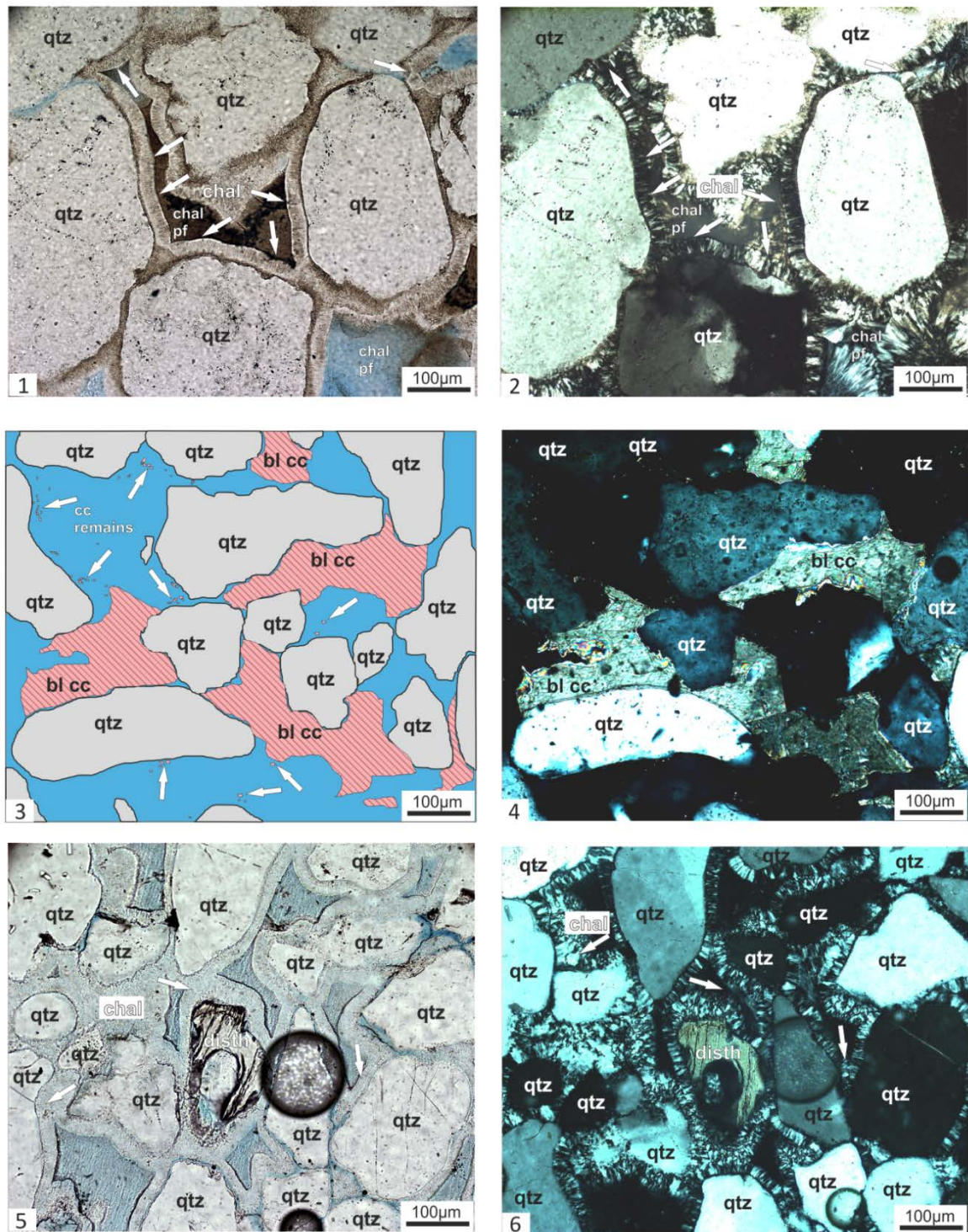


Fig. 22: Berriasian sandstones from well Neuruppin 2/87 show quartzarenites with chalcedonic overlays or fibrous fringe and pore-filling spherulitic fan-forming chalcedony 1, 5: under transmitted light, 2, 6: under crossed polars. Remnants of blocky calcite cement are shown in 4 and 5: under crossed polars. 5, 6: detrital quartz and disthene.

### 6.1.3 Hauterivian

The Hauterivian succession in Western Pomerania is represented by light and dark grey to greenish grey fine-grained clayey, bioturbated sandstones, as drilled in well Darßer Ort 1 (Fig. 23). These homogenous, mottled, partly glauconitic and calcareous sandstones yield

shell and belemnite fragments as well as pyrite nodules. Detrital components of the highly mature quartzarenites are subangular undulose and non-undulose mono-quartz, polycrystalline quartz, less well-rounded feldspars like microcline, as well as plagioclase and orthoclase grains. Plant remains and well-rounded glauconite grains embedded in a pore-filling clayey matrix are common (*Fig. 23, no. 1, 2*) with intergranular porosity values up to 2.2 %. Moreover, samples from well Darßer Ort 1 provide a glauconitic-clayey green matrix. The less consolidated, moderately to poorly sorted fine-grained greensandstones and siltstones yield authigenic components, which indicate different phases of cementation: (I) early blocky calcite cementation (*Fig. 23, no. 6*), (II) a rusty appearing fibrous dolomite-ankerite-cement (*Fig. 23, no. 6*) and (III) a brown-reddish rhombohedral siderite cement within the pore center (*Fig. 23, no. 6*).

Core material from well Teetz 1, dated to the Hauterivian without biostratigraphic evidence, yield greyish-white quartzose fine-grained sandstones with less than 1 % feldspar, shell fragments and intergranular porosity values up to 26 %, interbedded with thin clayey laminae. Between the sandstone stacks, silty clayey layers with up to 5 m thickness are interbedded. Well Zippelsförde 1 yields weakly silty and consolidated well-sorted fine-grained sandstones, showing xylithic plant remains, rootlets and weak bioturbation. Core material from well Zechlinerhütte 1 yield light grey weakly consolidated, bioturbated, massive to low angle stratified fine-grained sandstones. Xylithic plant remains and thin silty and clayey layers are interbedded. Well Gorlosen 12 drilled silty marlstones in the Lower Hauterivian, whereas the Upper Hauterivian provides clayey marlstones, interlayered by glauconite-rich fine-grained sandstone and silty layers, which yield pyrite (Hübner, 1971). Well Sanne 1 drilled upper Hauterivian organic-rich fine-grained dark-grey and greenish glauconite-rich less compacted sandstones, partly calcareous cemented. Interlayering marlstone layers and ooids are common (Ross, 1964). Well Eldena 1 drilled a basal calcareous sandstone superimposed by glauconitic and sandy claystone (Hoth et al., 1993). Authigenic components are a pore-filling calcite cement and a dolomite/ankerite cement.

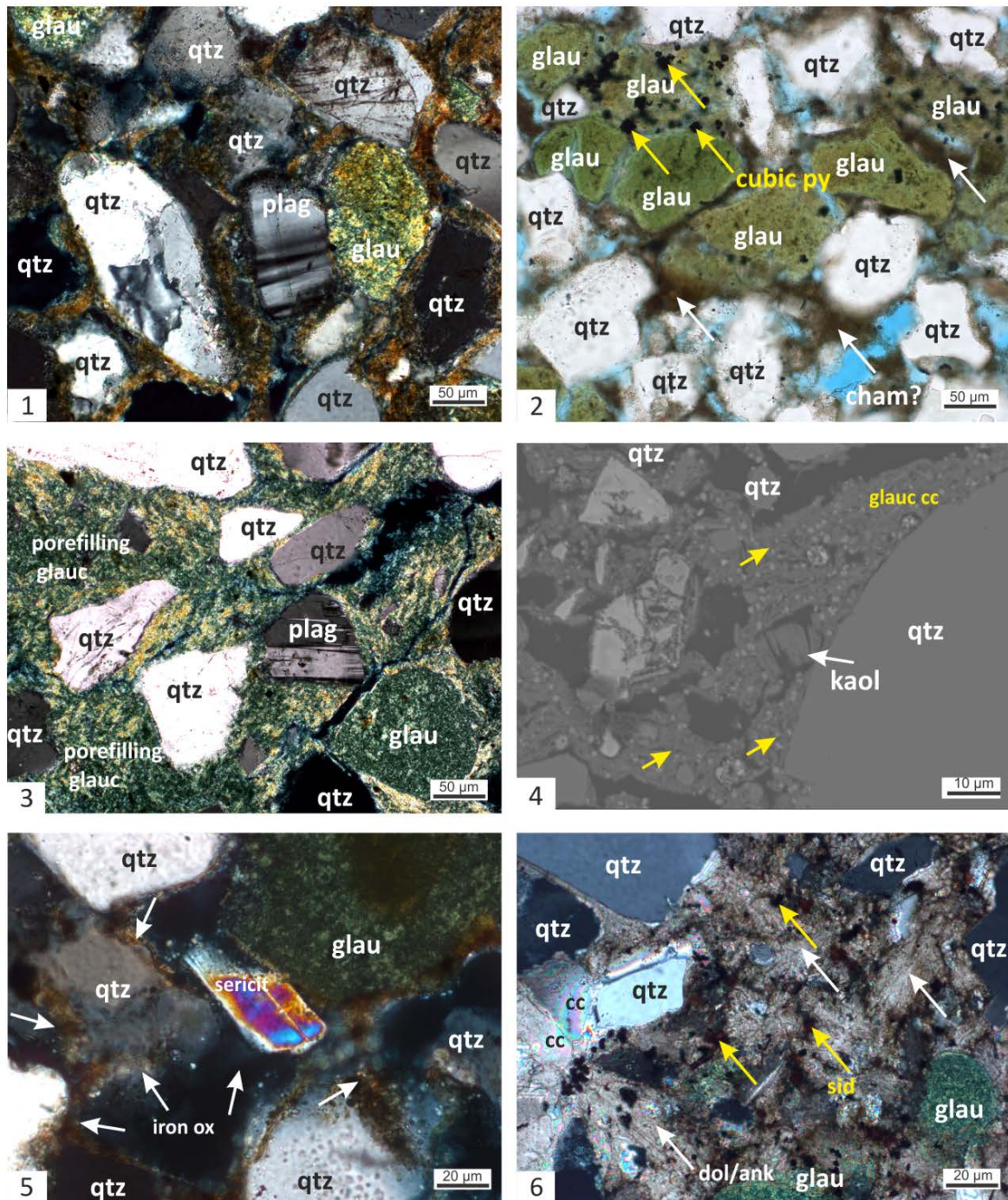


Fig. 23: 1: well DaOt 1: Hauterivian calcareous and glauconitic sandstone (crossed polars) show iron oxide cutans; 2: well; 3: well DaOt 1: Hauterivian greensandstones show glauconite grains and glauconitic matrix (transmitted light), 4: well DaOt 1: backscatter electron image, 5: well Uck 1: Hauterivian quartzose sandstone (crossed polars) show authigenic sericite, iron oxide cutans, 6: well DaOt1: Hauterivian calcareous greensandstone (crossed polars), authigenic (I) calcitic, (II) dolomite/ankerite and (III) rhombohedral siderite cement phase.

#### **6.1.4 Barremian**

Like Hauterivian sandstones, less consolidated Barremian sediments in Western Pomerania revealed greenish to dark grey organic-rich, fine-grained, calcareous and glauconitic sandstones in the Darß area. Detrital components are subrounded undulose and non-undulose mono-quartz, polycrystalline quartz, less subrounded feldspars like microcline and plagioclase, glauconite, biotite and less than 1 % muscovite. Pyrite nodules and shell fragments of bivalves are common. The moderately to poorly sorted fine-grained sandstones with intergranular porosity values of less than 1 % show authigenic cement, which precipitates in two phases: (I) early-formed calcite cement and a (II) dolomite/ankerite phase. Barremian strata, drilled in well Teetz 1 (*Fig. 24*), provide quartzose (97–98%) fine-grained to locally medium and coarse-grained less consolidated sandstones. The well to subrounded grains are moderately sorted, and quartzose grains often appear in a corrosive shape. Other detrital components are small amounts of feldspar minerals such as plagioclase, alkali feldspar, microcline and mica. Some samples yield remnants of glauconite grains. Furthermore, small amounts of volcanic and metamorphic lithoclasts were found (*Fig. 24, no. 1, 2*). Authigenic features are remnants of a former pore-filling carbonate cement, which is witnessed by floating grains and high intergranular porosity values of up to 28 % (*Fig. 24, no. 3*). Common heavy minerals are disthene and staurolite in detrital grain size (*Fig. 24, no. 3, 4*), epidote, zircon, staurolite disthene and garnet (*Fig. 24, no. 6*). Dark-grey, silty and partly mica-rich sandy claystones and marlstones, with intercalated partly calcareous cemented layers were drilled by the wells Gorlosen 12 and Eldena 1 in the Altmark-Prignitz Basin (Hübner and Rasch, 1971; Hoth et al., 1993).

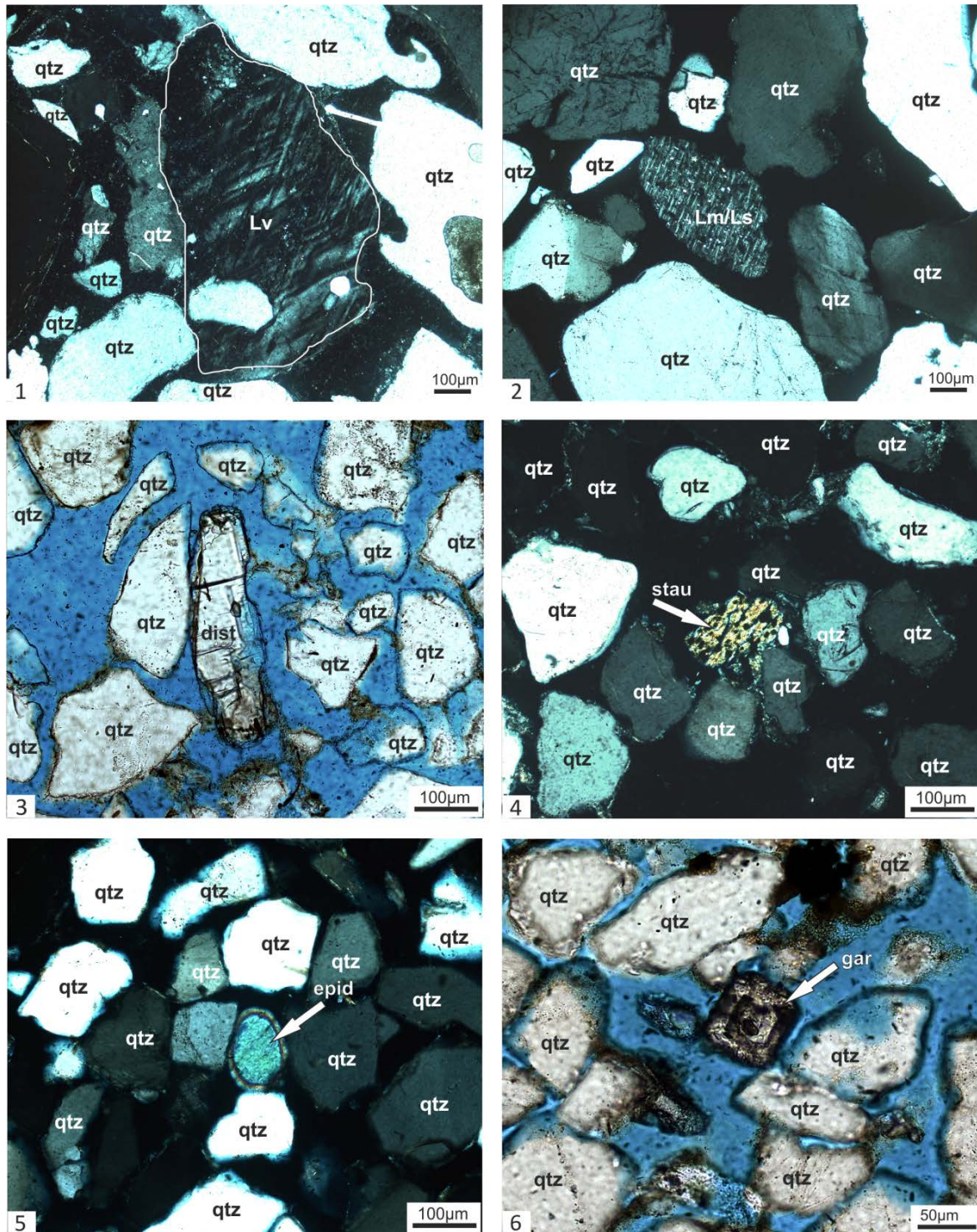


Fig. 24: Barremian (1-4) and Berriasian (5, 6) sandstones from well Teetz 1. 1, 2: quartzose sandstones under crossed polars (XP) with lithic fragments. 3: quartzose sandstone with high intergranular porosity values and a disthene grain of 250 µm size under transmitted light (TL). 4: quartzose sandstone and staurolite grain with sieve structure under XP. 5: quartzose sandstone and epidote grain under XP. 6: quartzose sandstone and garnet grain under TL.

### 6.1.5 Aptian – Lower Abian

In the northeastern part of the North German Basin, the basal, moderately to poorly sorted chalky fine-grained, glauconitic and clayey, calcareous sandstones comprise a high mature

detrital composition of subrounded to well-rounded mono- and poly-quartz, round glauconite grains and biogenic components like foraminifers and shale fragments (*Fig. 20, no. 3*). The detrital components are bounded by authigenic cement, like sparitic calcite and siderite-ankerite cement or a clayey or glauconitic matrix (*Fig. 20, no. 3, 4*). Opaque iron hydroxide phases like pyrite are abundant. Distal Aptian deposits are represented by greenish-grey to black calcareous silt- and claystones (Mutterlose and Bornemann, 2000). As reconstructed from documents of the well Darßer Ort 1, the hanging part of the Aptian strata is characterised by dark grey to greenish-grey, sandy, calcareous and glauconitic siltstones, including a 4 m thick blackish clay layer, which kept not preserved in well core material.

Lower Aptian claystones in the Altmark-Prignitz Basin, drilled by well Gorlosen 12, appear dark grey and partly silty with calcareous layers (Hübner and Rasch, 1971). According to Hoth et al. (1993), well Eldena 1 drilled claystones and marlstones, while the upper Aptian dated strata appear as silty, dark greyish-green marlstones. In the northern Altmark and Westprignitz area, the transgressive Aptian successions start with a c. 1 m thick middle- to coarse-grained calcareous and glauconitic sandstone. The overlying strata show a fining upward trend from sandy claystones to claystones.

Basal parts of the Albian were drilled in well Sanne 1 by fine-grained black-greenish sandstones, which yield fine-gravel pebbles and iron oxide nodules, followed by clayey, fossil-rich marlstones (Ross, 1964). In northeastern Germany, a maximum 5 m thick sandy and glauconitic sandstone horizon marks the transition to the Lower Albian. Wells Gorlosen 12 and Eldena 1 drilled Lower Albian dark-greyish, calcareous claystones and Middle to Upper Albian dark grey marlstones (Hoth et al. 1993).

#### **6.1.6 Middle – Upper Albian**

The moderately sorted, glauconite-rich siltstones and fine-grained sandstones of Middle Albian age in northeastern Germany reveal a detrital composition of undulose and non-undulose mono-quartz, polycrystalline quartz (17 %), glauconite (48 %), microcline, plagioclase (<1 %) and opaque minerals like pyrite and magnetite. Authigenic phases like ankerite-dolomite and siderite precipitated as pore-filling and rhombic cement (32 %, *Fig. 20, no. 2*). The reddish Upper Albian clayey marlstones are composed of dominantly carbonate mud with detrital mono- and poly-quartz grains as well as well-rounded glauconite grains. The basal transgressive marlstone shows layers of fine-grained sandstone and well-rounded glauconite grains. Shell fragments from *Inoceramus* and *Terebratula*, fish- and belemnite remains from the taxa *Neohibolites* are common.

Core material from the Altmark-Prignitz Basin, drilled in well Zippelsförde show Upper Albian homogeneous limestones, which are weakly silty and clayey layered. Bioclastic features like Echinodermata spicules are common. According to well reports from well Sanne 1 and Gorlosen 12, Upper Albian strata provides clayey and calcareous greyish-green marlstones, containing occasionally thin silt and clay laminae, fossil remains (Ross, 1964; Hübner and Rasch, 1971)

## **6.2 Heavy minerals**

### **6.2.1 Heavy mineral assemblage**

Detailed information on the heavy mineral assemblage of Wealden-type sandstones is given in samples of well Anklam 1/64 (*Fig. 25*) from the grain size fraction 0.063–0.35 mm yield 26–68 % zircon, 5–25 % tourmaline, 10–18 % rutile, 1–10 % epidote, 10–15 % disthene, 5–12 % staurolite, 1–11 % garnet, 1–10 % apatite, 1–5 % brookite and less < 3 % sillimanite. Furthermore, the samples contain pyroxene and amphibole, which were excluded from the statistics. The spectrum of silt- and fine-grained Berriasian to Valanginian sandstones in well Anklam 1/64 is characterised by a ZTR-index of nearly 70 %. High ZTR indices implicate high sediment maturity. Relating to shape and appearance, zircon grains are present as subrounded to well-rounded transparent grains under transmitted light (TL) and appear mostly with growth zoning under polarised light (PL). Typical interference colours in zircon grains range within 3<sup>rd</sup> order (Michel Levy colour scale). Triangular-shaped rounded tourmaline grains appear under TL greenish blue to greenish brown and under PL with brownish-green interference colours. Subrounded brownish-red rutile grains are characterised by cleavage and high relief. Angular, rounded epidote grains with cleavage appear transparent under TL and in 2<sup>nd</sup> order interference colours (Michel Levy colour scale) under PL. Transparent disthene grains appear in an elongated shape and cleavage under TL. A characteristic grey to brownish-orange interference colour represents the appearance under PL. The characteristic sieve-structured staurolite grains appear in a pale yellowish colour under TL and from light to dark grey under PL. Sieve-structured staurolite is filled with quartz. Well-rounded garnet grains show pale rose colours under TL and dark grey colours under PL. Cubic apatite grains appear under TL and PL in greyish interference colours. Amphibole yields a typical high relief and 90°-cleavage in the brownish to greenish-coloured grains under TL and PL. Similar coloured pyroxene grains with 120° and 60°-cleavage also appear with a high relief.

Samples from the Altmark-Prignitz Basin show larger disthene (*Fig. 22, no. 5, 6*) and staurolite (*Fig. 24, no. 3, 4*) grains in a detrital grain-size of ~ 125 µm within Berriasian to Barremian samples.



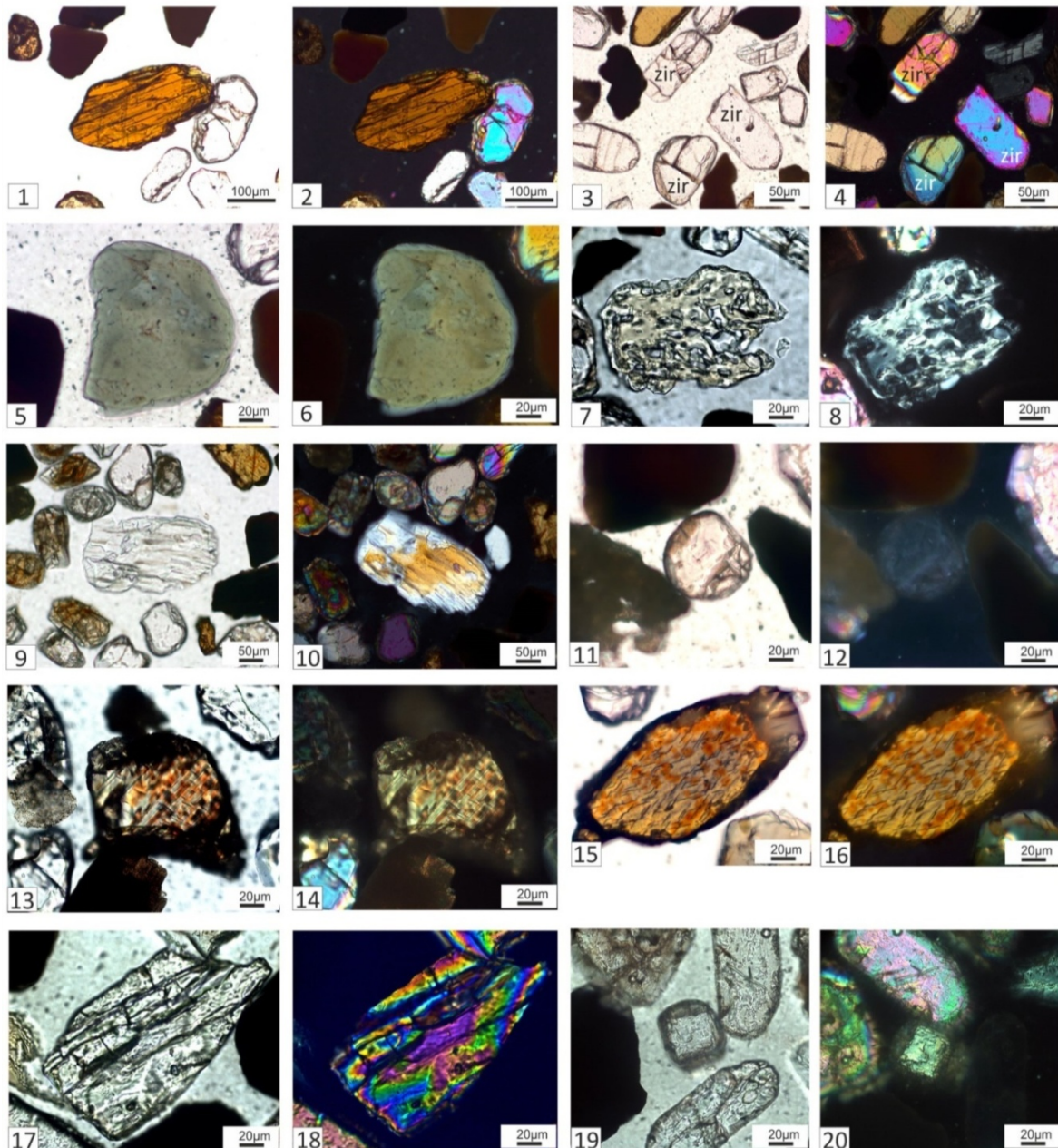


Fig. 25: Heavy mineral assemblage of well Anklam 1/64 1: rounded rutile grain under transmitted light (TL); brownish with cleavage and slight pleochroism, 2: rutile under polarised light (PL), 3: rounded zircon grains under TL, with cleavage (left) and inclusions (right), 4: zircon under PL; with typical 3rd-order interference colours (left) and zonation (right), 5: tourmaline under TL; typical green, well rounded grain shows pleochroism to brownish-green, 6: tourmaline under PL; 7: staurolite under TL; transparent to yellowish rounded grain with high relief show pleochroism and typical sieve-structure filled with quartz, 8: staurolite under TL; light to dark greyish pleochroism, 9: disthene-grain under TL; angular grains show cleavage and intermediate relief, 10: disthene under PL with pleochroitic greyish-white to orange-brown interference colours, 11: well-rounded garnet grain under TL, 12: isotropic garnet under PL, 13: pyroxene grain under TL shows high relief; brownish to green interference colours and 90°-cleavage, 14: pyroxene under PL, 15: amphibole grain under TL with brownish to green interference colours and 120°/60°- cleavage, 16: amphibole grain under PL, 17: angular epidote grain under TL; intermediate high relief with cleavage, 18: epidote grain under PL; typical 2nd-order interference colours, 19: apatite grain under NP with high relief, 20: apatite grain under PL with typical light to dark greyish interference colours.

### 6.2.2 Heavy mineral distribution

According to Dickinson et al. (1983), the origin of Lower Cretaceous deposits in the North German Basin based on generalised petrographic classifications (McBride, 1963) is from a Craton Interior. This is most likely the Fennoscandian High, as suggested by the analysis of heavy mineral assemblage and distribution of Berriasian to Valanginian-dated deposits from western Pomerania and the Prignitz Altmark Basin (Fig. 26). Differing from the other evaluated wells from this study, well Darßer Ort 1 show an epidote content of up to 40 % in average.

Compared to samples from the neighbouring Danish embayment (Larsen, 1966), the samples from the North German Basin show a similar heavy mineral assemblage consisting of the ultrastable magmatic and metamorphic minerals zircon, tourmaline, rutile, as well as epidote, disthene, staurolite, garnet and others (Fig. 26).

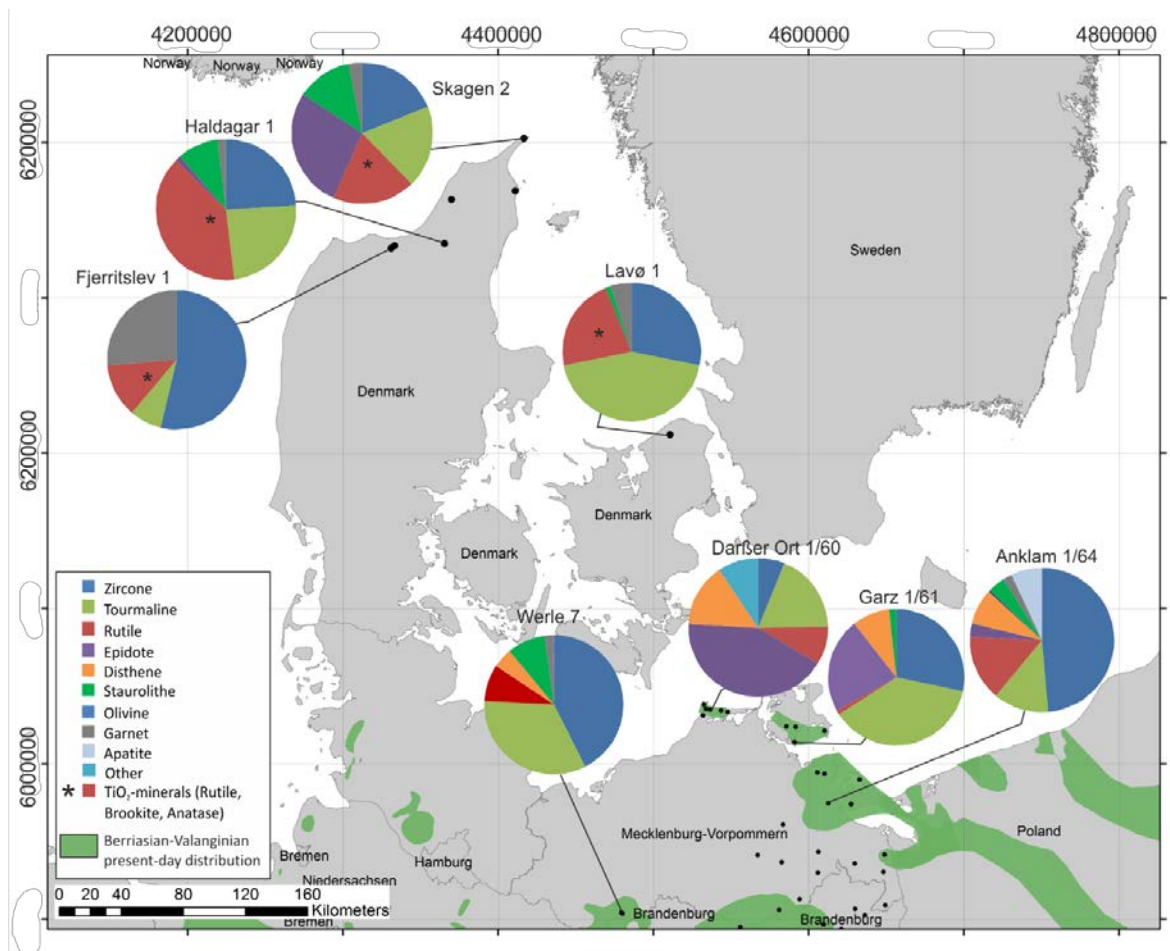


Fig. 26: Heavy mineral assemblage and distribution of Berriasian to Valanginian deposits in northeast North German Basin, northern Altmark-Prignitz Basin (Werle) and Denmark show assemblages of ultrastable heavy minerals transported from the Fennoscandian High. Heavy mineral data from wells Fjerritslev 1, Haldagar 1, Skagen 2, Lavø 1 according to Larsen (1966); Werle 7 according to Ludwig (1956); Darßer Ort 1 according to Haupt and Heppner (1962); Garz 1 according to Rudolph (1962), Anklam 1 according to results from this study.

## **6.3 Diagenesis and geochemical characterisation of Lower Cretaceous strata**

### **6.3.1 Upper Berriasian–lower Valanginian (Wealden-type) sandstones**

The highly mature Berriasian quartzarenite sandstones provide a high intergranular porosity of up to 33 %. The precipitation of cement is considered chemical compaction (Hesse and Gaupp, 2021), whereas mechanical compaction is caused by subsidence. Different diagenesis types from different depositional regimes, such as floodplain, deltaic/shallow-marine and fully marine, could be figured out. Due to the focus of this work, only a general overview is given within this study.

The grain fabric of these Wealden-type sandstones was stabilised by an early-diagenetic, carbonate cementation (*Fig. 27*) suggested by the carbonate residues surrounding the detrital grains of nonmatrix-rich sandstones (*Fig. 21, no. 5*), floating grains (*Fig. 21, No. 3*) and the corroded and etched detrital grain margins (Tucker, 2011). Calcite or dolomite is commonly the first fabric-stabilising cement in grain-supported sandstones such as quartzarenites. The precipitation of CaCO<sub>3</sub> in the shallow subsurface may happen through the evaporation of vadose or near-surface, phreatic groundwater (Tucker, 2011). A late-diagenetic dissolution of the carbonate cement caused the present-day high secondary porosity.

In matrix-rich samples, a clayey and partly carbonatic matrix was a stabilising feature within the grainfabric. Samples providing a thin clayey grain coating caused by infiltration of clayey suspension load in fluvial environments, which hamper the formation of early carbonate cement (Hesse and Gaupp, 2021), show higher compaction characterised by point contact of the quartz grains. Early diagenetic iron oxide-rich clayey grain coatings or cutans are referred to as pedogenic processes in the vadose zone of terrestrial-dominated sediments (Hesse and Gaupp, 2021). Syntaxial euhedral quartz overgrowths are separated from the grain by a small dusty rim, which may reflect early iron precipitation. However, quartz overgrowths are remnants from the former source area and rarely occur on several detrital monoquartz grains.

Eodiagenetic-formed pyrite (*Fig. 27*) occurs commonly in a cubic and a framboidal shape and attests the deposition under dysaerobic to anoxic conditions and the preservation of organic matter (Ulmer-Scholle et al., 2015) under the influence of bacterial activity. Sulphide comes from the bacterial reduction of sulphate, which is present in organic matter like plant debris (Tucker, 2011). The sphaerosiderite cement forms in reducing groundwaters and swampy paleosols (Tucker, 2011). Rarely and minor occurring authigenic clay minerals such as chlorite and kaolinite (dickite), dominantly present as booklets, form in specific areas in

the pore centre near dissolved feldspars, from partially dissolved detrital microcline feldspar (Tucker, 2011) or the clayey pore-filling matrix.

Rarely occurring chalcedony cement, sampled from quartzite layers in the wells Neuruppin 2 and Zippelsförde 1 (Fig. 22), occur as (I) chalcedonic overlays or fibrous fringe of equal thickness followed by a (II) pore-filling spherulitic fan-forming chalcedony. The first type fills primary or secondary pore space and appears as a ‘growth structure’ all over the quartzose grains. The following fan-forming spherulitic cement grows directly on the fibrous fringe. Both types of cement stabilised the grain fabric and caused a weak chemical (cement-induced) compaction, as shown by the point grain contacts. Chalcedony cement witness full marine ingressions by the precipitation from silica-saturated pore waters. Due to the existence of radiolarians, diatoms and siliceous sponges, which are composed of silica (Tucker, 2011), pore waters could be oversaturated with respect to silica. A late (telodiagenetic) evolution of porosity was caused by the dissolution of pore-filling cement.

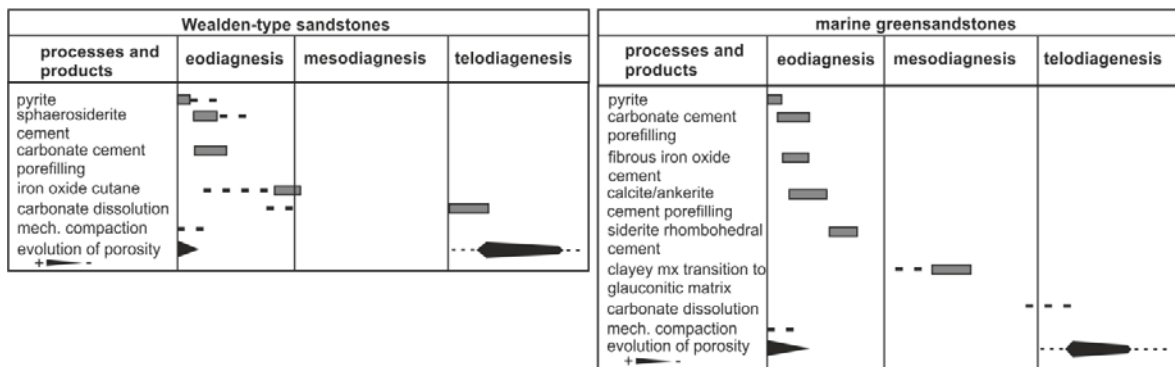


Fig. 27: preliminary paragenetic sequence of Lower Cretaceous sandstones in the North German Basin. Diagenetic features of middle to upper Lower Cretaceous Wealden-type Sandstones (left) and Hauterivian–Barremian marine greensandstones (right).

### 6.3.2 Upper Hauterivian–lower Barremian glauconitic sandstones

In shallow marine Hauterivian to Barremian shoreface greensandstones from northeastern Germany, glauconite is a common detrital component, indicating starved sedimentation and less terrigenous input (Hesse and Gaupp, 2021). The rounded glauconite grains within this succession occur as (I) homogenous fine-grained green or (II) zoned and altered by dark brownish-black oxide/hydroxide rims. The Formation of glauconite is related to oxic/suboxic conditions and the availability of  $Fe^{2+}$  from reduced iron-hydroxides and the formation in a shallow water depth < 500 m (Hesse and Gaupp, 2021).

Three eodiagenetic cement generations occur (Fig. 27): the (I) blocky calcite- and (II) dolomite/ankerite cement, as well as (III) a rhombohedral siderite cement. The calcite cement occurs as poikilotopic crystals, the ankerite cement appears in a rusty rhombic crystal shape. The third authigenic cement generation is a rhombohedral siderite cement, rarely accompanied by finely crystallised chamosite, precipitated during eodiagenesis in a

shallow marine environment from marine pore waters. Authigenic pyrite commonly occurs in a cubic and a framboid shape and attests the deposition under dysaerobic to anoxic conditions and is of an early diagenetic origin. Generally, compaction occurred in less cemented sandstones or where pore fluids caused cement dissolution. Samples from well Darßer Ort 1 show a greenish glauconitic matrix *Fig. 23* (no. 3 and 4), which was transformed from an early clayey matrix during mesodiagenesis. In the samples from the Altmark-Prignitz Basin, a telodiagenetic dissolution of early carbonate cement caused the high present-day secondary sandstone porosity.

#### **6.4 Geochemical characterisation of Lower Cretaceous sediments**

In cored well Ückeritz 1 (*Fig. 28*), the Jurassic-Lower Cretaceous transition from the Kimmeridgian to the lowermost Berriasian (Wealden-type) sediments is characterised by increasing  $\text{Al}_2\text{O}_3$ -,  $\text{K}_2\text{O}$ -,  $\text{Na}_2\text{O}_3$ -,  $\text{TiO}_2$ - and  $\text{MgO}$ - contents at a depth of 276 m. The interlayering Wealden-type strata change from fine-grained sandy parts, characterised by decreasing  $\text{Al}_2\text{O}_3$ -,  $\text{K}_2\text{O}$ -,  $\text{Na}_2\text{O}_3$ -,  $\text{TiO}_2$ - and  $\text{MgO}$ - contents and increasing  $\text{SiO}_2$ -contents (43%–98%), to clayey and silty parts, with contrary trends. Clayey parts are reaching maximum values at about 220 m and 240 m depth. Especially  $\text{Al}_2\text{O}_3$  values are increasing from <5 % up to 18.1 % (depth 220 m),  $\text{MgO}$  values from 0.4 to 1.6 % (depth 220 m) and  $\text{Na}_2\text{O}_3$  values increase from 0.02–0.6 % (depth 220 m). Furthermore, the clayey organic-rich tops of the paleo-histosols are characterised by increasing C-org-values varying from 5% to 9% and S-values (0.02–2.75 %). According to higher C-org values,  $\text{Fe}_2\text{O}_3$  shows a significant rise from >0.4 to 15.7 % (depth 224 m), related to the precipitation of iron hydroxide grain coatings under reducing conditions. The transition from Wealden-type sediments to the Hauterivian is marked by increasing  $\text{Al}_2\text{O}_3$ -values (1.7 %–2.7 %) and  $\text{CaO}$ -values (0.49 %–1.15 %). Under constantly increasing marine influence,  $\text{SiO}_2$ -values are decreasing from 91.8 % to 57.6 % (depth 166 m), whereas  $\text{CaO}$  rises from 1.2 % to 15.8 % (depth 166 m) at the top of the Hauterivian. At the transition to Albian strata,  $\text{Al}_2\text{O}_3$ -,  $\text{K}_2\text{O}$ -,  $\text{Na}_2\text{O}_3$ -,  $\text{TiO}_2$ - and  $\text{MgO}$ - contents are increasing, whereas  $\text{SiO}_2$ -values decrease significantly from 88 % (depth 167 m) to 29.2 % (depth 165 m). The Albian-Cenomanian transition shows a remarkable decrease in  $\text{SiO}_2$ -values (6.2 %, depth 163.5 m) and an increasing  $\text{CaO}$ -content of >41.4 % (depth 164 m).

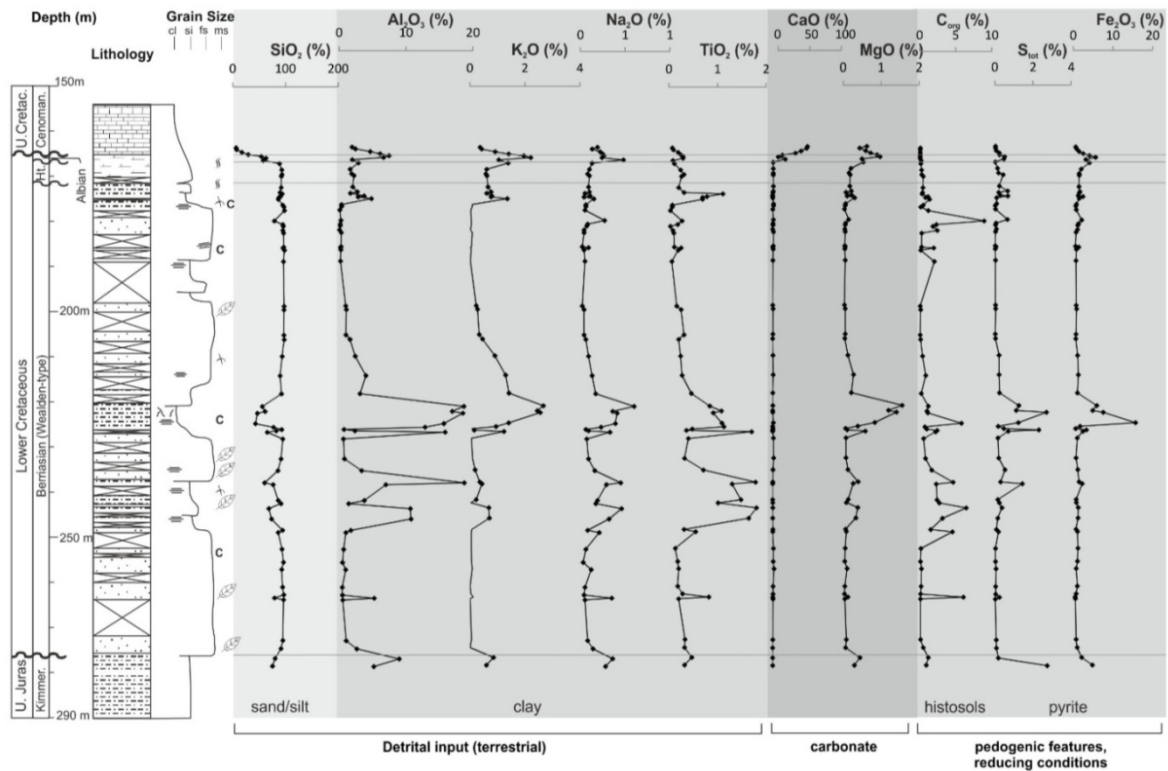


Fig. 28: Bulk rock geochemistry samples from well Ückeritz 1 show the characteristics of the terrestrial deltaic dominated Berriasian sand- and siltstones with clayey and organic-rich layers and histosols in contrast to the post-Berriasian calcareous sandstones, siltstones and limestones from a shallow marine environment.

## 6.5 Discussion

### 6.5.1 Heavy minerals

Samples for this study were evaluated from core sampling, unpublished well reports and the work of Larsen (1966). A compilation shown in Fig. 26 comprises the heavy mineral distribution of 8 cored wells from Berriasian–Valanginian sediments from Denmark and Northeast Germany. Concerning comparability, the heavy mineral assemblage consists of two grain size fractions: 0.063–0.1 mm and 0.1–0.2 mm, which can cause differences in the heavy mineral assemblage from transport selection. The heavy mineral distribution in Denmark represents an assemblage of the minerals zircon, tourmaline, rutile and garnet. Minerals like epidote, staurolite, disthene, anatase and brookite imply a metamorphic source area. The zircon-tourmaline-rutile-index (ZTR-index) depicts information about sediment maturity. Higher values are observed in modern sands derived from cratonic shields because of the extensive recycling of ancient sedimentary successions (Garzanti and Ando, 2007). Except for the northernmost well Skagen 2, the three danish wells Lavø-1, Haldagar-1 and Fjerritslev-1 constitutes a high ZTR-index of 40–80 % combined with 5–25 % garnet and 2–10 % staurolite. Well Skagen-2 comprises solely high epidote values of 25 %, which might be a result of the potential source area proximity of the Baltic Shield, which is also suggested by

petrographic classification after Dickinson et al. (1983). The epidote value is decreasing in the southern direction because of the relative instability related to transport selection. In comparison, the four north german wells also represent a high ZTR-index of 50–90 % combined with the minerals epidote, disthene, staurolite, garnet, apatite and sillimanite. The northernmost wells, Darßer Ort 1, Garz 1 and Anklam 1 represent the highest contents in epidote, disthene, staurolite and apatite, which suggest a higher content in material eroded from a metamorphic basement compared to samples from the other wells in western Pomerania. Again, well Werle 7 represents decreased contents of these minerals and the comparatively highest ZTR-index of 93 %.

According to Japsen et al. (2016), the southwestern Baltic shield experienced multiple major phases of uplift and subsidence during the Phanerozoic. The earliest Cretaceous, early Miocene and early Pliocene phases of uplift and exhumation and mid-Cretaceous inversion along the Sorgenfrei-Tornquist Zone could be documented. A sub-Cretaceous peneplain with hilly relief along the west and south coast of southern Sweden resulted from exhumation that began during the Middle Jurassic to the earliest Cretaceous and lasted until mid-Cretaceous transgression, correlating in time with regional cooling events identified from apatite fission track ages. This sub-Cretaceous relief was controlled by fluvial systems that eroded the basal plane of the relief towards sea level. Erosion of a 1–2 km thick cover above the Sub-Cretaceous hilly relief on the west and south coast of Sweden is estimated by Japsen et al. (2016).

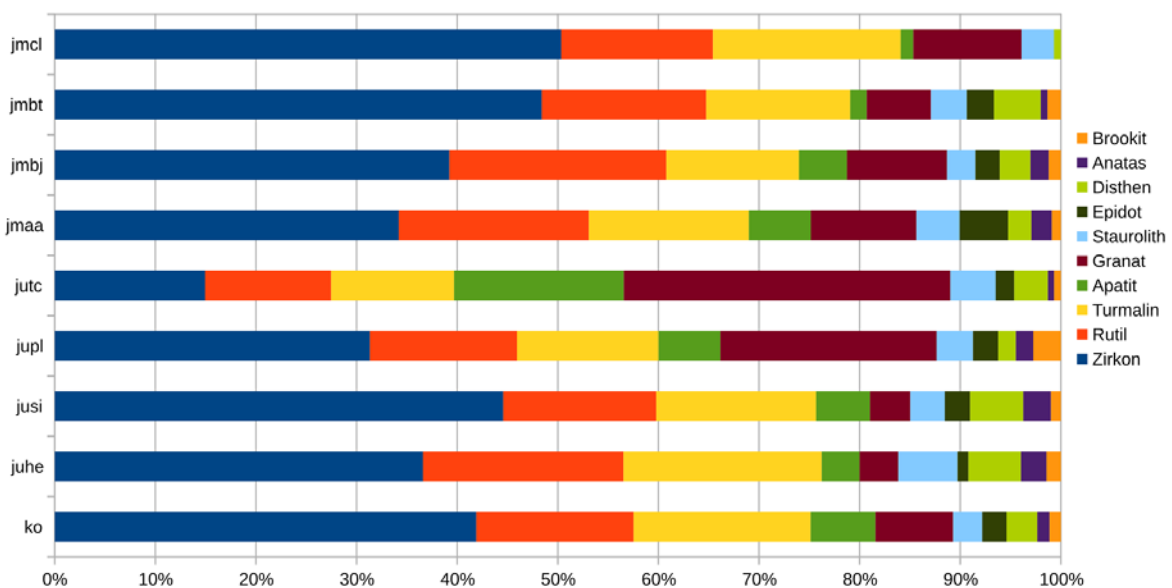


Fig. 29: Averaged heavy mineral assemblages from samples of northgerman wells from Upper Triassic to Middle Jurassic times (Franz et al, 2015). ko – Rhaetian, n=142; juhe – Hettangian, n=90; jusi – Sinemurian, n=145, jupl – Pliensbachian, n=120; jutc – Toarcian, n=149; jmaa – Aalenian, n=80; jmbj – Bajocian, n=41; jmbt – Bathonian, n=21; jmcl – Callovian, n=11; n<sub>total</sub> = 799.

High epidote-contents of up to 40 % in the wells Darßer Ort 1 and Garz 1 indicate an early Cretaceous erosion of metamorphic basement located in the source area on the southern Baltic Shield. Compared to Rhaetian–Callovian heavy mineral assemblages (Franz et al.

2015) from northern Germany (*Fig. 29*), such high epidote contents were not evaluated within 799 samples, which suggest an early Cretaceous uplift of a metamorphic basement region on the southern Baltic Shield. Mineral composition and transport selection point to the fact that the heavy mineral associations represent minerals from a magmatic and partly metamorphic source area of southern Sweden. This is supported by the blue and red luminescing Quartz grains from well Ückeritz. Blue luminescence of detrital quartz grains is caused by  $Ti^{2+}$ , indicating a magmatic origin, whereas red luminescence is caused by  $Al^{2+}$  and  $OH^-$ , indicating a metamorphic origin. The differences in the composition of the heavy mineral assemblages shown in *Fig. 26* could also be caused by transport from different terranes on the fennoscandian high. According to Olivarius and Nielsen (2016), different basement source terranes in southern Norway and southwestern Sweden were eroded during the Triassic, reflected in varying heavy mineral compositions and zircon ages.

### **6.5.2 Diagenesis**

Eodiagenetic pore-filling carbonate cement is indicated by the low contact strength, according to Fürchtbauer (1988), attested by mainly point contacts, occasionally floating detrital grains and high porosities up to 33 % in Berriasian to Albian sandstones. The early-stage carbonate cementation prevented the grain fabric from significant burial compaction. Caused by telodiagenetic dissolution, only thin residual carbonate cementation is visible in pore throats and surrounding grains in sandstone samples. Under a cathodoluminescence microscope, calcite shows an extensive bright orange luminescence, as shown in *Fig. 21 (no. 5)*. Dissolution-causing processes are changes in temperature, pressure and pore-fluid chemistry, which is associated with uplift and exhumation. By the dissolution of eo- to mesodiagenetic pore-filling cementations, these processes contribute to the development of secondary porosity. During the basin differentiation stage and the basin inversion stage (e.g. Jaritz, 1969; Nöldecke and Schwab, 1977; Ziegler, 1990), the Lower Cretaceous strata were uplifted to shallower depths in the North German Basin.

Mineral transformations observed within samples from e.g. the late Triassic Stuttgart Formation (Niegel and Franz, 2023) constrain the burial maximum to a temperature of at least 105°C, contrasting present-day fluid temperatures of 20–65°C. The reconstructed burial history of the well Wolgast 1/1A shows that Triassic–Quaternary successions, including Berriasian Wealden-type sandstones, witness repeated phases of uplift and erosion, which have resulted in regional and basin-scale unconformities, such as Base-Cretaceous Unconformity, the Base-Albian Unconformity and Base-Quaternary Unconformity (Niegel and Franz, 2023). For Lower Cretaceous samples from this study, subsidence and burial are assumed to Berriasian–Lower Albian times, interrupted by pre-Albian multiple uplifts.



Telogenetic exhumation and erosion combined to the dissolution of eodiagenetic carbonate cements is assumed to Late Cretaceous inversion and locally Paleozoic uplift.

Glauconitic greenish sandstones occur within the Upper Jurassic and Lower Cretaceous. Fine-grained and partly calcareous sandstone beds of Kimmeridgian, Upper Hauterivian, Barremian, Middle to Upper Aptian and Middle to Upper Albian contain detrital glauconite of up to 48 % and up to 38 % of a carbonatic, iron-rich and glauconitic matrix, (wells Darßer Ort 1, Garz 1 and Ückeritz 1). Glauconite could be formed from clayey smectite matrix and  $K^+$  ions from marine waters, forming iron-rich instable montmorillonite (Hesse and Gaupp, 2021).

According to Jeans et al. (2000), sand grade glauconite grains in the North Sea Basin of the Upper Jurassic and Lower Cretaceous age could be interpreted as secondary deposits. Strongly increased iron contents of 20.17 %  $Fe_2O_3$  (Haupt, 1961) in the glauconite-rich sediments, as analysed in Upper Aptian and Albian samples from well Darßer Ort 1, suggest an additional iron source than the hinterland (Borchert, 1964). Brockamp (1976) also described  $Fe_2O_3$  contents of 5.8 % in Barremian and up to 8.7 % in Albian strata of the neighbouring Lower Saxony Block, from a region 40 km around Hildesheim and contemporary volcanic activity as a potential source and referred the 20 % contents of montmorillonite at the Barremian/Aptian transition and up to 50 % within Albian strata to a chemical transformation from alkaline volcanic tuffs.

This theory is supported by the occurrence of angular-shaped quartz grains in Hauterivian and Upper Aptian samples of well Darßer Ort 1 from this study. Tuff occurrences are also known from the western North German Basin to be concentrated in the Berriasian, Upper Aptian and Lower Albian (Zimmerle, 1979), sampled in well Schüttof 3, located in the Hannover area. The often bioturbated, fine-grained, greenish vitric tuff layers display a relic vitroclastic structure. Zimmerle (1979) mentioned that the volcanic activity can be related to rifting phases during the North Atlantic opening, which is documented by volcanic necks in Portugal, northern Spain, Cornwall, Waddensee and southern Sweden.

## 7 Lower Cretaceous Depositional environments

Influenced by the constantly rising long-term Lower Cretaceous sea level (Haq et al., 2014), the eastern North German Basin extended during Lower Cretaceous times (e.g. Diener, 1974, Ziegler 1990), which is shown in the stratigraphic distribution and thickness maps (see *chapter 8.2*) and the successively establishing fully marine conditions in the Albian. However, strong regressive trends during Upper Jurassic, Berriasian, Hauterivian and Barremian times forced the formation of evaporitic, lagoonal, terrestrial and deltaic-dominated strata and condensed sections in marine swell areas. Especially the northeasternmost part of the working area is characterised by deposits from a terrestrial influenced deltaic environment during the Berriasian, witnessed by pedogenic features and terrestrial pollen and spore species. However, Hauterivian–Albian deposits from a shallow marine environment are suggested by brackish-marine and marine fauna as well as bioturbation. According to available core material, well reports and present-day strata thickness, the most information is given about Berriasian strata. Consequently, this section can be described in more detail than the others mentioned. Therefore, a Berriasian basin-wide cross-section and a Middle Berriasian facies map (Wealden 3) could be presented within this study (*Fig. 30*).

### 7.1 Upper Jurassic

The northeastern Usedom and Rügen area provide bioclastic calcareous sandstones composed of shell fragments, peloids and drusy calcite cement at grain contacts and irregular grain coatings. Evaporitic claystones and marlstones providing ooid layers are common in the eastern Altmark-Prignitz Basin.

#### Interpretation:

The occurrence of bioclastics, such as shell fragments in the sandstones, points to near-shoreface or beach sands and carbonate cement precipitation from marine pore waters, indicating a near-surface vadose zone environment and suggesting regressive conditions (Tucker, 2011). Ooids are built in high-energy coastal shoals with elevated temperatures, which are supersaturated with respect to  $\text{CaCO}_3$ . They represent a kind of lag sediment under repeatedly changing environmental conditions and low terrigenous sediment influx (Einsele, 1992). Most Jurassic ironstones formed during long periods of high but short-term fluctuating sea levels in epicontinental seas (Van Houten and Arthur, 1989). Peloids are also most common in sediments of protected environments such as lagoons and tidal flats produced by gastropods. Evaporitic claystones may be deposited on neighbouring tidal flats behind barriers.

The progradation of tidal flats typically forms fine-grained sediments and is capped by soil or sabkha evaporate beds (Tucker, 2011).

## 7.2 Upper Berriasian (Wealden-type)–Valanginian strata

The wells Darßer Ort 1 and Garz 1 yield very weakly to non-bioturbated, non-calcareous stacking sets of 1 m to 30 m thick fining upward units or massive, up to 30 m thick sandstone complexes. Grain size ranges from sandstone to siltstones and organic-rich claystone with thin coal layers. The less compacted brownish-grey, fine-grained sandstones comprise thicknesses of 0.5 m to 25 m and are mostly unstratified to low-angle cross-bedded or horizontal bedded. Root trace fossils, xylithic plant remains and wood are common features. Superimposed by mostly organic-rich, black to dark grey laminated heterolithic bedded clay- and siltstones, the fining upward sequences are covered by a dark-grey to black organic-rich claystone, a coal layer, or a maximum 0.5 m thick histosol. Silt- and claystones often provide slicken sides and xylithic plant remains. In the basal part of the well, de-stratified claystones yield iron-bearing nodules and fine-grained sandstones show an erosional base and locally yield mudclasts. On gamma logs, the fining upward sequences start with a sharp based sandstone unit and show serrated curves combined to an increasing gamma value, ending up in silt- or claystones (*Fig. 31*). In contrast, the up to 30 m thick single sandstone sequence is based with a sharp gamma-ray signal at the bottom and the top, characterised by less serrated decreased and relatively stable gamma values.

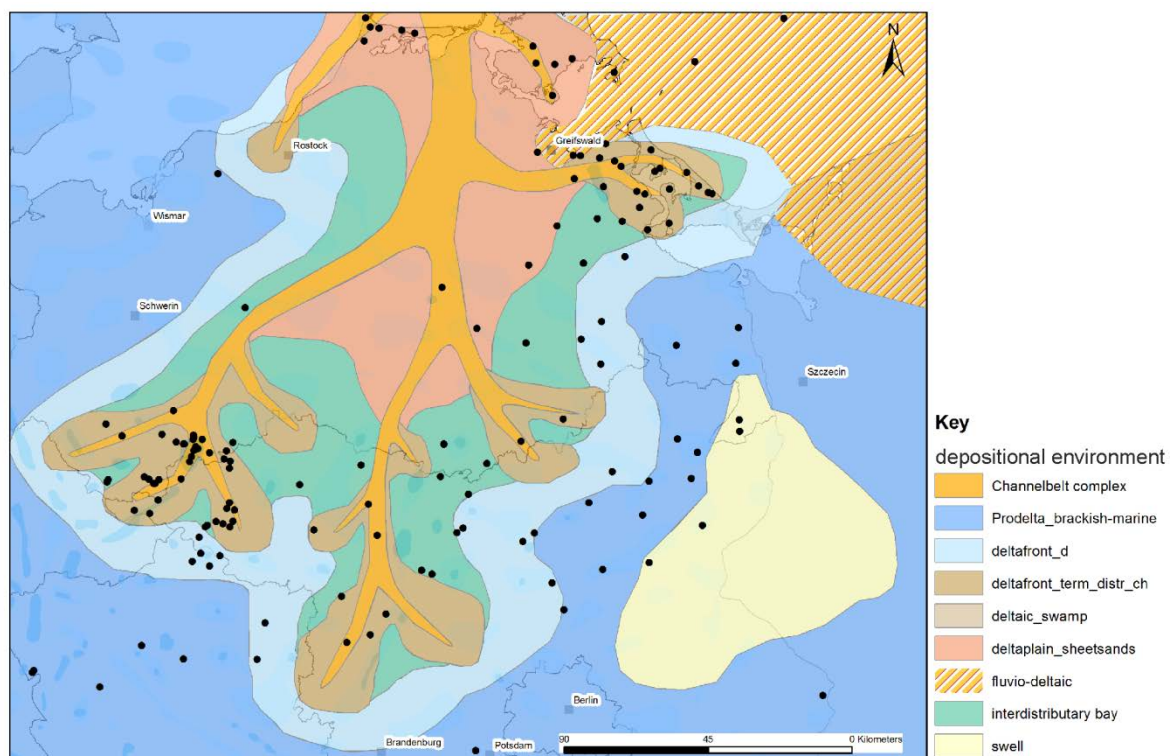


*Fig. 30: Schematic reconstruction of depositional environments and facies during mid-Berriasian mrs 2 / Wealden 3. Black points are referred to the evaluated wells.*

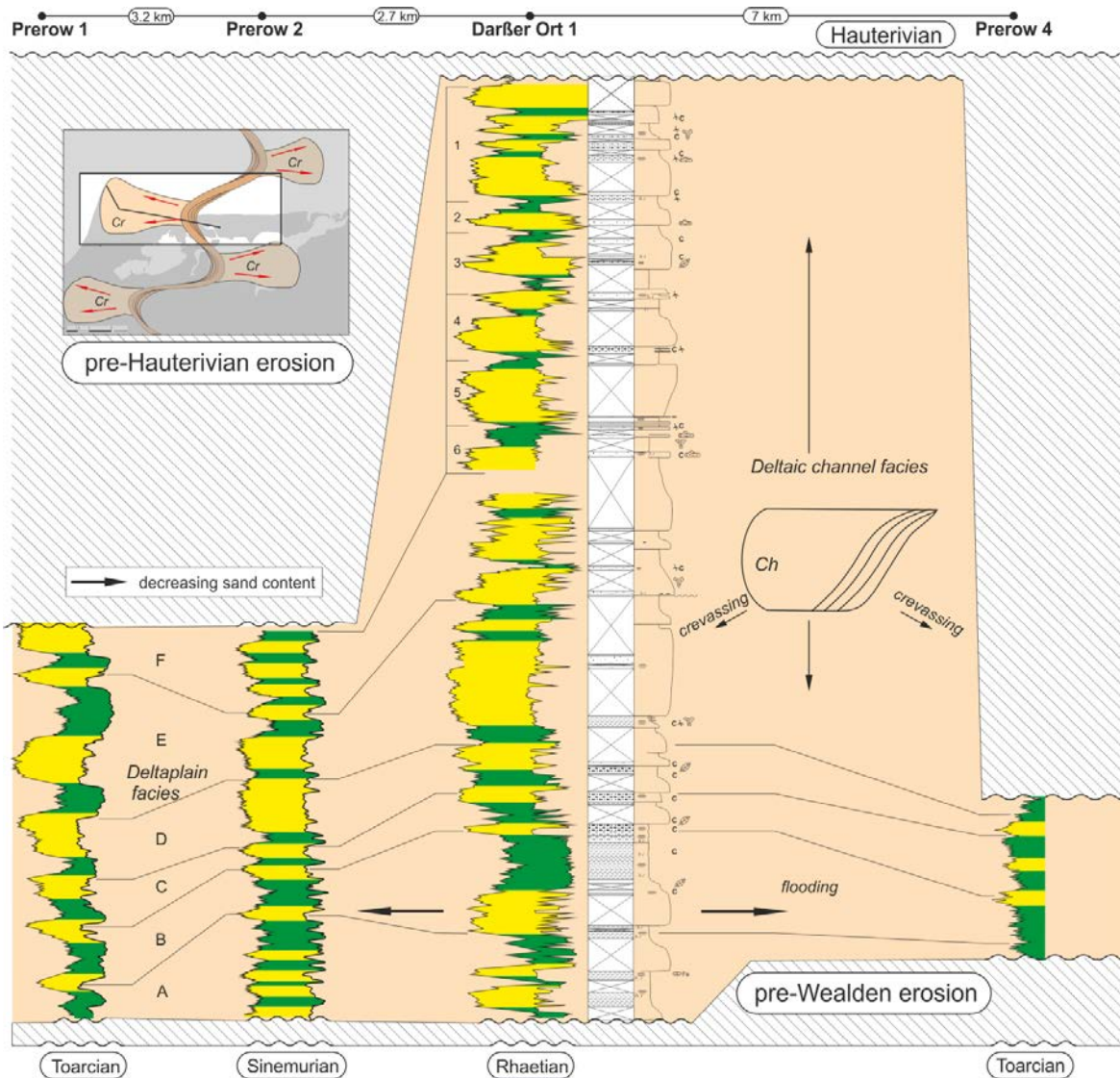


Fig. 31: Facies section from the Darß area, yellow coloured parts show the sand content, and the green parts show clayey to silt content. The section line is shown in the small map top left. The section represents channel belt facies and overbank areas; the black arrows show decreasing sand contents on the delta plain away from deltaic channel facies.

**Interpretation:**

*Lithofacies S1 and Sh:* The low angle cross-bedded (*S1*) to horizontal laminated (*Sh*) sandstones with an erosional base and mudclasts were interpreted as sandy bedforms, which are occurrences of plane beds deposited on initially dipping surfaces (Miall, 2006). Therefore, these sections were interpreted as crevasse splays but can also represent sheetsands.

*Lithofacies Sm:* massive sandstone complexes were interpreted as channel belt deposits of sediment gravity flow. A characteristic occurrence of this facies is in small channels resulting from bank collapse (Miall, 2006).

*Lithofacies Ft:* Interlamination of mud, silt, and very fine-grained sand is common in overbank areas and represents deposition from suspension and weak traction currents (Miall, 2006). Very small-scale ripples may be present in the sand and silt

beds. Undulating bedding, scattered bioturbation, desiccation cracks, plant roots, coal streaks and scattered pedogenic nodules may be present in overbank fines, interlayered by sheetsands.

The described stratal patterns of stacked fining upward successions point to overbank deposits from an upper delta plain environment, supported by the evidence of wet and dry lowland spore and pollen species. Coastal and pioneer elements witness marine incursions from a near-shore environment (Döring, 1965a,b; Heunisch, 2019). Channels and crevasse-splays deposits point to a lower delta plain environment. A schematic reconstruction of the depositional environments is given in *Figure 30*.

Deltaic deposits, as described above, were also observed in the Altmark-Prignitz Basin drilled in the wells Werle 19, Zechlinerhütte 1. Well Teetz 1 yields a section starting with dark organic-rich weakly bioturbated claystones interbedded with up to 0.5 m thick siltstone layers, bivalve shells and xylithic plant remains. Gamma values show a quiet run of high values with several thin negative excursions. Followed by heterolithic, flaser bedded, or massive fine to medium-grained sandstones intercalated with laminated sandy silt- and mudstones containing plant detritus, the Berriasian succession ends with a fining upward unit. These 4 to 5 m thick units start with fine-grained sandstone, followed by laminated siltstone and end in organic-rich claystone. Core material from the wells Werle 19 and Neuruppin 2 revealed intercalated marlstone or quartzitic sandstone layers up to 2 m thickness.

#### Interpretation:

Dark organic-rich, laminated to silty claystones with marine ostracod fauna and shell layers points to deposits from an offshore environment from an inland sea. These shales suggest temporarily restricted bottom water circulation, which caused anoxic conditions, witnessed by the formation of pyrite and organic-rich dark claystone layers (Sparfeld, 1973; Tucker, 2011).

Horizontal flaser bedded clayey and silty deposits with intercalated massive sand layers, plant remains and weak bioturbation point to prodelta to distal bar deposits from the lower delta plain (Einsele, 1992).

The intercalated chalcedonic cemented layers from well Neuruppin 2 show fibrous fringe cement and porifera spicules, suggesting temporary marine incursions. According to Sparfeld and Dreyer (1970), the ostracod species determined in well Sanne 1 are attributed to meso- to oligohaline-influenced, in the late Berriasian poly-

## *Lower Cretaceous* Depositional environments

to euhaline shallow and coastal waters in the eastern part, connected to open marine waters. Decreased sedimentation rates and temporary dry falling, attested by desiccation cracks, are evident for regressive phases.

In the eastern North German Basin, mostly upper Valanginian-dated successions kept preserved from erosion in the Altmark-Prignitz Basin. The few information given by well reports shows bioturbated silt- and fine-grained calcareous sandstones. The micro- and macrofossil taxa attest to a euhaline shallow marine and the near-shore environment connected to open marine waters. Good water circulation and oxic conditions allowed a benthic marine ostracod and foraminifer fauna (Sparfeld and Dreyer, 1970a). Amongst others, ostrea and uncertain ammonite remains suggest strong water currents, whereas plant remains and megaspore fauna suggest a nearshore environment. However, temporarily anoxic bottom waters caused euxinic conditions (Sparfeld and Dreyer, 1970).

### Interpretation:

Silt, interlayered with fine-grained calcareous sandstones, bioturbation and plant remains, points to deposits from the prodelta or the delta front (Einsele, 1992). Wave action is suggested by bivalve and ammonite remains.

### 7.2.1 Sporomorph Ecogroup Model

Due to the facies analysis of well Darßer Ort 1 (Fig. 32) based on a sporomorph ecogroup model (Heunisch, 2019) according to Abbink et al. (2004), the Berriasian Wealden-type strata of NE-Germany is with up to ~80 % dominantly characterised by continental dry lowland (*Gleicheniidites* spp.) and wet lowland species (*Cicatricosisporites* spp.), indicating wetter and warmer climate conditions, and the occurrence of coastal and pioneer species such as *Classopolis* and *Perinopollenites elatoides*. According to Heunisch (2019), coastal elements indicate short marine incursions. *Perinopollenites elatoides* may suggest cooler and wetter climate conditions (Abbink, 2004a). Spore and pollen tables analysed by Heunisch (2019) are listed in Appendix A. Short marine incursions are suggested by the aquatic brackish-marine taxa *Botryococcus* sp., while open marine species are lacking.

The sporomorph ecogroup model of well Ückeritz 1 (Bornemann and Heunisch, 2017; Fig. 33) show a terrestrial-dominated environment associated with Wealden-type facies with alternating marine influences. Compared to well Darßer Ort 1, only the minor *Gleicheniidites*- and *Deltoidospora* species could be identified according to the Sporomorph zonation (Döring, 1965a, b; 1966). Consequently, the terrestrial-dominated samples were considered Wealden-facies and, therefore, to a Lower Cretaceous age (Bornemann and Heunisch, 2017). Dry and wet lowland and hinterland taxa comprise 90 % of terrestrial-dominated samples. Indirect marine incursions via the Polish Trough are witnessed by the occurrence of coastal elements like increasing pioneer, tidal, marsh and coastal species. Short marine incursions are witnessed by 40 % of brackish-marine freshwater to marine species and a decreased amount of 20 % in dry lowland and hinterland elements (Bornemann and Heunisch, 2017). Dinocysts (Abbink et al. 2004a, b) and foraminifera testified in depths of 214–224 m (Appendix A) indicate a short, fully marine incursion. The brackish-marine freshwater taxa *Botryococcus* sp. indicates brackish-marine to limnic environments and show increasing occurrence towards short marine incursions. Generally, the fast-changing facies shift from terrestrial to marine could be indicative for transgressions (Bornemann and Heunisch, 2017) or erosional gaps.

Lower Cretaceous Depositional environments

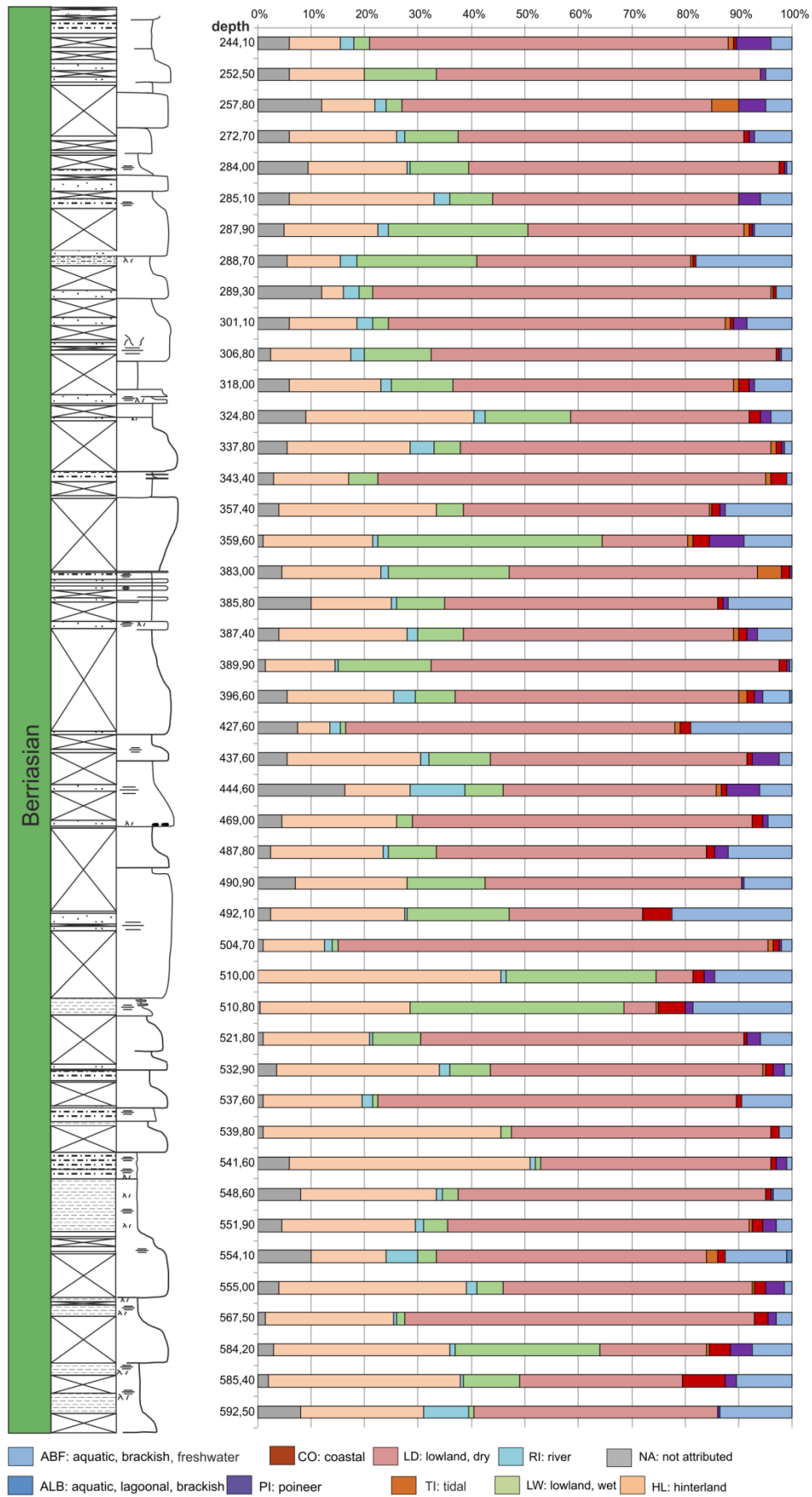


Fig. 32: Sporomorph ecogroup model of Berriasian successions from well Darßer Ort 1 according to Heunisch (2019) shows a depositional environment that is dominantly (~80 %) influenced by wet/dry lowland and hinterland spore and pollen taxa. A minor aquatic brackish-marine influence makes up 20 %.



## Lower Cretaceous Depositional environments

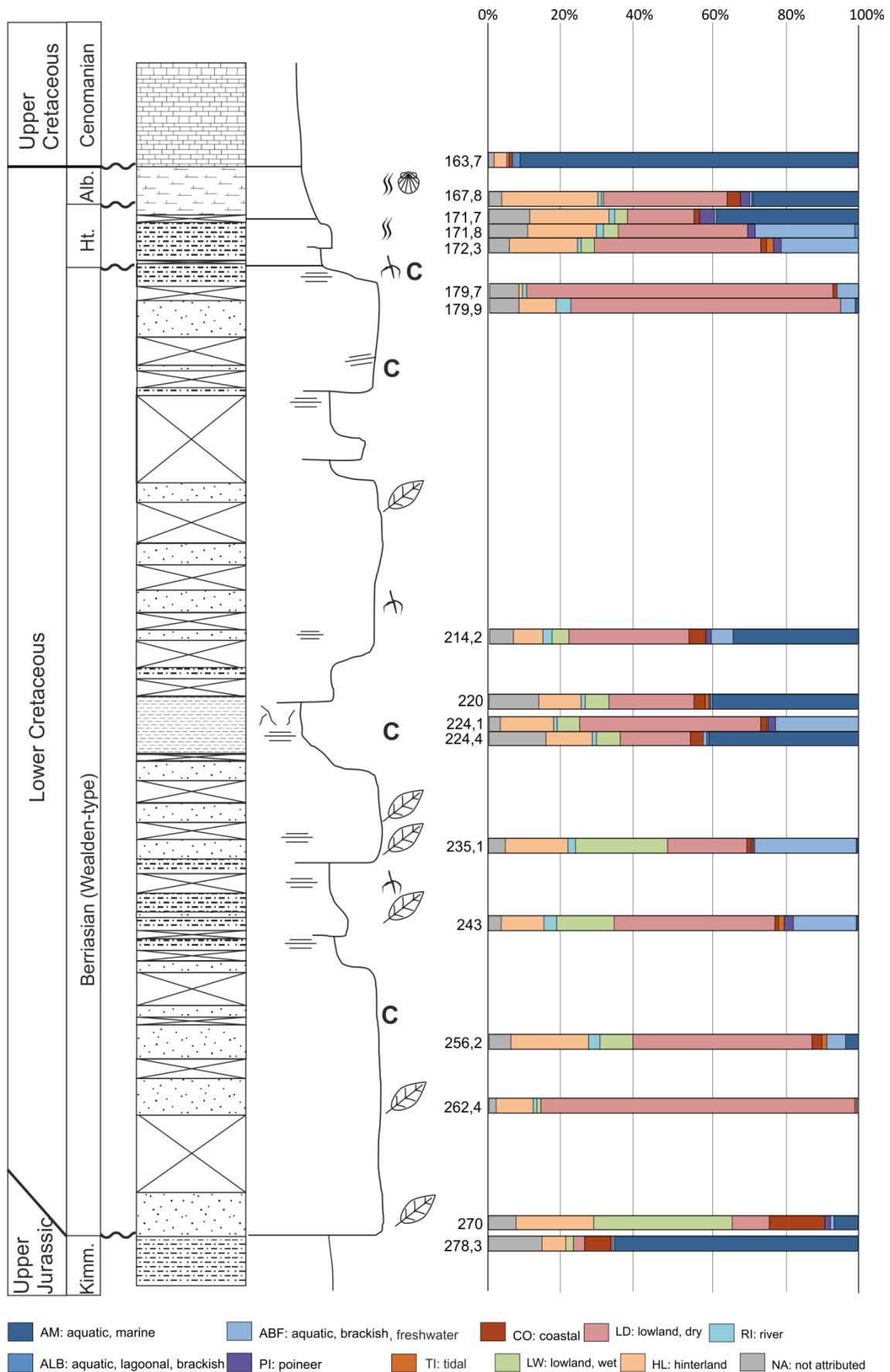


Fig. 33: Sporomorph ecogroup model of Lower Cretaceous successions from well Ückeritz 1 (Bornemann and Heunisch, 2017) show a depositional environment influenced by dry and wet lowland and hinterland spore and pollen taxa, make up to 90 %. Marine ingressions via the Polish Trough are witnessed by up to 40 % marine and freshwater taxa, testified by foraminifers and dinocysts.

### 7.3 Hauterivian–Barremian

A marine transgression flooded the North Western Pomeranian High via the Prignitz-Altmark area and from another direction via the Polish Trough in the early Hauterivian (Diener, 1974). Belemnite-, lamelibranchiata- and ammonite remains, carbonaceous plant remains and weak bioturbation are quite common in the Hauterivian and Barremian fine-grained and glauconitic sandstones (*Fig. 8*). Single sandstone stacks include up to 50 m thickness, separated by thin clay- or marlstone layers. Strong currents are suggested by abraded belemnite and ammonite remains. According to Tröger (1966), the benthic bivalves and brachiopod species are domestic in near-shore habitats. A few coarse-grained sandstone layers and fine gravel layers are intercalated (Diener, 1974). The transgressive base (*Fig. 8*) is marked by a medium to coarse-grained transgressive layer, with partly iron ooids and concretionary iron-rich nodules.

In the Altmark-Prignitz Basin, the basal Hauterivian strata are characterised by weakly bioturbated transgressive greensands and decreased sedimentation rates (Sparfeld and Dreyer, 1970, 1970a). Followed by fine-grained massive to low-angle stratified carbonate cemented sandstones. The single sandstone stacks are up to 15 m thick and interbedded with silty-clayey flaser-bedded or marly layers with up to 5 m thickness. In the western Altmark-Prignitz Basin, dark-grey silty and clayey marlstones, siltstones and greenish-grey sandy partly glauconitic claystones are common in Hauterivian and Barremian strata, as drilled in Werle 19.

#### Interpretation:

Basin extension (Schott, 1967; Diener, 1974; Diener et al., 2004), strong currents suggested by abraded bioclastic shell fragments and the near shore domestic species indicate a shallow marine to coastal environment. The described patterns, as well as glauconite grains of these well-sorted and bioturbated massive to cross-stratified sandstone points to shoreface deposits. This is supported by the occurrence of carbonate cement, rhombohedral siderite and fine-crystallised chamosite cement, which precipitate from pore waters in shallow marine environments. Fine-grained organic-rich and carbonatic siliciclastic sediments were deposited in distal and deeper parts of the basin with increased water depths in the shelf transition zone. Marine foraminifera and belemnite remain, indicating an open marine environment. The formation of glauconitic sandstone layers witnessed a starving sediment input and condensed sections during strongly regressive conditions.

#### 7.4 Aptian–Lower Albian

In Northeast Germany, basal and weakly bioturbated, fine-grained, moderately to poorly sorted glauconitic sandstones with biogenic components and quartzose detrital input superimposed by a dark grey to greenish-grey, sandy, calcareous and glauconitic siltstones, including a 4 m thick blackish clay layer are common. A decrease in benthic fauna individuals and a high content of agglutinated foraminifer species witness temporary regressive conditions, restricted water circulations and oxygen-depleted bottom waters, characterised by high pyrite and other iron oxide precipitations (Diener, 1974, Tucker, 2011).

In the northwestern and southwestern Altmark-Prignitz Basin, Lower Aptian black shales containing fish remains, informal called “Blättertonmergel”, was drilled by the wells Dömitz 4 and Waddekath 35. In the northern Altmark and Westprignitz area, the transgressive Aptian successions start with a c. 1 m thick middle- to coarse-grained calcareous and glauconitic sandstone. The overlying strata show a fining upward trend from sandy claystones to claystones. In northeastern Germany, a maximum 5 m thick sandy and glauconitic sandstone horizon marks the transition to the Lower Albian.

##### Interpretation:

The Aptian mature fine- grained moderately to poorly sorted glauconitic sandstones with biogenic components covered by sandy, calcareous and glauconitic siltstones and claystone layer are indicative of a shallow-marine upper lower shoreface sand, witnessed by bioturbation, marine foraminifer and ostracod species. The succession reflects a deepening fining upward trend starting with a basal transgressive and coarse reworking horizon, followed by finer siliciclastics from more distal and deeper parts of the basin with increased water depths in the shelf transition zone.

The formation of organic-rich black shale successions suggests anoxic bottom waters and low water circulation (Sparfeld, 1972; Tucker, 2011) as well as less terrigenous detrital input away from the coast and linked to increased water depths during transgressive conditions and basin extension.

#### 7.5 Middle–Upper Albian

Resulting from large-scale changes in basin configuration, Middle to Upper Albian strata are characterised by a change in lithology and facies represented by the bioturbated Middle Albian organic-rich siltstone shelf deposits of the Darß, Rügen and Usedom area and the Altmark-Prignitz Basin. Phosphorous nodules on the Upper Albian base and sandy marlstones suggest temporary reworking (*Fig. 8*) of the underlying Lower Cretaceous or

Upper Jurassic strata during regressive conditions. Attested by the unconformable contact of Upper Albian on Hauterivian strata, the former Usedom Basin trough was a swell region on the axis Heringsdorf – salt pillow Hohendorf to Lubmin (Diener, 1974; Petzka et al., 1964). Followed by reddish clay and marlstones, also called 'Flammmergel', the Upper Albian deposits witness an ongoing transgressive trend from distal siliciclastic shelf to pelagic deposits. Benthic lammellibranchiata remains from *Inoceramus*, benthic foraminifera and ostracods species, and planktic foraminifera like *Hedbergella* are common.

Interpretation:

Benthic and planktic macro and microfossil taxa indicate an open marine environment. Shell fragments of *Terebratula* and *Inoceramus* witness increased water depths of > 300 m, euhaline waters, medium water action and oxygen-rich bottom waters combined to decreased sedimentation rates (Sparfeld, 1972). During Albian times the successive flooding of the North German Basin is attested by the formation of pelagic clayey marlstones. According to Tucker (2011), typical grey mudrocks of the open-marine shelf are deposited below the wave base and, in some cases, rich in fossils. Epifaunal and infaunal forms with some pelagic forms and bioturbation, are common. Towards the Cenomanian, the ongoing transgressive trend developed a pelagic to hemipelagic limestones and mudrocks deposition.

## 8 Geothermal Potential of Lower Cretaceous sandstones

The underground temperature in the North German Basin is mainly influenced by the terrestrial heat flow, ranging from 50–90 mW/m<sup>2</sup> and increase in depth with an average of 32 K per kilometer. The latter is locally varying up to 50 K per km. The highest thermal conductivity is given in anhydrite and halite lithologies with up to 5 W/(m\*K), followed by sandstones with values ranging from 3–5 W/(m\*K) (Wolfgramm et al., 2014). Lateral variability in underground temperature is mainly caused by the different and heterogeneous lithologies. Therefore, underground temperature modeling should be done by evaluating values from well temperature logs, bottom hole temperatures, pumping and lift tests for only small areas. Increased temperatures could be found on top of a salt plug related to good thermal conductivity.

Another important factor is the solution and dissolution potential of fluids and rocks, which should be low with respect to remineralisation and porosity loss in sandstones. The composition of deep brines strongly influences the thermic capacity of geothermal plants as well as the technical dimensioning of the plant and its operation (Wolfgramm et al., 2011, 2014). With increasing brine salinity and composition, density and viscosity cause a decrease in thermal conductivity (Wolfgramm et al., 2011). According to Wolfgramm et al. (2011), the geothermal aquifer waters in the North German Basin primarily originated from seawater in the pore space or evaporitic waters and secondary changed by diagenetic reactions and/or mixing with fluids from surrounding stratigraphic units. The fluid mineralisation and salinity of Mesozoic brine correlate to increasing depth until 2000–3000 m depth and salinities up to 250 mg/l while the pH value decreases. The highest salinities were measured from Zechstein and Rotliegend brines with salinities up to > 280 mg/l / 330 mg/l Wolfgramm et al. (2011). The Lower Cretaceous sodium and chloride-enriched brines were mainly taken from sites near salt plug rim synclines and showed an increasing salinity with increasing depths of up to 20–25 g/l per 100 m depth (Wolfgramm et al., 2014). This is more than twice as high as the usual trend of 10g/l per 100 m depth away from salt structures. The mineralisation of Berriasian samples (*Fig. 34*) shows values ranging from 43 g/l in depths of 406 m–218 g/l in depths of 1550 m. The overlying Hauterivan samples revealed mineralisation values ranging from 64 g/l in depths of 1000 m and 170 g/l in depths of 1710 m. The single Albian sample shows 68 g/l in 560 m depth.

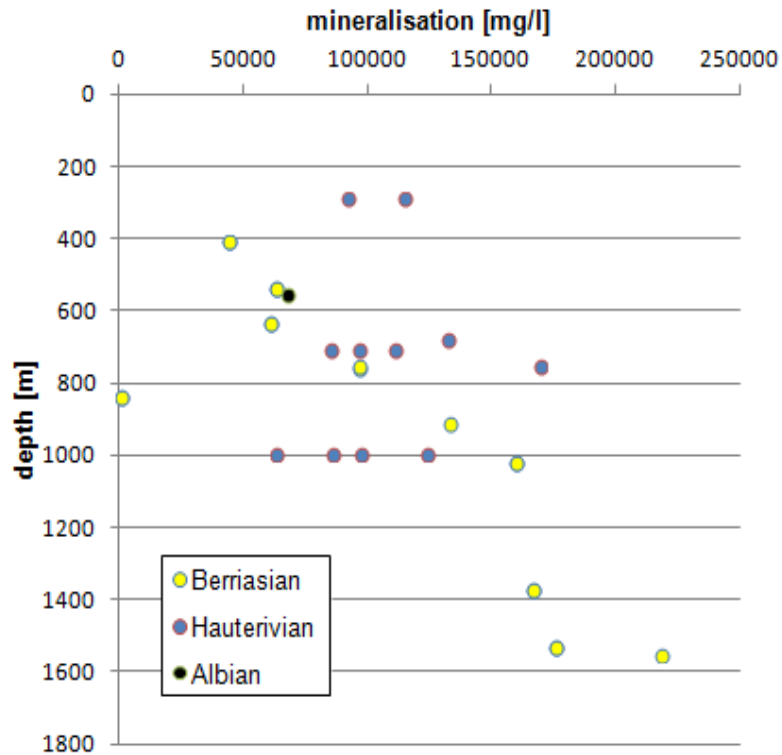


Fig. 34: Mineralisation from Lower Cretaceous brines in the North German Basin. Maximum measured mineralisation of 218 g/l (total dissolved solid) within Berriasian brines at depths of 1600 m (n=30), according to unpublished project data.

### 8.1 Geothermal utilisation in the North German Basin

The potential of geothermal reservoirs in the northeastern North German Basin has already been investigated since the 1970s in the former GDR, mainly based on the use of data evaluated in huge exploration campaigns of hydrocarbons of the 1950–1970s (e.g. Diener et al., 1989; Wormbs et al., 1989; Katzung, 1984; Katzung et al., 1992). The following exploration focused on Mesozoic hydrothermal reservoirs in northern Brandenburg and Mecklenburg-Vorpommern, resulting in the reservoir development at Waren, Neubrandenburg and Neustadt-Glewe (Table 2). In western Germany, e.g. Schulz et al. (1994); Hänel et al. (1984) evaluated geothermal reservoirs first. Followed by a re-evaluation of results from the eastern and western basin parts, data were compiled to the internet system GeotIS (e.g. Schulz and Röhlung, 2000; Kabus et al., 2003, Schulz et al., 2007). Since 2011, the public availability of basic geothermal data has been provided by the geo-informational system GeotIS (Agemar, 2014).

The Mesozoic sandstone reservoirs in the North German Basin yield different sandstone reservoir complexes, referred to as profitable hydrothermal reservoirs. Until now, these complexes yielded a few geothermal power plant sites, utilised for balneological, heat production and deep aquifer purposes, as shown in Table 2.

Table 2: Examples of deep geothermal power plant sites in porous and fractured reservoirs in the North German Basin.

Site	reservoir complex	depth (m)	aquifer temp./ borehole temp. (°C)	main utilisation	exploitation system	Install. year
Neustadt-Glewe	Rhaetian	2240	99 (97)	heat supply	doublet system	1994
Waren	Rhaetian	1540	63 (61)	heat supply	doublet system	1984
Neubrandenburg	Rhaetian	1250	80 (55)	aquifer storage	doublet system	2004
Templin	Rhaetian-Hettangian	1620	67	balneology		
Neuruppin	Aalenian	1650	63 (56)	heat supply balneology	doublet system	2007
Prenzlau	Zechstein	2786	108 (55)	heat supply	Deep borehole heat exchanger	1994

So far, the Schilfsandstein, Rhaetian and Liassic sandstones and the Zechstein limestones seem to be the most promising porous and fractured geothermal reservoirs. They were drilled in depths ranging from 1200 to 2800 m (Table 2), which ensure high temperatures of up to 99°C to provide a heat energy supply for districts and cities. Although the existing sites have proven efficiency for more than thirty years, the explorations risks for new ones still remain high.

In general, there is a distinction between open and closed systems. A geothermal doublet system (see chapter 8.1.1) is a conventional example of available systems, such as operating in Waren, Neuruppin and Neustadt Glewe (Table 2). The latter was also operated for power production using an Organic-Rankine-Cycle (OCR) system until 2012 when it was dismantled. An OCR unit is a system based on a closed-loop thermodynamic cycle for generating electric and thermal power. Therefore, it is exploiting multiple sources, such as traditional fuels, waste heat or renewable energy; in Neustadt Glewe, geothermal energy uses an organic working fluid to reach its critical point at lower temperatures and pressures than water (Schuster et al., 2010). A so-called binary system uses the water from the geothermal reservoir to heat the secondary working fluid, which is vaporised and used to turn the turbine/generator units (Madhawa Hettiarachchi et al., 2007).

In 1994 a deep borehole heat exchanger (BHE) was installed in Prenzlau. This site is an example of a closed system. To use this heat source, new drillings and abandoned boreholes can be used to install such a plant (Kohl et al., 2002). Therefore, a common way is to install a co-axial pipe in a liner within an outer steel pipe (casing) optimises thermal and hydraulic behaviour by providing an injection of cold water through the annulus and the production of warm water through the centered co-axial pipe, both within one well. On the

way down to the borehole bottom, the water takes up heat from the surrounding rock and from the base of the heat exchanger, the hot water flows back to the surface via the centered co-axial pipe. This closed water circulation does not use water in the subsurface. Back on the surface, the water passes cascade through radiators and ceiling- and floor-heating systems, providing heat to buildings (Doelling and Schulte, 2010).



### 8.1.1 Hydrothermal doublet system

Geothermal district heating is realised with two or more geothermal wells, including one production well and one re-injection well (Fig. 35). According to Wolfgramm et al. (2014), the following general conditions are necessary for a successful long-term operation of a geothermal heating station using a doublet system:

- effective reservoir thickness > 20 m corresponding to an effective permeability thickness of 10 Dm
- permeability > 500 mD
- porosity > 20 %
- productivity > 75 m<sup>3</sup> (h MPa)<sup>-1</sup>
- reservoir water temperatures > 65°C (direct heat production)
- reservoir water temperatures > 100°C (direct power production)

The transmissivity also affects the geothermal potential. For a groundwater aquifer, transmissivity (T) in [m<sup>2</sup> \*s] is defined by the hydraulic conductivity ( $k_f$ ) in [m\*s<sup>-1</sup>] and the strata thickness (M) in [m].

$$T = k_f * M$$

The product of permeability ( $k$ ) (instead of hydrothermal conductivity ( $k_f$ )) and the aquifer thickness determines the transmissivity (T) in [m<sup>3</sup>], which could be exactly determined by a pumping test. Due to drilling costs, the aquifer depth should not exceed 3000 m (Schulz et al., 1994).

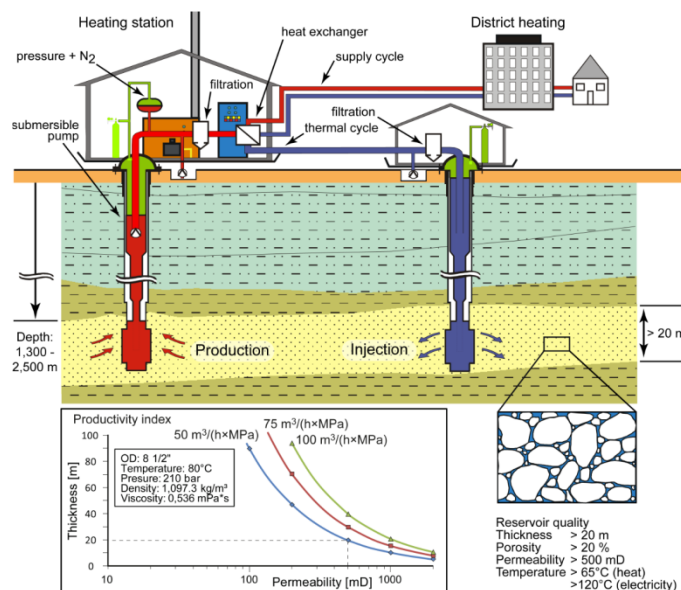


Fig. 35: Schematical operation procedure of a hydrothermal doublet system (Franz, 2018, modified from Rockel et al., 1997). A productivity index of at least 50 m<sup>3</sup>/h x MPa is needed for an efficient operation. Further necessary reservoir quality parameters are given on the right side bottom concerning temperature, porosity, and permeability.

### 8.1.2 Aquifer thermal energy storage in porous sandstone aquifers

Thermal energy storage (TES) systems provide energy savings and contribute to reducing environmental pollutants. Water has a high heat capacity and low cost and TES can be used for heating and cooling. Long-term or seasonal storage has a storage capacity of three to four months, depending on several requirements. Great volumes involving great amounts of energy can be stored to store solar heat collected in summer for space heating in winter or to provide heating and cooling by storing solar heat underground in summer and cold in winter (Novo et al., 2010). While the heat pump extracts heat from the water in winter, it extracts heat from the building in summer to store it in the underground water. Regarding the large volume necessary for seasonal heating and cooling, heat stores are mostly built near the surface. Using natural water from saturated and permeable underground layers as a storage medium is called Aquifer Thermal Energy Storage (ATES). Thermal energy is extracted from groundwater from the aquifer and re-injected at a modified temperature at a nearby separate well. High permeable and water-saturated sandstones without groundwater movement cost-effective seasonal storage (Novo et al., 2010). According to Schmidt et al. (2003), the geological requirements are a natural 20 to 50 m thick aquifer layer with high hydraulic conductivity ( $k_f > 1 \times 10^{-5}$  m/s) and impermeable layers on top and below. The natural groundwater flow needs to be very low and the water chemistry needs to be suitable at high temperatures. The heat capacity is 30 - 40 kWh/m<sup>3</sup> (Schmidt et al. 2003).

One example is the heat storage operating at the Reichstag in Berlin, where two aquifer thermal energy stores were built. A 29 m thick Hettangian sandstone layer, filled with low mineralised (29 g/l) thermal water, is fed with waste heat at a temperature of 70 °C, which is later recovered with a temperature ranging from 65–20°C to provide heat supply for the building (Kabus and Seibt, 2000). Another underground store was built in the near-surface quaternary freshwater aquifer to provide cold water to cool the buildings. The water from this cold store is cooled down in winter up to 5 °C and feeds in summer the high-temperature cold system of the buildings via heat exchangers at a temperature level of 16 °C / 19 °C (Kabus and Seibt 2000). For heat storage, water is pumped from the cold side of the underground storage, charged with waste heat from cogeneration units and from cooling and fed to the “warm” side of the aquifer storage, which is at a distance of 300 m. The discharge process works vice versa: water is pumped off from the warm side while heat is absorbed, e.g. direct heating and fed to the “cold” side of the store.

### **8.1.3 Hydrogen storage in porous sandstone aquifers**

Another possibility to utilise porous sandstone aquifers is for Underground Gas Storage (UGS). Due to the different properties of the storage gases, the underground aquifer rocks need to fulfil certain conditions. The basic properties are a good reservoir quality referring to high porosities and permeabilities as well as an impermeable over- and underlying layer. The porous caprock must be water-saturated and hydraulically tight for the gas up to the capillary threshold pressure. This is caused by water trapped within the extremely low-permeable caprock (Reitenbach et al., 2015) e.g. rock salt or claystones. The tightness of a clayey caprock is influenced by the capillary threshold pressure, which will drain the water out of the caprock in case it is exceeded. Therefore, the caprock will become permeable to gas.

There are several issues due to underground hydrogen storage. The corrosion of steel parts is the main problem of sulphate bacteria activity. Besides bacterial metabolism, there can be multiple mineral dissolutions and precipitation in underground hydrogen storage. Caused by the acidification of formation water, for instance, pore-filling carbonate- and sulphate minerals (Flesch et al., 2018) like calcite, dolomite, siderite, gypsum, anhydrite and barite, as well as feldspars and clay minerals of the chlorite group can be dissolved at reservoir temperatures > 100°C and working pressures > 15 MPa (150 bar), but also illite may be formed (Allan et al., 2011). Some H<sub>2</sub>-induced redox reactions, such as pyrite reduction and re-precipitation of sulphide in pyrrhotite, may be significant at low temperatures (Truche et al., 2013). The steel parts of wells can promote abiotic reactions in the near wellbore area, resulting in casing corrosion and chemical alteration (Pichler et al., 2010, Truche et al., 2013)

## 8.2 Characterisation of Lower Cretaceous Geothermal reservoirs

So far, the Lower Cretaceous sandstone aquifers were not utilised as a hydrogeothermal aquifer in the North German Basin. This study aims to understand reservoir characteristics better and propose three potential geothermal sites concerning the main parameters as aquifer depth, temperature, thickness, facies, and the availability of distributional structures to provide the power supply.

In general, potential reservoirs provide high mature sandstones and their quality is locally limited to strong varying thicknesses, facies changes and the geometry of the fluvio-deltaic channel belts. Increased strata thicknesses are especially bound to rim synclines of salt plugs, graben structures and locally smaller subbasins (see *chapter 5*). As the underlying Mesozoic (Rhaetian, Liassic) reservoirs, the Lower Cretaceous deposits are dominated by (I) Berriasian fluvio-deltaic strata from an upper and lower delta plain: (a) levee/crevasse-splays complex according to the channel belt, (b) distal crevasse splays and proximal sheetsands, (c) interdistributary bay sheet sands, paralic swamps, (d) delta plain sheetsands and delta front successions and (II) Hauterivian to Barremian shallow marine shoreface sands. So far, these sandstone reservoirs seem to be the most promising ones within the Lower Cretaceous successions of the northeastern North German Basin (*Fig. 36*).

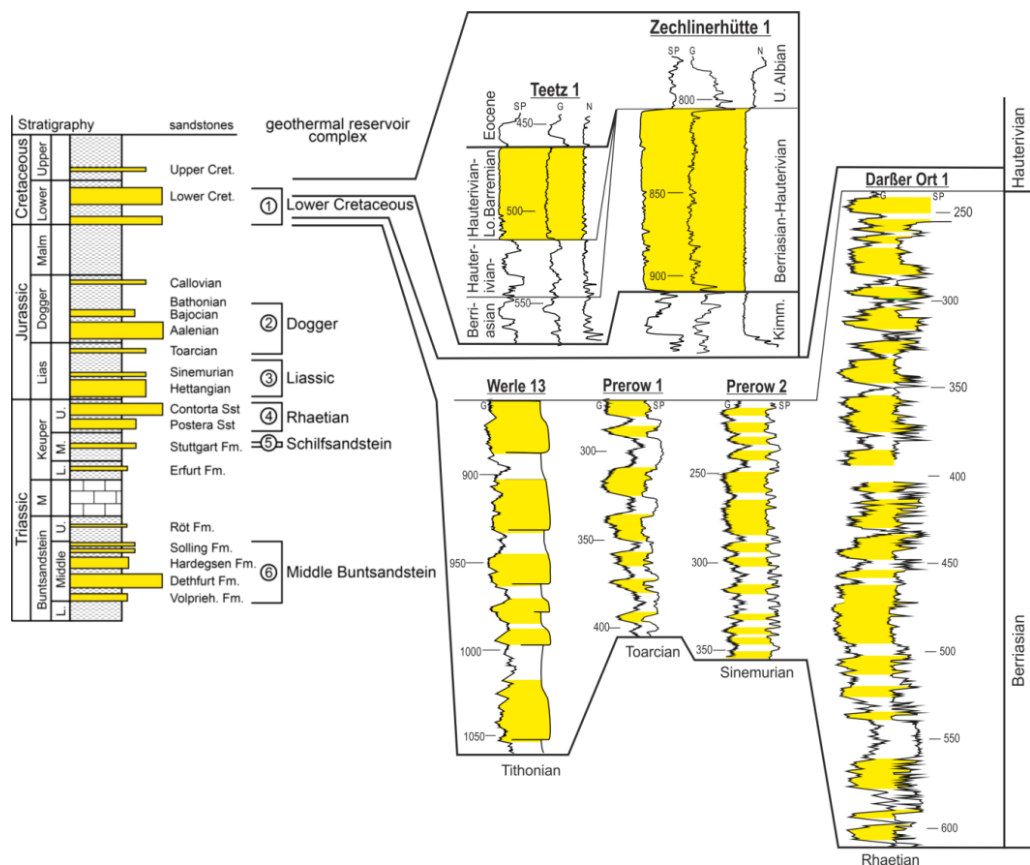


Fig. 36: Left side – Mesozoic geothermal reservoir complexes. Right side – potential Lower Cretaceous geothermal reservoir complexes. Berriasian to Barremian sandstones in the Altmark-Prignitz Basin and Berriasian deltaic sandstones in Western Pomerania (bottom).

### 8.2.1 Petrophysical parameters

Reservoir temperature values were taken from GeotIS (Agemar et al., 2014) and well reports, which are included in the temperature model (Agemar et al., 2014). Calculated temperatures range from 23 °C in 400 m to 43 °C in 900 m depth. The potential Lower Cretaceous reservoirs are situated in depths of 160 m to 1000 m. Higher depths up to 1900 m and, therefore, higher temperatures of up to 74 °C are known from salt plug rim synclines as drilled, for example, in well Gt Pritzwalk 2. Porosity and permeability data were taken from well reports or point counting results from this study.

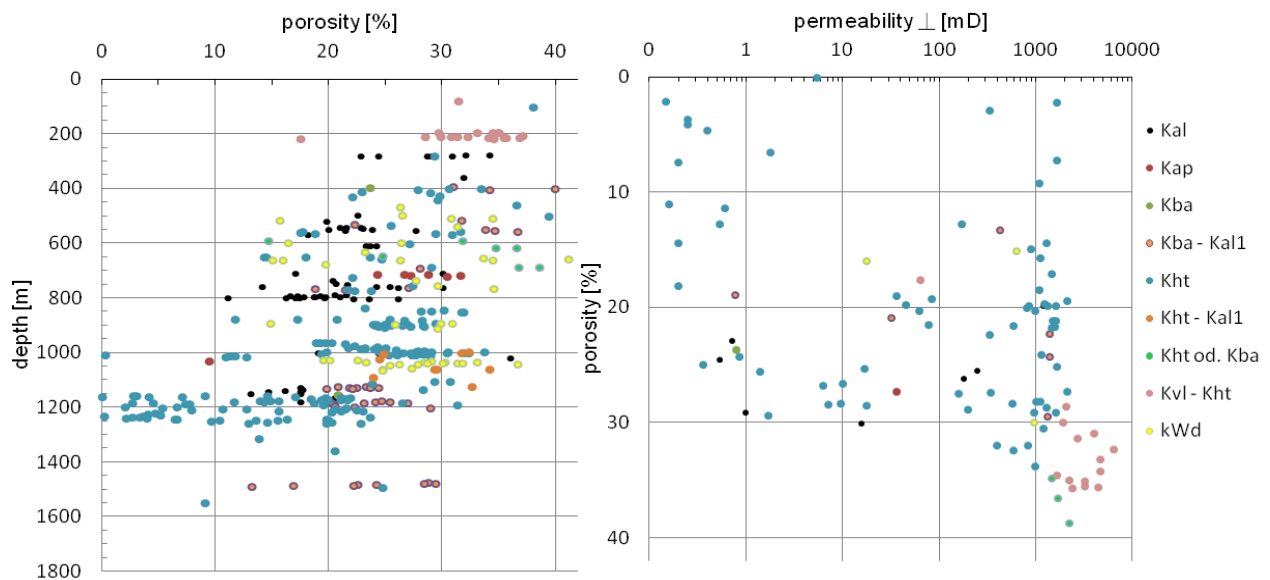


Fig. 37: Left: measured porosity data from Lower Cretaceous lithologies in relation to sample depth (n=380). Right: the relationship between porosity and permeability (n=161). Kal – Albian; Kap – Aptian; Kba – Barremian; Kht – Hauterivian; Kvl – Valanginian; kWd – Wealden-type (Berriasian).

Porosity values measured in Lower Cretaceous samples show a mean porosity of 23 %. The most promising values of 30 up to 40 % are given in Berriasian Wealden-type and Hauterivian to Barremian sandstones in depths of 200 to 800 m. However, promising porosity values in the range from 30 to 37 % are also given in depths of 800 to 1200 m. Relevant permeability values range from 100 mD up to 7000 mD, especially Hauterivian and Barremian samples provide considerable permeability values coupled to porosities higher than 25 % (Fig. 37).

Due to the evaluation of the sandstone reservoirs, cumulative sandstone thickness and distribution maps could be presented, as shown in Figures 39–44. The sandstone thickness maps show the distribution and cumulative thickness of geothermal sandstone reservoirs in the Berriasian (Fig. 39 and Fig. 40), Hauterivian (Fig. 42 and Fig. 43) and Barremian – Lower Albian strata (Fig. 44). While the dashed lines show a presumed distribution, the continuous lines mark a verified distribution, concluded from well data evaluation and distribution maps

after Diener (1974). According to facies changes, the areas of high sandstone thicknesses were former deltaic depositional areas or swell regions within a shallow marine shoreface environment. According to heavy mineral data from this study, the sediment was transported from Scandinavia to the North German Basin. Generally, porosity data were available from well reports and had been evaluated by the work of this study. The less compacted core material from sandstone and sandy material makes it nearly impossible to capture permeability data within this and former studies. However, a few data were provided by well reports where permeability could be measured or reconstructed from well logs.

### 8.2.2 Berriasian sandstone reservoirs

The early Cretaceous Berriasian depositional environment was dominated by a brackish-marine and deltaic depositional system, extending from the northeastern part of the Darß peninsula and Rügen island to the Altmark Prignitz area. The highly mature quartzose sandstones provide high porosities of up to 33 % (own results) and permeability of up to 1000 mD (well data) in less consolidated sandstones. The adjacent areas of western and southern Berlin are associated with a lower delta plain environment and are strongly influenced by marine incursions, which are reflected in the occurrence of calcareous sandstones, shell fragment layers, bioturbation and the biostratigraphic record. Two main reservoir complex types (*Fig. 38*) could be figured out:

- Type I: Fluvio-deltaic sandstone stacks, characterised by alternating fine- to medium-grained sandstones, siltstones and claystones, interlayered by coal seams, associated with deltaic channel belt facies, such as crevasse-splays, sheetsands and floodplain sediments. Single sandstone layer thickness: 1-15 m.
- Type II: The second complex is characterised by large single homogenous fine- to medium-grained sandstone stacks, which could be interlayered by clayey and marly horizons associated with a deltaic channel facies depositional environment. Single sandstone layer thickness: 20-40 m.

The first reservoir complex type is widely distributed (*Fig. 39*) on the Darß and Rügen islands to the Altmark-Prignitz Basin. The cumulative sandstone thickness ranges from 100 m in the Darß Graben to 200 m in rim synclines of salt plugs in the Altmark-Prignitz Basin. Single sandstones layer are 5 to 20 m thick. These fining upward sequences are superimposed by siltstones and covered by an organic-rich claystone top or coal seam, locally a pedogenic horizon. Sandstone porosities reach values up to 24 %. The second homogenous sandstone complex, distributed in the Usedom sub-basin, provides single sandstone thicknesses of 15 m up to 30 m (*Fig. 38*) and sandstone porosities up to 33 %. Cumulative sandstone thickness range from 10 to 90 m in the vicinity of the Polish Trough,

whereas single sandstone stacks are separated by 2 to 5 m thick clay- and siltlayers (Fig. 38).

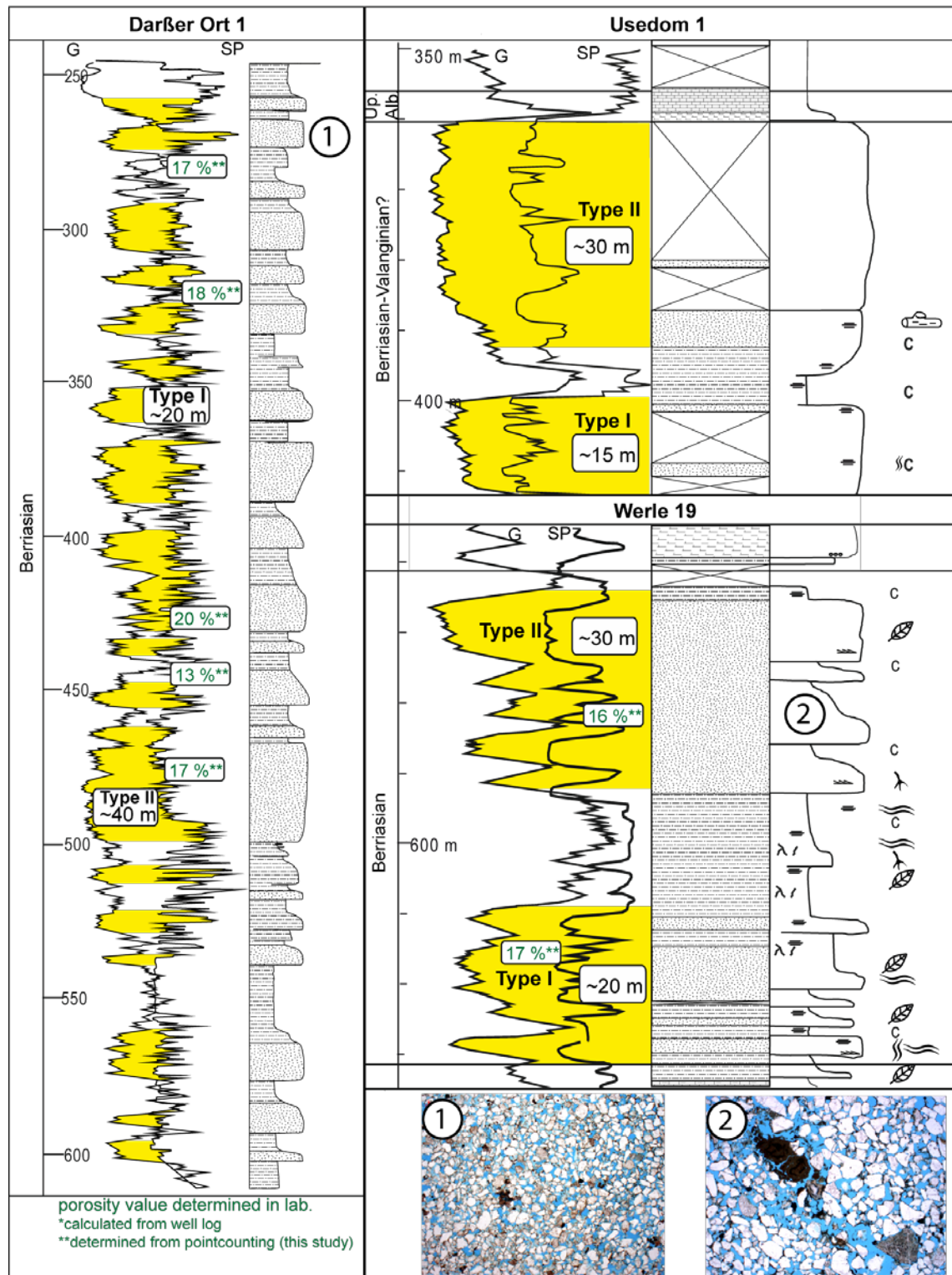


Fig. 38: Potential Berriasian geothermal reservoirs. Left: alternating sandstone stacks in Berriasian deltaic dominated channel belt facies, interlayered by silt- and claystones. Right: homogenous Berriasian-Valanginian? sandstone layers up to 30 m in thickness, partly interlayered by silt- and claystone layers.

Geothermal Potential of Lower Cretaceous sandstones

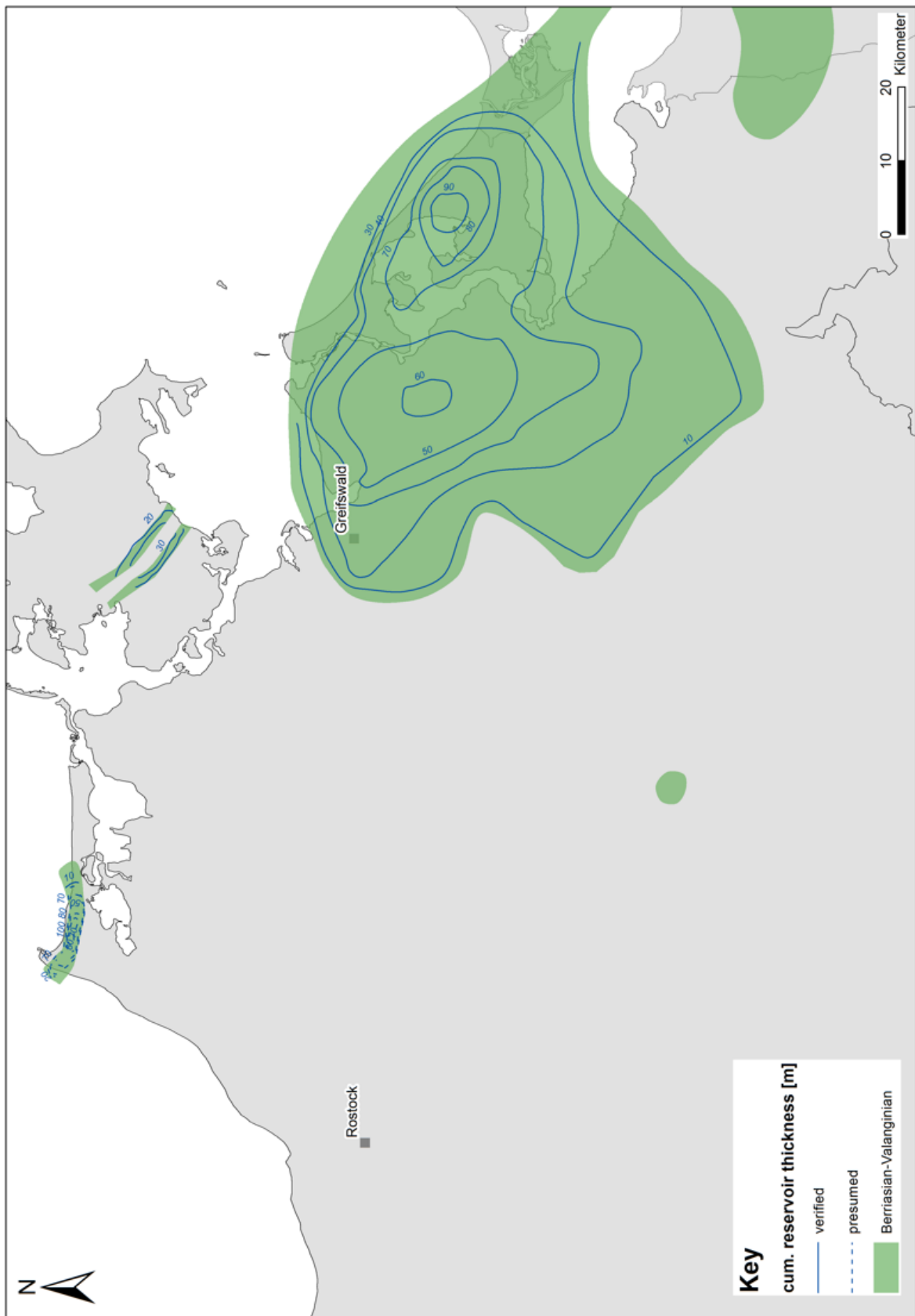


Fig. 39: Cumulative thickness of Berriasian (- Valanginian) sandstone reservoirs in the northeastern North German Basin, after Diener (1974) and own results.



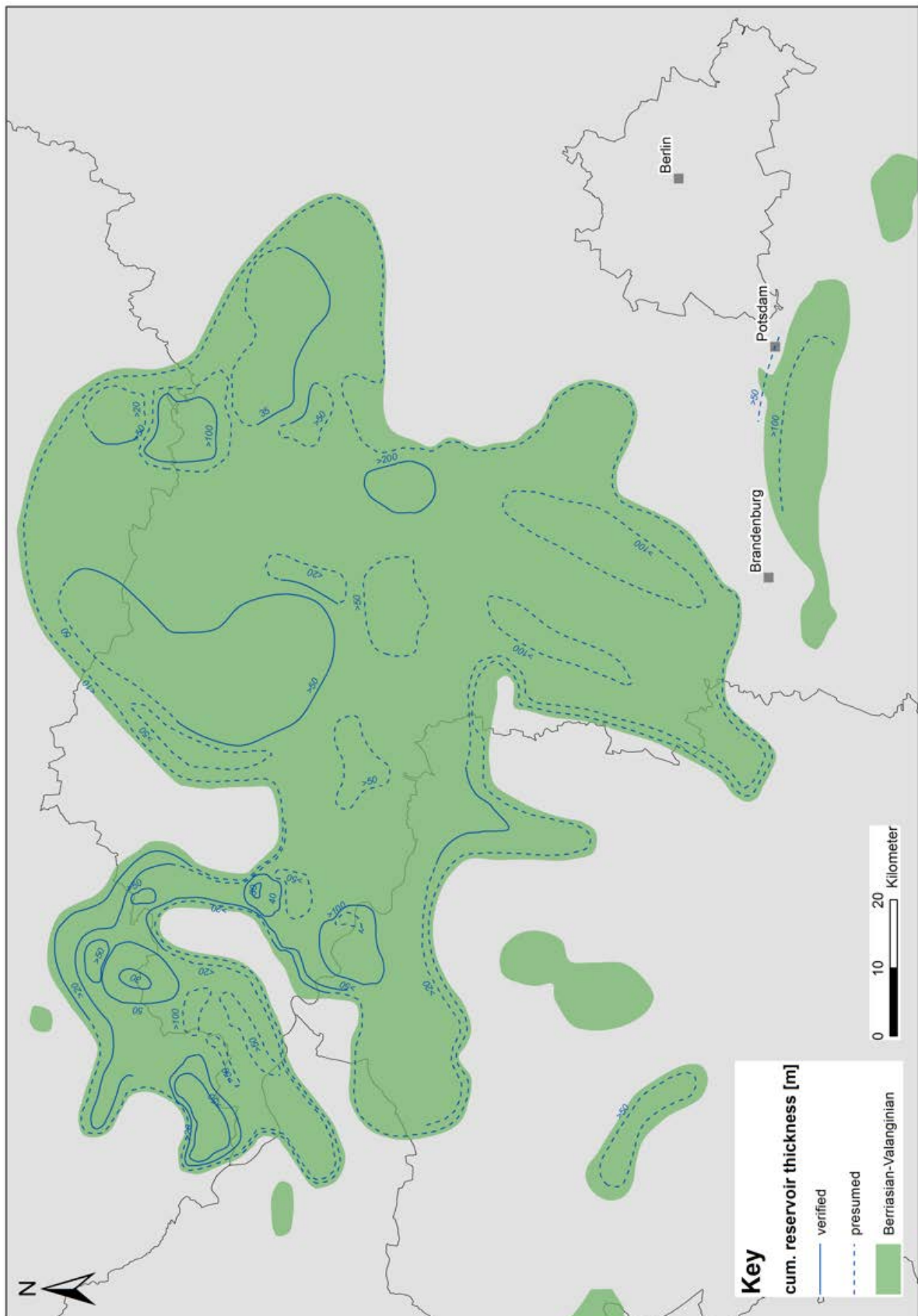


Fig. 40: Cumulative thickness of Berriasian (- Valanginian) sandstone reservoirs in the Altmark-Prignitz Basin, after Diener (1974) and own results.

### 8.2.3 Hauterivian – Barremian sandstone reservoirs

Hauterivian to Barremian fine- to medium-grained sandstones and greensandstones were deposited in a shallow-marine shoreface environment. Besides the carbonate-cemented sandstones, less consolidated thick sandstone stacks are common, deposited in the former swell areas of northern Western Pomerania and the northeastern Altmark Prignitz area. There, the sediment accumulation was locally strongly influenced by the formation of salt plug rim synclines. The cumulative thickness of Hauterivian sandstones (*Fig. 42*) ranges from 10–20 m in the Usedom area and from > 15 up to >50 m, locally 110 m (*Fig. 41*) in the Altmark-Prignitz Basin (*Fig. 43*). Within Barremian strata, sandstone thickness (*Fig. 44*) ranges from roughly 30 m in the Darß Graben to 90 m in the Altmark-Prignitz Basin. Sandstone porosities of up to 26 % (own results) and values of 35 % are known from well log calculations Diener et al. (1988) (*Fig. 37*). Coupled to permeability values ranging from 200 mD up to 2000 mD, poroperm values remain high according to increasing depth. In contrast, the successions in Western Pomerania were widely eroded and provided mostly cemented sandstones with thicknesses of up to 40 m.

Due to mainly silty-clayey and marly lithologies and the decreased thickness combined with carbonate cement, Aptian strata do not provide a good geothermal reservoir potential. The 15–20 m thick sandstones from the Darß Graben are mainly cemented by calcite- and ankerite. Diener et al. (1988) suggested that the widely-distributed base Lower Albian sandstone is not considered a potentially good geothermal reservoir due to its decreased thickness of 3–5 m. However, due to erosional gaps and missing strata, this sandstone layer locally can extend an underlying sandstone horizon. For this reason, the Lower Albian is included in the cumulative thickness maps of the Barremian (*Fig. 44*).

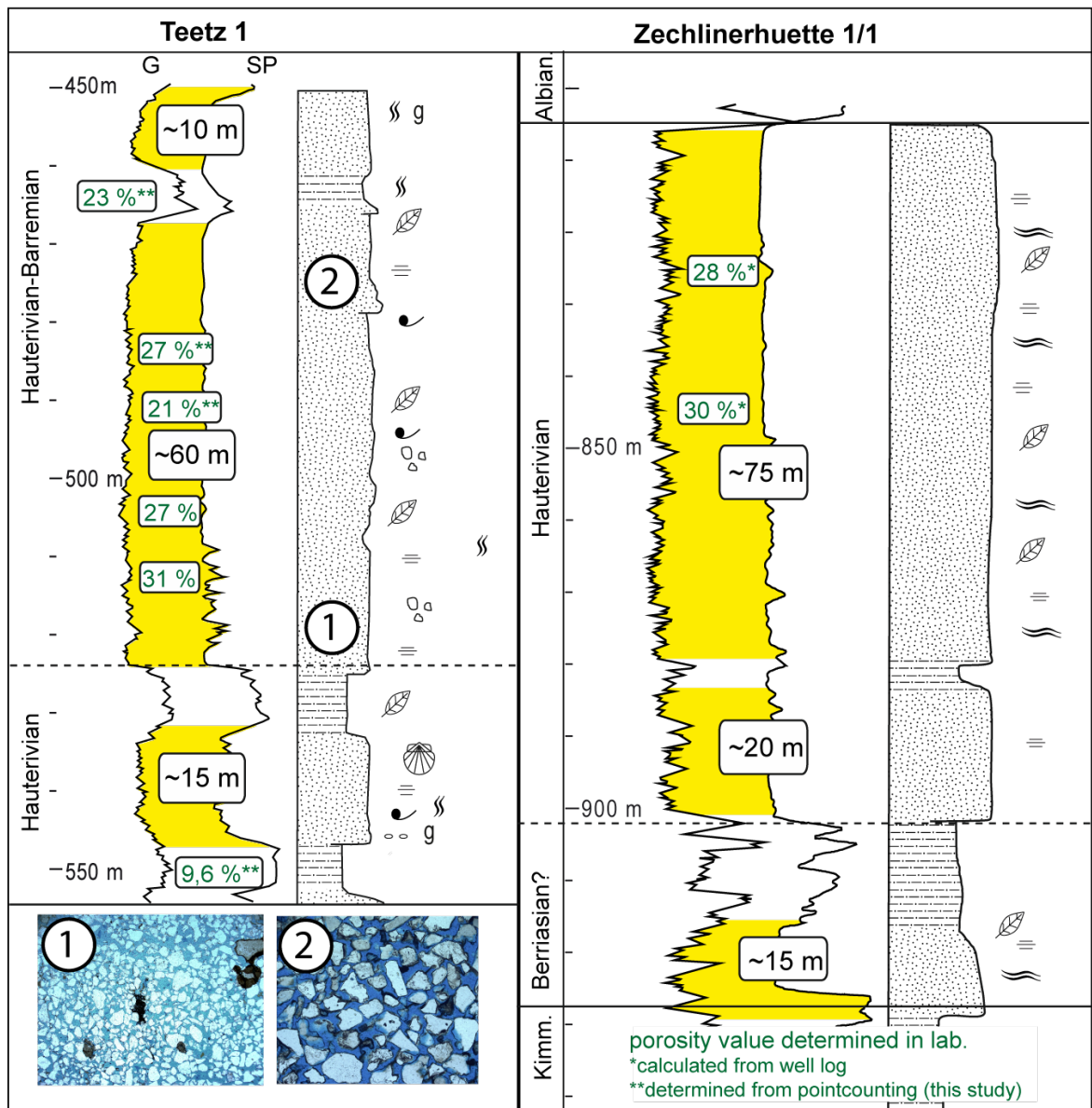


Fig. 41: Potential Hauterivian to Barremian geothermal reservoirs. The relatively homogenous sandstone stacks provide thicknesses up to 75 m and porosities up to 31 %. Single sandstone stacks are separated by 3–15 m thick silty-clayey layers.

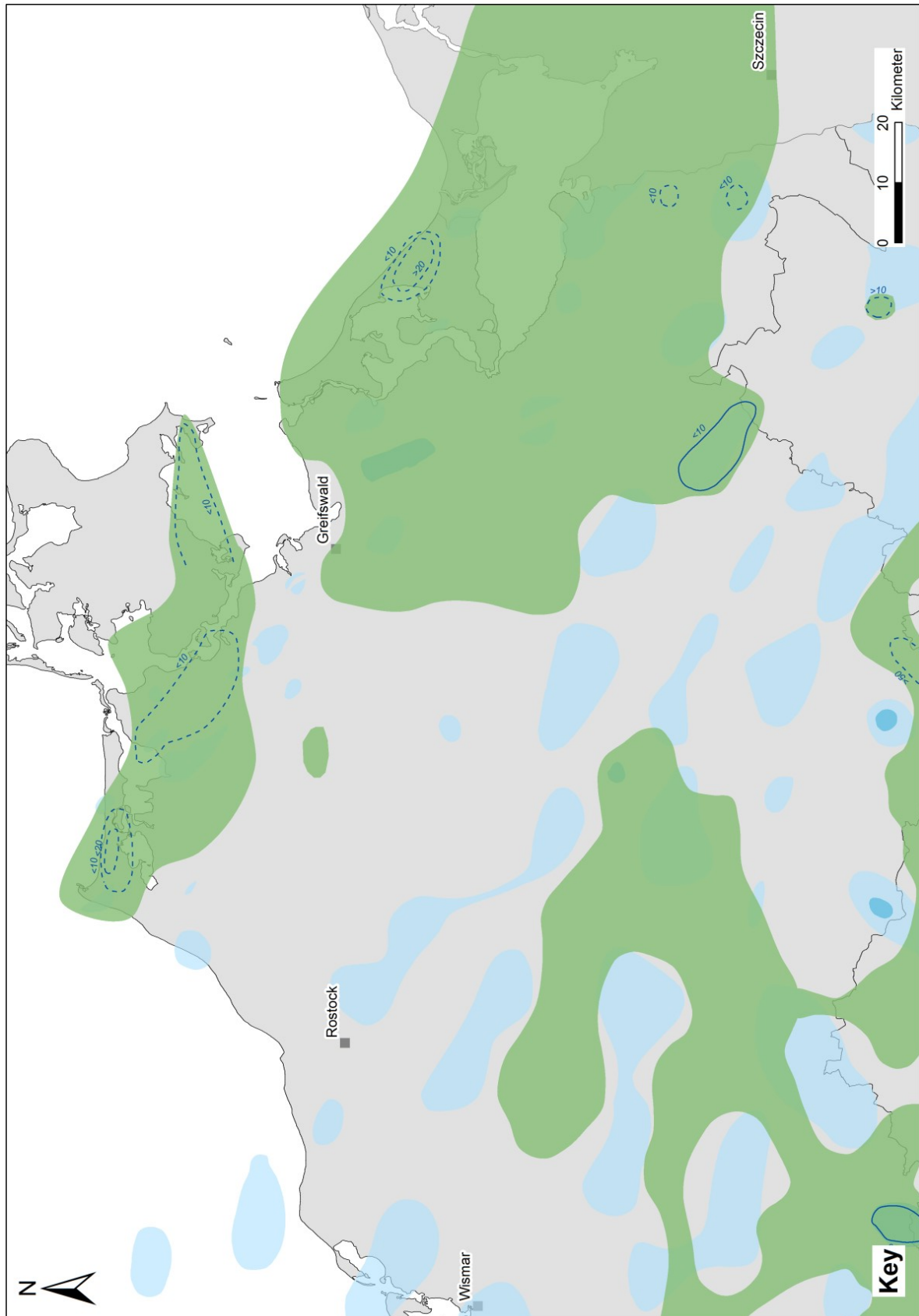


Fig. 42: Cumulative thickness of Hauterivian sandstone reservoirs in Western Pomerania, modified from Diener (1974) and own results.

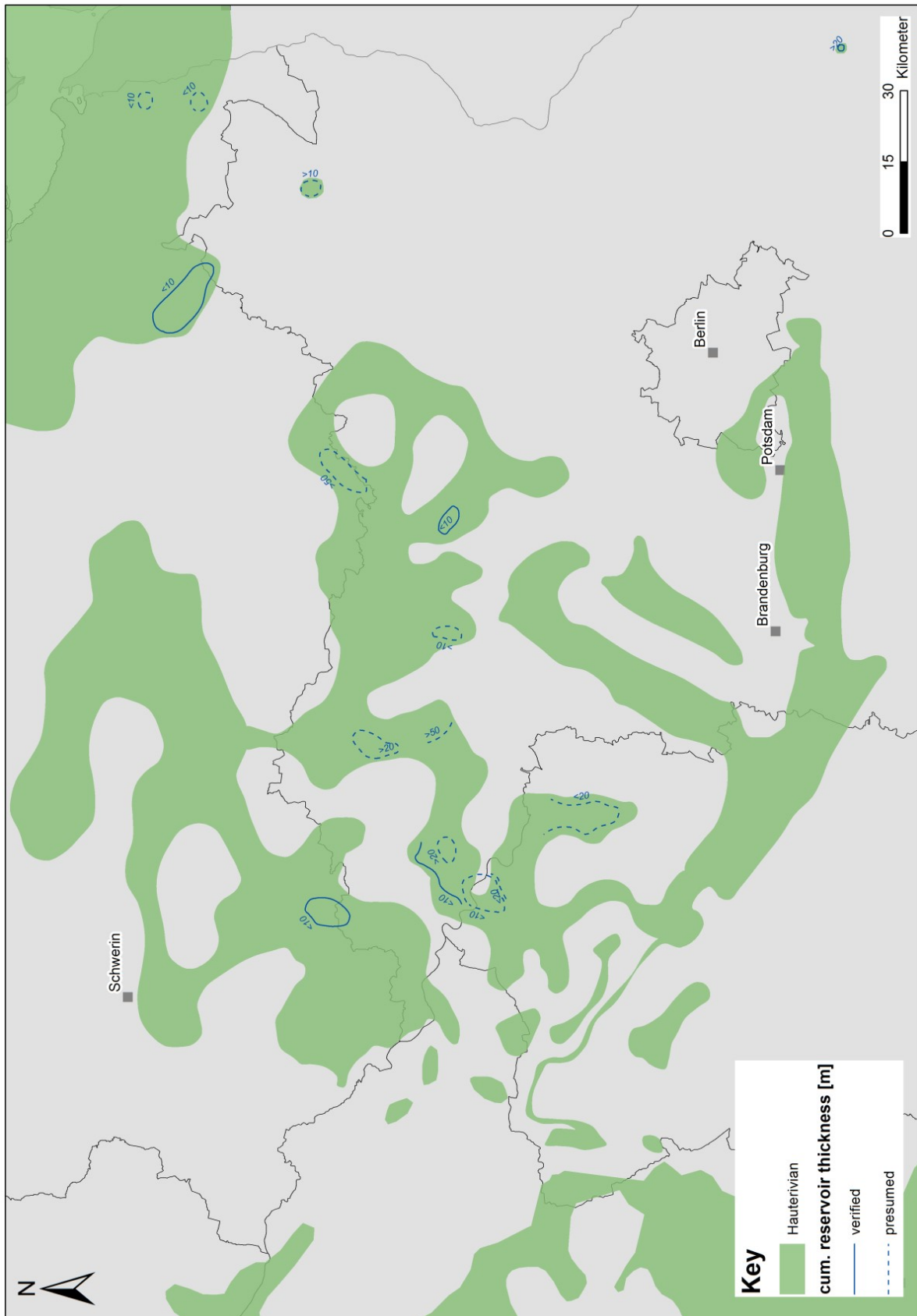


Fig. 43: Cumulative thickness of Hauterivian sandstone reservoirs in the Altmark Prignitz Basin, modified from Diener (1974) and own results

Geothermal Potential of Lower Cretaceous sandstones

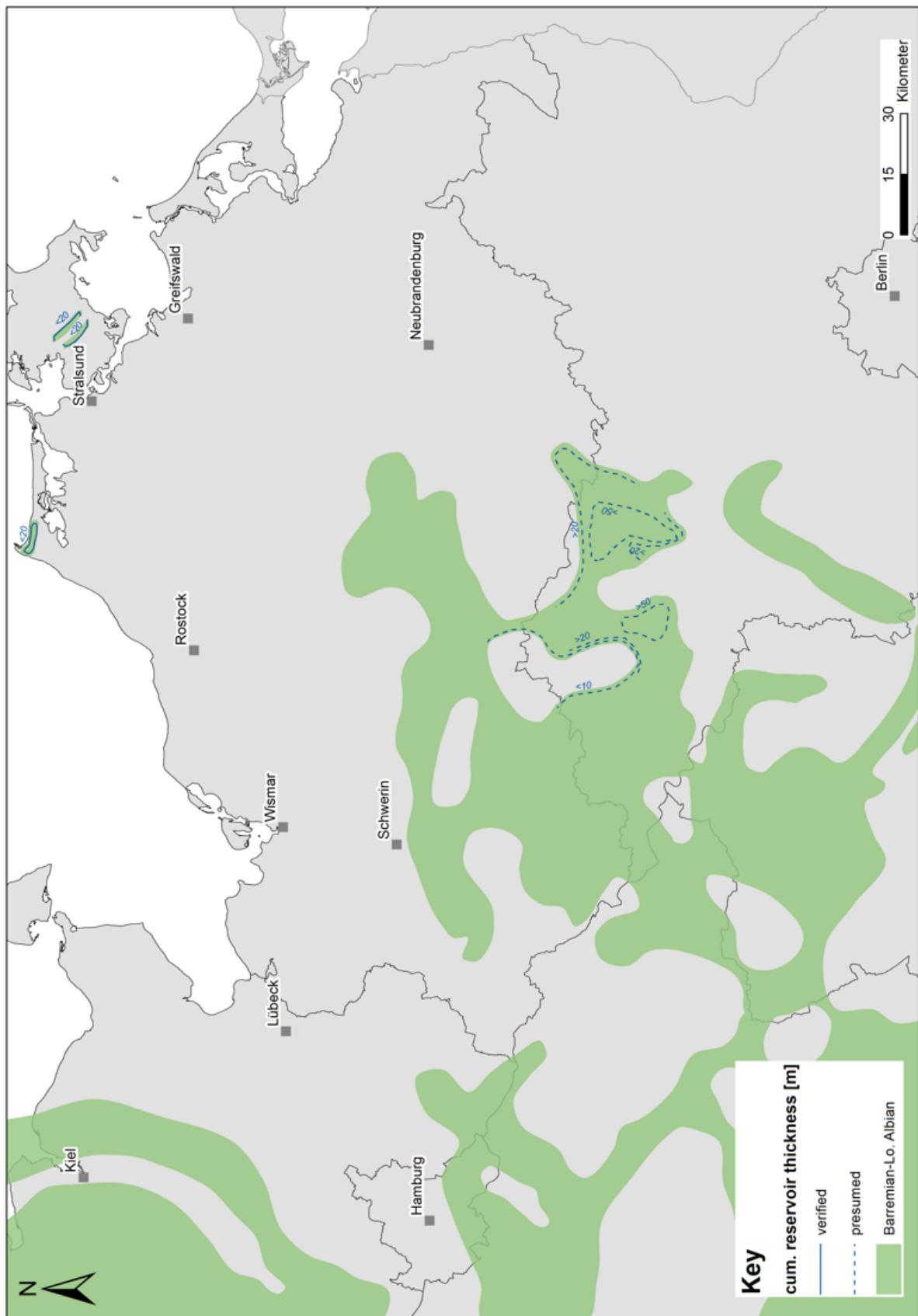


Fig. 44: Cumulative thickness of Barremian to Lower Albian sandstone reservoirs in the Altmark-Prignitz Basin, modified from Diener (1974) and own results.

### 8.3 Exploration examples

According to Diener et al. (1988, 1989) and Becker and Lenz (1991), highly effective sandstone reservoirs in depths of 150 m to 1000 m could be predicted in northeast Germany. In the vicinity of salt plugs, the strata were subsided into depths of > 1000 m and locally up to 1900 m e.g. Gt Pritzwalk 2. Limiting factors are locally decreased sandstone thicknesses due to post-depositional erosion and decreased temperatures at maximum  $\pm 40$  °C (Agemar et al., 2014; this study) combined to shallower depths < 1000 m. Therefore, the following three exploration sites are proposed for potential geothermal utilisation using a hydrothermal doublet system. For these potential sites, cumulative sandstone thickness, facies, depth and power supply infrastructures were evaluated. An alternative utilisation as Aquifer Thermal Energy Storage or Underground Gas Storage will also be discussed.

#### 8.3.1 Proposal 1: Wittstock/Dosse region

The proposed region is located in the rim-syncline near the salt structure Wrdenhagen/Königsberg. The development of three aquifer horizons is possible in combination with the overlying quarternary and tertiary aquifers (*Table 3*). Considering well data from Teetz 1 and Wredehagen 1, a nearly 120 m thick Lower Cretaceous potential reservoir could be provided in depths of 450–570 m. The basal part is separated by c. 5–10 m thick clay layers at 545–555 m and 530–525 m, whereas the overlying part provides silty fine-grained sandstones, separated by thin clayey laminae. Porosity data predict good values ranging from 21–31 %, and according to GeotIS (compiled well data, Agemar et al., 2014), moderate–good permeability data  $10^{-4}$ – $10^{-5}$  m/s but only moderate and relatively cool reservoir temperatures ranging from  $28$ – $31 \pm 4$  °C at 600 m depth. It can be concluded that the thermal energy extracted from this reservoir to provide heat supply using a doublet system would not be cost-efficiently. Therefore, a utilisation as Aquifer Thermal Energy Storage or Underground Gas Storage could be feasible regarding the good reservoir properties concerning porosity and permeability. Additionally, results from petrographical analysis of well Teetz 1 from this study confirm less cemented sandstones and high porosities. Potential customers for Aquifer Thermal Energy Storage could be the hospitals Kyritz (KMG Klinikum Kyritz) or Wittstock (KMG Klinikum Wittstock), a municipal energy supply system provided by the town of Wittstock.

Table 3: Properties of the potential reservoir in the Wittstock/Dosse region.

Stratigraphy	Aquifer	Reservoir thickness (m)	Porosity (%) permeability	Depth (m)	Temperature (°C)
Pleistocene	Coarse-grained sand, fine-gravel	60		0-60	14 ± 3 (100 m depth)
Tertiary	Clay/claystone, siltstone	0		60-390	
Oligocene-Eocene					
Barremian-Hauterivian	fine-grained sandstone, silty, thin clay laminae	70	21-31 % T/H =	450-525	28 ± 4 (500 m depth)
Hauterivian	fine-grained sandstone, thin clay laminae	15	10 <sup>-4</sup> – 10 <sup>-5</sup> m/s	530-545	
Berriasian	fine-grained sandstone, silt- and claystone	15		555-570	31 ± 4 (600 m depth)

### 8.3.2 Proposal 2: Rheinsberg region

The proposed region is located in the rim-syncline near the salt structure Dollgow. Quarternary and tertiary stratigraphy was reconstructed from well Gransee 2, and Hauterivian–Berriasian strata from well Gransee 3. The well Gransee 3 and the well Zechlinerhuetten 1, located 10 km away, give the reservoir information (Table 4). The development of three aquifer horizons would be possible in combination with the overlying quarternary and tertiary aquifers. Considering well data, a ~100 m thick Lower Cretaceous potential reservoir could be provided in depths of 1580–1675 m. The potential reservoir is a homogenous silty fine-grained sandstone, partly heterolithic bedded and separated by thin clayey laminae. Porosity data predict good values ranging from 28–30 %, and according to GeotIS (compiled well data, Agemar et al., 2014), suitable reservoir temperatures of ~67 ± 3 °C at 1600 m depth. Permeability data are not available. It can be concluded that this reservoir is suitable for geothermal use by a doublet system, irrespective of the cost efficiency. Alternatively, utilisation as Aquifer Thermal Energy Storage or Underground Gas Storage could be feasible regarding the good reservoir properties concerning porosity and permeability. Potential customers could be hospitals or municipal energy suppliers.



Table 4: Properties of the potential reservoir in the Rheinsberg region.

Stratigraphy	Aquifer	Reservoir thickness (m)	Porosity (%) permeability	Depth (m)	Temperature (°C)
<b>Pleistocene</b>	Silty coarse-grained sand, fine gravel, and tills	50	n.a.	0-50	14±3 (100 m depth)
<b>Tertiary Miocene</b>	Silty fine- medium-grained sandstones, coal/lignite layers	105	n.a.	135-241	28±4 (500 m depth)
<b>Hauterivian-Berriasian</b>	fine-grained sandstone, silty, thin clay laminae	70	28-30 %	1580-1675	67±3 (1600 m)

### 8.3.3 Proposal 3: Werle region

The proposed region is located in the rim-syncline and the vicinity of the salt structure Werle, which was extensively prospected during the 1950s to 1970s. Considering well data from Werle 3, 19, 20, 23 and 101, a nearly 70–100 m thick Lower Cretaceous potential reservoir could be provided in 780–930 m (Table 5). Varying aquifer depths from 600 to 1000 m results from sediment accumulation in rim-synclines. The maximum 25 m thick single sandstone stacks are interbedded by siltstone- and up to 30 m thick clay layers. Porosity data predict moderate to good values ranging from 19,5 % in silty layers to 30 % in and, according to GeotIS (Agemar et al., 2014), relatively cool reservoir temperatures range from  $44 \pm 3$  °C at 900 m depth. In summary, the aquifer is suitable for geothermal use by a doublet system, irrespective of the cost efficiency. Concerning the good reservoir properties concerning porosity and permeability, utilisation as Aquifer Thermal Energy Storage or Underground Gas Storage could also be feasible. Potential customers could be the town of Grabow's municipal energy supply system.

Table 5: Properties of the potential reservoir in the Werle region.

Stratigraphy	Aquifer (Werle 23)	Reservoir thickness (m)	Porosity (%) permeability	Depth (m)	Temperature (°C)
<b>Berriasian</b>	Fine-medium-grained sandstone, siltstone, claystone	71	19-30 % n.a.	786-930	44 ± 3 (900 m) 50 ± 3 (1000 m)

## 9 Conclusions

The results of this study show the importance of evaluating how tectono-stratigraphic and eustatic features influence the present-day petrophysical characteristics, distribution and thickness of Lower Cretaceous sandstone aquifers. The main outcomes of this study enhance the knowledge of the bio- and sequence stratigraphy and palaeogeography of the Lower Cretaceous in the eastern North German Basin and provide new insights into the basin evolution, granulometric, petrophysical and petrological information of the potential sandstone aquifers.

Biostratigraphic zonation in the eastern North German Basin is partly provided by brackish-marine marker species. Dominating terrestrial and shallow-marine conditions do not enable completely the same biostratigraphic time control as applied in the western North German Basin. However, characteristic ostracod, spore, pollen, foraminifera and dinocyst species could be identified combined with lithostratigraphic characteristics a time control on the Lower Cretaceous strata is enabled. The eastern basin part was well connected to boreal and tethyal waters, although regressive conditions temporarily hampered faunal migration. Sea-level fluctuations triggered the progradation of deltas during regression, especially in Berriasian times.

Despite the dominating extensional tectonic regime assigned to Lower Cretaceous times, the study area revealed widespread erosional patterns implying differential uplift and erosion. A pre-Late Cretaceous uplift of the Pompeck Block eroded up to 450 m of Berriasian to Albian strata and several hundred meters of Upper Jurassic strata in the northeastern North German Basin. The formation and activity of swell areas and salt movement contributed much to basin differentiation, the formation of local sub-basins and strata thickness. Three main unconformities could be figured out. Generally, the stratigraphic most complete successions kept preserved in syn-tectonic graben structures in northeast Germany and the rim synclines of salt plugs. However, they also lack a complete stratigraphic succession, except in the vicinity of the Lower Saxony Basin.

Petrographic analysis shows that the investigated sandstones are highly mature and influenced by diagenetic features, which enable high porosities and high permeabilities depending on the depositional environment. The grain fabric was stabilised by an eodiagenetic carbonate cement, which was dissolved during telodiagenetic uplift. Differences between porosity, permeability and lithofacies are documented. Channel-belt sandstones and shallow-marine shoreface sandstones yield higher values and thicker sandstone stacks than sheetsands or crevasse splays due to the occurrence of grain coatings, clayey matrix associated with terrestrial environments and occurring cementation. Glauconite and

phosphorous nodules formation indicate starved sedimentation and less terrigenous input during Hauterivian to Albian times. The analysis of the grain-size distribution shows a constant trend, which suggests a relatively stable sediment source area. Corresponding to the heavy mineral assemblage, which is characterised by an ultrastable magmatic and partly metamorphic heavy mineral assemblage located on the Fennoscandian High.

The analysis of the depositional environments revealed deposits from a lagoonal or tidal flat, deltaic channel belt facies and alternating sand-, silt- and claystone successions from an upper and lower delta plain. Furthermore, delta front, prodelta and shoreface deposits were analysed, and full marine incursions are suggested by chalcedony cement layers. Condensed sections, desiccation cracks and delta progradation are evident for regressive phases as well as the formation of evaporitic and lagoonal environments. The ongoing subordinated basin extension and flooding are characterised by the formation of shoreface sands, fine clastics from the shelf transition zone and pelagic limestones and mudrocks combined to a fully marine microfauna.

Lower Cretaceous strata locally provide highly effective sandstone reservoirs regarding thickness, permeabilities and porosities. The most promising reservoir sandstones were located within the Berriasian Wealden-type channel-belt sandstones and Hauterivian to Barremian shallow-marine shoreface sandstones. Limiting factors are locally strong varying sandstone thickness and decreased temperatures due to post-depositional erosion and shallow depths.

## **10 Further perspectives**

A comprehensive understanding of depositional environments is much important to the analysis and exploration of geothermal aquifers. Sedimentary basin evolution influences the formation and development on depositional environments, lithofacies patterns resulting in the potential aquifer depth, thickness and petrophysical characteristics. These factors are essentially for the prediction of hydrogeothermal aquifer availability and quality. Yet again, this study shows that the evaluation of aquifer characteristics is also site-specific and therefore a detailed analysis is necessary. Although the understanding of basin evolution and litho-stratigraphic development has been improved by this study, the following points need further examination:

- (I) A more extensive lithofacies analysis and declaration of facies type enable a better direct correlation from the depositional environment to petrophysical reservoir parameters and therefore a better reservoir prediction.
- (II) Time resolution is a main point in the understanding of basin evolution. Due to mainly sandy lithologies, the preservation of microfossils is limited. However, re-evaluation of core samples from this study gave new insights in the fossil record. The re-evaluation of further samples regarding microfossils would improve the time control of the Lower Cretaceous deposits and enable the application of a sequence-stratigraphic framework.
- (III) This framework would enhance the understanding of basin differentiation for the prediction of thickness and distribution patterns of potential sandstone aquifer horizons.
- (IV) The evaluation of thermochronological data like e.g. apatite and zircon fission track or fluid inclusions would improve the reconstruction of thermal basin history and the understanding of the basin evolution.

## Curriculum vitae

Name Sandra Franke  
Geburtsdatum 23.10.1989  
Geburtsort Saalfeld (Saale)

### Ausbildung

1996-2000 Grundschule Kamsdorf  
2000-2008 Heinrich-Böll-Gymnasium, Saalfeld

### Studium

2008-2014 Diplom-Studiengang in Geologie, Universität Jena  
2014-2016 Wissenschaftliche Hilfskraft an der Universität Jena

### Beruf

2016-2019 Wissenschaftliche Mitarbeiterin im Projekt GeoPoNDD, Universität Göttingen. Wissenschaftliche Mitarbeiterin am Geowissenschaftlichen Zentrum, Arbeitsgruppe Angewandte Geologie, Projektmitarbeit zur Charakterisierung der geothermischen Unterkreidereservoirs im Norddeutschen Becken.

2019-2021 Wissenschaftliche Mitarbeiterin am Landesamt f. Bergbau, Energie und Geologie, Hannover. Referat Geologische Grundlagen und AG Endlagerung,  
-Stellungnahmen nach § 21 StandAG,  
-Bohrkernaufnahme, Aufschlussdokumentation, Qualitätsmanagement Bohrdaten.

seit 02/2022 Mitarbeiterin im Fachbereich Geothermie, JENA GEOS Ingenieurbüro GmbH, Jena.  
-Standortanalysen und Machbarkeitsstudien zu geothermischen Potenzialen für Quartier- und Gebäudeumrüstung und (Quartier)-Neubau.  
-FuE-Projekte zur Wasserstoffspeicherung  
-Bohrbetreuung

## **Bibliography**

Abbink, O.A. 1998. Palynological identification in the Jurassic of the North Sea region. Laboratory of Palaeobotany & Palynology contribution series 8, 1–192.

Abbink, O.A., van Konijnenburg-van Cittert, J.H.A., Visscher, H., 2004a. A sporomorph ecogroup model for the northwest European Jurassic–Lower Cretaceous I: concepts and framework. *Neth. J. Geosci. (Geol. Mijnbouw)* 83 (1), 17–31.

Abbink, O.A., van Konijnenburg-van Cittert, J.H.A., van der Zwan, C.J., Visscher, H., 2004b. A sporomorph ecogroup model for the northwest European Jurassic–Lower Cretaceous II: application to an exploration well from the Dutch North Sea. *Neth.*

AGEB, 2022. Energieverbrauch in Deutschland im Jahr 2021. – Energieverbrauch 2021 wächst durch Pandemie und Wetter. Arbeitsgemeinschaft Energiebilanzen (AG Energiebilanzen). Berlin.

Agemar, T., Alten, J.-A., Ganz, B., Kuder, J., Kühne, K., Schumacher, S. & Schulz, R. 2014. The Geothermal Information System for Germany – GeotIS. – *ZDGG, German Journal of Geology*, 165, 2: 129-144.

Ahrlrichs, N., Hübscher, C., Noack, V., Schnabel, M., Damm, V., & Krawczyk, C. M. 2020. Structural evolution at the northeast North German Basin margin: From initial Triassic salt movement to Late Cretaceous - Cenozoic remobilization. *Tectonics*, 39

Al Hseinat, M., & Hübscher, C. (2017). Late Cretaceous to recent tectonic evolution of the North German Basin and the transition zone to the Baltic Shield/southwest Baltic Sea. *Tectonophysics*, 708, 28–55.

Allan, M. M., Turner, A., Yardley, B. W. D. 2011. Relation between the dissolution rate of single minerals and reservoir rocks in acidified pore waters. *Appl Geochem* 26:1289–1301

Bachmann, G. H.; Voigt, T.; Bayer, U.; Eynatten, H. von; Legler, B.; Littke, R.; Breitzkreuz, Ch.; Geißler, M.; Schneider, J.; Kiersnowski, H.; Stollhofen, H.; Barnasch, J.; Beutler, G.; Franz, M.; Kästner, M.; Mutterlose, J.; Radies, D.; Reicherter, K.; Voigt, S.; Kley, J.; Sirocko, F.; Lehné, R.; Hübscher, Ch.; Winsemann, J.; Stackebrandt, W. 2008. Basin Fill. In: *Dynamics of Complex Intracontinental Basins* (Eds. Littke, R., Bayer, U., Gajewski, D., Nelskamp, S.), 156–245.

Bachmann, G., Geluk, M., Warrington, G., Becker - Roman, A., Beutler, G., Hagdorn, H., et al. (2010). Triassic. In H. Doornenbal, & A. Stevenson (Eds.), *Petroleum geological atlas of the southern Permian Basin area* (pp. 149–173). Houten, Netherlands: European Association of Geoscientists & Engineers.

Badley, M. E., Price, J. D., Rambech Dahl, C., & Agdestein, T., 1988. The structural evolution of the northern Viking Graben and its bearing upon extensional modes of basin formation. *Journal of the Geological Society* 145.3, 455-472.

Baldschuhn, F & Kockel, F. 1996. *Geotektonischer Atlas von Nordwestdeutschland* (Bundesanstalt für Geowissenschaften und Rohstoffe, Hannover)

Bally, A. W., Snelson, S. 1980. Realms of subsidence. In: *Facts and Principles of World Petroleum Occurrence* (Ed. A.D. Miall), *Can. Soc. Pet. Geol. Mem.*, 6 (1980), pp. 9-94.

Bartenstein, H., Brand, E., 1951. Mikropaläontologische Untersuchungen zur Stratigrafie des Nordwestdeutschen Valendis. Abh. Senck. Naturfosch. Ges., 485, 239-336.

Bartenstein, H. 1962. Die Biostratigrafische Einordnung des NW-Deutschen Wealden und Valendis in die schweizerische Valendis-Stufe. Paläont.Z, H.-Schmidt-Festband, 1-7.

Becker, U., Lenz, G. 1991. Zusammenstellung und Auswertung der Testergebnisse ausgewählter Speicher des Mesozoikums. Blatt Neubrandenburg/Torgelow. Teilbericht in: Geothermische Ressourcen im Nordteil der DDR, Blatt Neubrandenburg/Torgelow. (Ed. Diener, I. et al., 1989).

Beutler, G., Junker, R., Niediek, S., Rößler, D. 2012. Tektonische Diskordanzen und tektonische Zyklen im Mesozoikum Norddeutschlands. Zeitschrift der Deutschen Gesellschaft für Geowissenschaften 163/4, 447–468.

Borchert, H. 1964. Über Faziestypen von marinen Erzlagerstätten. Berichte der geologischen Gesellschaft in der DDR. 9. Band, Heft 2, 163-193.

Bornemann, A., Heunisch, C. 2017. Mikropaläontologischer Untersuchungsbericht der Kernbohrung Ückeritz 1/64. LBEG Hannover, unpublished. pp. 10.

Brockamp, O. 1976. Vulkanismus in der Unter- und Oberkreide in Norddeutschland. Aufsatz. Sedimentpetrografisches Institut der Universität Göttingen.

Bruns, B., Di Primio, R., Berner, U. and Littke, R. 2013. Petroleum system evolution in the inverted Lower Saxony Basin, northwest Germany: a 3D basin modeling study. *Geofluids* 13, 246-271

Bundesministerium für Wirtschaft und Klimaschutz (BMWK), 2022. Geothermie für die Wärmewende – Bundeswirtschaftsministerium startet Konsultationsprozess. Pressemitteilung Energiewende vom 11.11.2022. <https://www.bmwk.de/Redaktion/DE/Pressemitteilungen/2022/11/20221111-geothermie-fuer-die-waermewende.html>, Stand: 28.03.2023.

Christensen, O. B. 1965. The Ostracod Genus *Dicrorygma* POAG 1962 from Upper Jurassic and Lower Cretaceous. Geological Survey of Denmark, II. No. 90. Copenhagen.

Cooper, M. A., Williams, G. D., De Graciansky, P. C., Murphy, R. W., Needham, T., De Paor, D., Stoneley, R., Todd, S., Turner, J.P., and Ziegler, P. A. 1989. Inversion tectonics—a discussion, in: *Inversion tectonics*, edited by: Williams, G. D., and Cooper, M. A., Geological Society, London, Special Publications, 44.1, 335-347.

Cord-Ruwisch R, Seitz HJ, Conrad R. 1988. The capacity of hydrogenotrophic anaerobic bacteria to compete for traces of hydrogen depends on the redox potential of the terminal electron acceptor. *Arch Microbiol* 149:350–357

Deutschmann, A., Meschede, M., & Obst, K. 2018. Fault system evolution in the Baltic Sea area west of Rügen, NE Germany. Geological Society, London, Special Publications, 469(1), 83-98.

Dickinson, W., Beard, L., Brakenridge, G., Erjavec, J., Ferguson, R., Inman, K., Knepp, R., Lindberg, F., Ryberg, P., 1983. Provenance of North American Phanerozoic sandstones in relation to tectonic setting. *Geological Society of America Bulletin* 94, 222–235.

Diener, I. 1968. Kreide. In: *Grundriß der Geologie der Deutschen Demokratischen Republik* (Ed. Zentrales Geologisches Institut Berlin).

Diener, I. 1974. Stratigraphie, Lithologie und Paläogeographie der Unterkreide in der DDR Ernst-Moritz-Arndt Universität Greifswald, 286 pp. (PhD thesis).

Diener, I., Katzung, G., Kühn, P., Pasternak, G., Rusitzka, I., Tessin, R., Wormbs, J. 1988. Geologische Expertise über die Zweckmäßigkeit der Weiterführung geothermischer Untersuchungen im großraum Berlin. Teil 2. (Ed. Zentrales Geologisches Institut Berlin).

Diener, I., Wormbs, J., Rusitzka, I., Pasternak, G., Tesch, M., Toleikis, R., 1989. Geothermische Ressourcen im Nordteil der DDR(II) – Blatt Neubrandenburg/Torgelow (unpublished). VEB Kombinat Geologische Erkundung Nord, Zentrales Geologisches Institut.

Diener, I., Rusbült, J, Reich, M., 2004. Unterkreide. In Geologie von Mecklenburg-Vorpommern ( Ed. Katzung, G.), 164-173.

Dincer, I, Dost, S., Li, X., 1997. Performance analyses of sensible heat storage system for thermal applications. International Journal of Energy Research, 21, pp. 1157-1171

Doelling, R., J., Schulte, I. 2010. Deep Groundsourced Heat Exchanger with Coaxial Pipe, Closed Water Circuit –Improvement Proposals in Project Development and Technical Pipe Conception. Proceedings World Geothermal Congress 2010. Indonesia.

Dörhöfer, G., 1977. Palynologie und Stratigraphie der Bückeberg-Formation (Berriasium-Valanginium) in der Hilsmulde (NW-Deutschland). - Geol. Jb., A42: 1–122; Hannover.

Dörhöfer, G., Norris, G. 1977a. Palynostratigraphische Beiträge zur Korrelierung jurassisch-kretazischer Grenzsichten in Deutschland und England. N. Jb. Geol. Paläont. Abh., 153: 50-69, Stuttgart.

Dörhöfer, G., Norris, G. 1977b. Discrimination and Correlation of Highest Jurassic and Lowest Cretaceous Terrestrial Palynofloras in North-West Europe. Palynology 1, 79-93, Austin, Texas.

Dörhöfer, G., (1977c): Palynologie und Stratigraphie der Bückeberg-Formation (Berriasium-Valanginium) in der Hilsmulde (NW-Deutschland). - Geol. Jb., A42: 1–122; Hannover.

Döring, H., 1963. Bericht über die sporen- und planktonstratigraphische Einstufung des „Wealden“ der Bohrung Usedom 1/60. Zentrales Geologisches Institut, Berlin.

Döring, H., 1965a. Die sporenpaläontologische Gliederung des Wealdens in Westmecklenburg (Struktur Werle). Zeitschrift für das Gesamtgebiet der Geologie und Mineralogie sowie der Angewandten Geophysik – Geologie, Beiheft 47, Jg 14, 1-118.

Döring, H., 1965b. Stratigrafischer Verbreitung der Sporengattung Gleicheniidites und Trubasporites im Jura-Kreide-Grenzbereich. Abhandlungen des Zentralen Geologischen Instituts. Heft 1, 191-209.

Döring, H., 1966. Sporenstratigrafischer Vergleich zwischen dem Wealden Norddeutschlands und Südenglands. Beiheft zur Zeitschrift Geologie, Beiträge zur Sporenpaläontologie. II, Band 55/1966, 102-129.

Döring, H. 1966a. Sporenstratigraphische Untersuchungen in unterkretazischen Ablagerungen der Bohrung Darßer Ort 1/60. Bericht-Nr. 53/66. Zentrales Geologisches Institut, Berlin.



Döring, H., Eiermann, H., Haller, W., Wienholz, E., 1970. Bericht Nr. EE 74/70. Biostratigraphische Untersuchungen des Malm und Wealden im südlichen Mittelrügen. Zentrales Geologisches Institut, Berlin. unpublished.

Döring, H., Eiermann, H., Haller, W., Wienholz, E., 1969/70. Biostratigraphische Untersuchungen im Malm und Wealden der Insel Rügen. Geologisches Jahrbuch Band 5/6. 711-783.

Dreyer, E. 1969., Mikropaläontologische Bearbeitung einiger Proben der Bohrung Ückeritz 1. Forschungsinstitut für die Erkundung und Förderung von Erdöl und Erdgas, Gommern.

Dreyer, E., 1971. Mikropaläontologie der Unterkreide der Bohrung Brome 2/63. Forschungsinstitut für die Erkundung und Förderung von Erdöl und Erdgas, Gommern.

Einsele, G., 1992. Sedimentary Basins. Evolution, Facies, and Sediment Budget. 628 pp. Berlin, Springer-Verlag.

Elstner, F., 1991. Abriß der Stratigraphie, in Das Gasfeld Thönse in Niedersachsen – Ein Unikat - . Niedersächsische Akademie der Geowissenschaftlichen Veröffentlichungen, Heft 6, 11-14.

Elstner, F., Mutterlose, J., 1996. The Lower Cretaceous (Berriasian and Valanginian) in NW Germany. *Cretaceous Research* 17, 119-133.

Erbacher, J., Hiss, M., Luppold, F., Mutterlose, J., 2014. Bückeberg-Gruppe. In: LithoLex (online database). BGR, Hannover (last updated 24 November 2014).

v. Eynatten, H. v., Voigt, T., Meier, A., Franzke, H.-J., Gaupp, R., 2006. Provenance of the Cretaceous clastic Subhercynian Basin fill: constraints to exhumation of the Harz Mountains and timing of inversion tectonics in Central Europe. - *International Journal of Earth Sciences*. 97, 1315-1330.

v. Eynatten, H., Voigt, T., Meier, A., Franzke, H.-J., and Gaupp, R.: Provenance of the clastic Cretaceous Subhercynian Basin fill: constraints to exhumation of the Harz Mountains and the timing of inversion tectonics in the Central European Basin, *Int. J. Earth Sci.*, 97, 1315–1330, 2008.

v. Eynatten, H., Dunkl, I., Brix, M., Hoffmann, V.-E., Raab, M., Thomson, S. N., Kohn, B., 2019. Late Cretaceous exhumation and uplift of the Harz Mountains, Germany: a multi-method thermochronological approach- *International Journal of Earth Sciences*. 108, 2097-2111.

v. Eynatten, H., Kley, J., Dunkl, I., Hoffmann, V.-E., and Simon, A., 2020. Late Cretaceous to Paleogene exhumation in central Europe – localized inversion vs. large-scale domal uplift, *Solid Earth*, 12, 935–958

Flesch, S., Pudlo, D., Albrecht, D., Jacob, A., Enzmann, F., 2018. Hydrogen underground storage—Petrographic and petrophysical variations in reservoir sandstones from laboratory experiments under simulated reservoir conditions. *International Journal of Hydrogen Energy*, Volume 43, Issue 45, 20822-20835,

Folk, R. L., & Ward, W. C., 1957. Brazos River bar [Texas]; a study in the significance of grain size parameters. *Journal of sedimentary research*, 27(1), 3-26.

Franz, M., Wolfgramm, M., Barth, G., Nowak, K., Zimmermann, J., Budach, I., Thorwart, K., 2015. Schlussbericht Verbundprojekt: Identifikation hydraulisch geeigneter Bereiche innerhalb der mesozoischen Sandsteinaquifere in Norddeutschland.

Franz, M., Barth, G., Zimmermann, J., Budach, I., Nowak, K. & Wolfgramm, M., 2018. Geothermal resources of the North German Basin: exploration strategy, development examples and remaining opportunities in Mesozoic hydrothermal reservoirs. In: Mesozoic Resource Potential in the Southern Permian Basin. Ed. by B. Kilhams, P. A. Kukla, S. Mazur, T. McKie, H. F. Mijnlief & K. van Ojik. London: The Geological Society, 193–222.

Frisch, U., Kockel, F., 2004. Kreide. In Der Bremen-Knoten im Strukturnetz Nordwest-Deutschlands: Stratigraphie, Paläogeographie, Strukturgeologie (Eds. Frisch, U., Kockel, F.) Berichte aus dem Fachbereich Geowissenschaften der Universität Bremen 223.

Fritzsche, H., Doß, H., 1980. 2. Ergebnisbericht zum AP Fuhlendorf. Fuhlendorf 1.1 und Nachinterpretation Zechstein Barther Bodden. VEB Kombinat EE Gommern. 138 Anlagen.

Füchtbauer, H., 1988. Sedimente und Sedimentgesteine. E. Schweizerbart'sche Verlagsbuchhandlung, Stuttgart.

Garzanti, E., Ando, S., 2007. Heavy Mineral concentration in modern sands: implications for provenance interpretation. *Developments in Sedimentology*, Vol. 58, 517-545.

Graversen, O., 2004a: Upper Triassic-Lower Cretaceous seismic sequence stratigraphy and basin tectonics at Bornholm, Denmark, Tornquist Zone, NW Europe. *Marine and Petroleum Geology* 21, 579-612.

Graversen, O., 2004b: Upper Triassic-Cretaceous seismic stratigraphy and structural inversion offshore SW Bornholm, Tornquist Zone, Denmark. *Bulletin of the Geological Society of Denmark*, 51, 111-136.

Hänel, R., Kleefeld, M., Koppe, I., 1984. Geothermisches Energiepotential, Pilotstudie: Abschätzung der geothermischen Energievorräte an ausgewählten Beispielen in der Bundesrepublik Deutschland.- Abschlußbericht, Archiv-Nr. 96 276, Bd. I-IV; Hannover

Haq, B.U., Hardenbol, J., Vail, P.R. 1987. Chronology of fluctuating sea levels since the Triassic. *Science* 235, 1156-1167.

Haq, B.U., Hardenbol, J., Vail, P.R. 1988. Mesozoic and Cenozoic chronostratigraphy and cycles of sea-level change. *Soc. Econ. Paleontol. Mineral.* 42, 71–108.

Haq, B.U., Al-Qahtani, A.M. 2005. Phanerozoic cycles of sea-level change on the Arabian Platform. *GeoArabia* 10, 127–160.

Haq, B.U. 2014. Cretaceous eustasy revisited . *Global and Planetary Change* 113, 44-58.

Hardenbol, J., Robaszynski, F., 1998. Introduction to the Upper Cretaceous. In: de Graciansky, P.-C., et al. (Eds.), *Mesozoic and Cenozoic Sequence Stratigraphy of European Basins*. SEPM Special Publication, 60, pp. 329–332.

Haupt, J. 1961. Untersuchungsbericht zur Glaukonitentstehung einer Probenserie der Teufe 165-170 m. 11/61. VEB Geologische Erkundung Nord. unpublished

Haupt, J., Heppner, R. 1962. Abschlussbericht des VEB Geologische Erkundung Nord über die Kartierungsbohrung Darßer Ort 1/60. 18 Anlagen. unpublished.

Hallam, A. 1971. Mesozoic Geology and the Opening of the North Atlantic. *The Journal of Geology* Vol. 79, 2.

Henkel, S., Pudlo, D., Gaupp, R., 2013. Research sites of the H2STORE project and the relevance of lithological variations for hydrogen storage at depths. *Energy Procedia* 40. 25–33.

Hesse, R., Gaupp, R. 2021. *Diagenese klastischer Sedimente*. Springer Verlag. pp. 513.

Heunisch, C. 2019. Palynologischer Untersuchungsbericht der Kernbohrung Darßer Ort 1/60. LBEG Hannover, unpublished. pp. 7.

Hiss, M., Niebuhr, B., Teipel, U. 2018. Die Kreide in der Stratigraphischen Tabelle von Deutschland 2016. *Zeitschrift der Deutschen Gesellschaft für Geowissenschaften* 169/2, 247–266.

Hoth, K., Rußbült, J., Zagora, K., Beer, H., Hartmann, O. 1993. Die tiefen Bohrungen im Zentralabschnitt der Mitteleuropäischen Senke - Dokumentation für den Zeitabschnitt 1962 - 1990.- *Schriftenreihe für Geowissenschaften*, 2: 1-145; Berlin.

Hübner, Rasch, 1971. Abschlussmonatsbericht der Forschungsbohrung E-Gorlosen 12/71. VEB Erdöl und Erdgas Grimmen, unpublished.

Hübscher, C., Hansen, M., Trinanes, S., Lykke - Andersen, H., & Gajewski, D. (2010). Structure and evolution of the Northeastern German Basin and its transition onto the Baltic Shield. *Marine and Petroleum Geology*, 27(4), 923–938.

Japsen, P., Green, P. F., Bonow, J. M., Erlström, M., 2016. Episodic burial and exhumation of the southern Baltic shield: Epeirogenic uplifts during and after break-up of Pangea. *Gondwana Research* 35, 357-377.

Jaritz, W. 1969. Epirogenese in Nordwestdeutschland im höheren Jura und in der Unterkreide. *Geologische Rundschau* 59, 114-124

Jaritz, W. 1980. Einige Aspekte der Entwicklungsgeschichte der nordwestdeutschen Salzstöcke. *Zeitschrift der deutschen geologischen Gesellschaft* 131, 387-408

Jans, C. V., Wray, D. S., Merriman, R. J., Fisher, M. J. 2000. Volcanogenic clays in Jurassic and Cretaceous strata of England and the North Sea Basin. *Clay Minerals* 35, 25-55.

Kabus, F., Lenz, G., Wolfgramm, M., Hoffmann, F., Kellner, T., 2003. Studie zu den Möglichkeiten der Stromerzeugung aus hydrothermalen Geothermie in Mecklenburg-Vorpommern. *GTN-Bericht* 4383, 148 S.

Kabus, F., & Seibt, P., 2000. Aquifer thermal energy storage for the Berlin Reichstag building-new seat of the German parliament. In *Proceedings of the World Geothermal Congress*. 3611-3615.

Katzung, G. 1984. *Geothermie-Atlas der Deutschen Demokratischen Republik*. Zentrales geologisches Institut Berlin. p. 27

Katzung, G., Diener, I., Kühn, P., 1992. Temperaturverteilung im Untergrund Ostdeutschlands und für die Nutzung der geothermischen Ressourcen in Betracht kommenden Aquifere. *Braunkohle* 1992, 27–32.

- Katzung, G., Ehmke, G. 1993. Das Prätertiär in Ostdeutschland. Strukturstockwerk und ihre regionale Gliederung. Verlag Sven von Loga. Köln.
- Köhler, E., König, H. 1965. Ergebnisbericht Reflexionsseismik Darß-Wustrow (Spezial). VEB Erdöl- und Erdgaserkundung Grimmen. 62 Anlagen.
- Kemper, E. 1973. Das Berrias (tiefe Unterkreide) in NW-Deutschland. Geologisches Jahrbuch A9, 47-67
- Kemper, E. 1979. Die Unterkreide Nordwestdeutschlands. Ein Überblick. In: Aspekte der Kreide Europas (Ed. Wiedemann, J.) Int. Union of Geol. Sciences, Serie A6, 1-9
- Kleinitz W, Boehling E (2005) Underground gas storage in porous media—operating experience with bacteria on gas quality. Paper SPE 94248 presented at the SPE Europec/EAGE Annual Conference held in Madrid 13–16 June 2005
- Kley, J., & Voigt, T. 2008. Late Cretaceous intraplate thrusting in central Europe: Effect of Africa-Iberia-Europe convergence, not Alpine collision. *Geology*, 36(11), 839–842.
- Kockel, F. 1998. Geotektonischer Atlas von Nordwest-Deutschland 1:300 000. Die paläogeographische und strukturelle Entwicklung Nordwestdeutschlands, Band 1: Geschichte der Erforschung, Datengrundlage, Methodik, großregionale Stellung NW-Deutschlands, Schollengliederung des Sockels, Typisierung der Strukturen des Oberbaues, Zeitlichkeit der Bewegungen, thermische und Reifungsgeschichte, Subsidenzgeschichte. Bericht Nr. 115557: 77 S., Hannover (Bundesanst. Geowiss. Rohstoffe) [unveröff.]
- Kohl, T., Brenni, R., Eugster, W. 2002. System performance of a deep borehole heat exchanger. *Geothermics* No. 31. 687-708.
- Kölbel, H. 1944. Die tektonische und paläogeographische Geschichte des Salzgitterer Gebietes. – Abh. Reichsamt f. Bodenforsch., N.F, 207: 1–100.
- Kölbel, H. 1967. Allgemeiner Überblick über die paläogeografische und tektonische Stellung des Nordostdeutschen Tieflandes nebst Einführung in die Problemstellung. *Berichte der Deutschen Gesellschaft für Geologische Wissenschaften* 12 1/2, 51-64.
- Kossow, D., & Krawczyk, C. M. (2002). Structure and quantification of processes controlling the evolution of the inverted NE - German Basin. *Marine and Petroleum Geology*, 19(5), 601–618.
- Kossow, D., Krawczyk, C. M., McCann, T., Strecker, M., & Negendank, J. F. W. (2000). Style and evolution of salt pillows and related structures of the northern part of the Northeast German Basin. *International Journal of Earth Sciences*, 89(3), 652–664.
- Krauss, M., Meyer, P. 2004. Das Vorpommern-Störungssystem und seine regionale Einordnung zur Transeuropäischen Störung. *Z. geol. Wiss.* 32, 2–4, pp. 227–246, Berlin.
- Kubon, R. 1966. Ergebnisbericht der VEB Geologische Erkundung Nord über die Kartierungsarbeiten im raum Rügen (Tertiär-Rhät). unpublished.
- Krzywiec, P. 2002. Mid-Polish Trough inversion – Seismic examples, main mechanisms and its relationship to the Alpine – Carpathian collision. *Continental collision and the tectonosedimentary evolution of forelands: European Geophysical Society Special Publication*, 1, 151–165

Kyrkjebø, R., Gabrielsen, R. H., Faleide, J. I., 2004. Unconformities related to the Jurassic–Cretaceous synrift–post-rift transition of the northern North Sea. *Journal of the Geological Society* 161.1. 1-17.

Larsen, G. 1966. Rhaetic-Jurassic-Lower Cretaceous sediments in the Danish Embayment (A Heavy Minerals Study). *Danmarks Geologiske Undersøgelse II. Række*, 91, 1-127.

Larson, R. L., 1991. Geological consequences of superplumes. *Geology*, 19. 963-966.

Leszczynski, K., 1997. The Lower Cretaceous depositional architecture and sedimentary cyclicity in the Mid-Polish Trough. *Geological Quarterly* Vol. 41, No. 4, 509-520.

Leszczynski, K. 1998. The Lower Cretaceous. In: *Paleogeographic atlas of epicontinental Permian and Mesozoic in Poland (1:2 500 000)* (eds. R.Dadlez, S.Marek and J. Pokorski). *Pol.Geol. Inst.Warszawa*.

Leszczynski, K., Waksmundzka, M. 2013. The palynofacies pattern for the Lower Cretaceous of central Poland. *Geological Quarterly* Vol. 57, No. 1, 101-112.

Linke, F., Krauss, M. 1966. *Ergebnisbericht Reflexionsseismik Rügen SW (Tiefe Horizonte)*. unpublished.

Lovley DR, Goodwin S. 1988. Hydrogen concentration as an indicator of the predominant terminal electron-accepting reactions in aquatic sediments. *Geochim Cosmochim Acta* 52:2993–3003

Ludwig. 1956. *Sedimentpetrographische Untersuchungen des Wealden und Portland der Bohrung Werle 7*. Staatl. Geol. Kommission der DDR – Sedimentpetrographisches Labor. Berlin.

Malz, A., Nachtweide, C., Emmerlich, S., and Schimpf, L. 2020. Mesozoic intraplate deformation in the southern part of the Central European Basin – Results from largescale 3D modelling, *Tectonophysics*, 776, 228–315,

Marek, S. 1964. Paleogeographical and stratigraphical sketch of the Lower Cretaceous in the Polish Lowlands. *Kwart. Geol.*, Vol. 8, No. 2, 282-290.

Marek, S. and Raczynska, A. 1979. Lithostratigraphic subdivision of epicontinental Lower Cretaceous in Poland and proposals for its rearrangement (in Polish with English summary). *Kwart. Geol.*, Vol. 23, No. 3, 631-637.

Marek, S. 1988. Paleothickness, lithofacies and paleotectonics of the epicontinental Lower Cretaceous in Poland. *Kwart. Geol.*, Vol. 32, No. 1, 157-174.

Marek, S. 1997. Kreda dolna. Litostratygrafia i lithofacje. Formalne i nieformalne jednostki litostratigraficzne. In: *The epicontinental Permian and Mesozoic in Poland* (eds. S. Marek, M. Pajchłowa) *Pr. Państw. Inst. Geol.*, 153. p. 351.

Madhawa Hettiarachchi H., D., Golubovic Mihajlo, Worek, W. M., Ikegamy, Y. 2007. Optimum design criteria for an Organic Rankine Cycle using low-temperature geothermal heat sources. In: *Energy*, No. 32, 1698-1706.

McBride, E. F., 1963. A classification of common sandstones. *Journal of Sedimentary Petrology* 33, 664–669.

Meinhold, R., Unger, E., Wienholz, R. 1960. Neue Erkenntnisse über den prätertiären Untergrund des Fischlandgebietes der DDR. Internat. geol. Congr., Rep. 21, See. Norden 1960, Ti.11, 87-100, Kopenhagen 1960.

Miall, A.D. 2006. The Geology of fluvial deposits – Sedimentary Facies, Basin Analysis and Petroleum Geology. 4<sup>th</sup> corrected printing.p.599.

Mutterlose, J., 1992b.Die Unterkreide-Aufschlüsse (Berrias-Hauterive) im Nördlichen Wiehengebirgsvorland (N-Deutschland). Geologie und Paläontologie in Westfalen 21, 39-113.

Mutterlose, J., 1995. Die Unterkreide-Aufschlüsse des Osning-Sandsteins (NW-Deutschland) – Ihre Faune und Lithofazies. Geologie und Paläontologie in Westfalen 36, 1-85.

Mutterlose, J., Bornemann, A., 2000. Distribution and facies patterns of Lower Cretaceous sediments in northern Germany: a review. Cretaceous Research 21, 733-759

Mutterlose, J., Bodin, S., Fähnrich, L., 2014. Strontium-isotope stratigraphy of the Early Cretaceous (Valanginian-Barremian): implications for Boreal-Tethys correlation and paleoclimate. Cretaceous Research 50, 252-263.

Muñoz, Y. A., 2006. The thermal history of the western Lower Saxony Basin, Germany. RTWH Aachen. (unpublished PhD thesis). p. 165.

Niegel, S., Franz, M., 2023. Depositional and diagenetic controls on porosity evolution in sandstone reservoirs of the Stuttgart Formation (North German Basin). Marine and Petroleum Geology. 151.

Nöldeke, W., Schwab, G. 1977. Tectonic development of platform cover of north german-polish depression, with special respect to north of GDB. Zeitschrift für Angewandte Geologie 23 (8), 369-379.

Nøttvedt, A., Gabrielsen, R., Steel, R., 1995. Tectonostratigraphy and sedimentary architecture of rift basins, with reference to the Northern North Sea. Marine and Petroleum Geology. 12. 881-901.

Amaya V. Novo, Joseba R. Bayon, Daniel Castro-Fresno, Jorge Rodriguez-Hernandez, 2010. Review of seasonal heat storage in large basins: Water tanks and gravel–water pits, Applied Energy, Volume 87, Issue 2, Pages 390-397.

Odin, G.S., Matter, A. 1981. De glauconarium origine. Sedimentology 28, 611–641.

Olivarius, M., Nielsen, L. 2016. Triassic paleogeography of the greater eastern Norwegian-Danish Basin: Constraints from provenance analysis of the Skagerrak Formation. Marine and Petroleum Geology 69. pp.168-182.

Panfilov M, Gravier G, Fillacier S 2000. Underground storage of H2 and H2-CO2-CH4 mixtures. Paper A003 presented at the EAGE 10th European Conference on the Mathematics of Oil Recovery held 4–7 Sept 2016 in Amsterdam

Pelzer, G., Wilde, V., 1987. Klimatische Tendenzen während der Ablagerung der Wealden-Fazies in Nordwesteuropa. Geologisches Jahrbuch A96, 239-263.

Pelzer, G. 1998. Sedimentologie und Palynologie der Wealden-Fazies im Hannoverschen Bergland. Georg August Universität Göttingen, 274 pp (unpublished PhD thesis).

Pelzer, G., Riegel, W., Wilde, V., 1992. Depositional controls on the lower Cretaceous Wealden coals of northwest Germany. In Controls on the distribution and quality of Cretaceous coals ( Eds. McCabe, P.J., Parrish, J.T.), Special Paper 267. Geological Society of America, 227-244.

Petmecky, S., Meier, L., Reiser, H., Littke, R., 1998. High thermal maturity in the Lower Saxony Basin: intrusion or deep burial? *Tectonophysics* 304, 317-344.

Petzka, E., Bartsch, D., Eiermann, H. 1964. Zwischenbericht des VEB Geologische Erkundung Nord über das Kartierungsobjekt Doggersenke Usedom (unpublished) VEB Geologische Erkundung Nord.

Pichler M. 2010. Assessment of hydrogen-rock interactions during geological storage of CH<sub>4</sub>-H<sub>2</sub> mixtures. Master Thesis, Leoben

Prössl, K. 1990. Dinoflagellaten der Kreide. – Unter-Hauterive bis Ober-Turon – im niedersächsischen Becken. – *Palaeontographica B*, 218: 93-191; Stuttgart.

Raczynska, A. 1967. Lower Cretaceous stratigraphy and sedimentation in western Poland. *Biul. Inst. Geol.*, 210, 129-179, Warszawa

Raczynska, A. 1979. The stratigraphy and lithofacies development of the younger Lower Cretaceous in the Polish Lowlands. *Pr. Inst. Geol.*, 89.

Reitenbach, V., Ganzer, L., Albrecht, D., & Hagemann, B. 2015. Influence of added hydrogen on underground gas storage: a review of key issues. *Environmental Earth Sciences*, 73, 6927-6937.

Rockel, W., Hoth, P. & Seibt, P. 1997. Charakteristik und Aufschluss geothermaler Speicher. *Geowissenschaften* 15, 244–252.

Ross, G. 1964. Schichtenverzeichnis der Bohrung Fe Sanne 1/64. unpublished.

Rusbült, J. 1964. Untersuchungsbericht Nr. 461 (Z). Mikropaläontologischer Untersuchungsbericht zur Bohrung Heringsdorf 4/63. VEB Erkundung Nord. unpublished.

Rudolph, I. 1962. Untersuchungsbericht zur Schwermineralanalyse der Bohrung Garz 1/61. VEB Erkundung Nord. unpublished.

Sahagian, D., Pinous, O., Olfieriev, A., Zakharov, V. 1996. Eustatic curve for the Middle Jurassic–Cretaceous based on Russian platform and Siberian stratigraphy: zonal resolution. *AAPG Bull.* 80, 1433–1458.

Scheck-Wenderoth, M., Krzywiec, P., Zühlke, R., Maystrenko, Y., Froitzheim, N. 2008. Permian to Cretaceous Tectonics. In *The Geology of Central Europe Volume 2: Mesozoic and Cenozoic* (Ed. McCann, T.), 923–997, Geological Society.

Schlanger, S. O.; Jenkins, H. C. 1976. Cretaceous anoxic events: Causes and consequences. *Geologie en Mijnbouw*, 55, 179-184.

Schmidt, T., Mangold, D., Müller-Steinhagen, H. 2003. Seasonal thermal energy storage in Germany. In: *ISES solar word congress, Göteborg, Schweden*.

Schnabel, M., Noack, V., Ahlrichs, N., Hübscher, C. 2021. A comprehensive model of seismic velocities for the Bay of Mecklenburg (Baltic Sea) at the North German Basin margin: implications for basin development. *Geo-Mar Lett* 41, 20.

Schneider, A.C., Heimhofer, U., Heunisch, C., Mutterlose, J. 2017. The Jurassic-Cretaceous boundary interval in non-marine strata of northwest Europe - New light on an old problem, *Cretaceous Research*, 1-13.

Schneider, A. C., Heimhofer, U., Heunisch, C., Mutterlose, J. 2018. From arid to humid – The Jurassic – Cretaceous boundary interval in northern Germany. *Review of Paleobotany and Palynology* 255, 57-69.

Schott, W. 1967. Paläogeografischer Atlas der Unterkreide von Nordwestdeutschland. Bundesanstalt für Bodenforschung Hannover

Schulz, R., Beutler, G., Röhling, H.-G., Werner, K.-H. 1994. Regionale Untersuchungen von geothermischen Reserven und Ressourcen in Nordwestdeutschland. Niedersächsisches Landesamt für Bodenforschung, Hannover.

Schulz, R., Röhling, H.-G., 2000. Geothermische Ressourcen in Nordwestdeutschland. *Zeitschrift für Angewandte Geologie* 46, 122–129.

Schulz, R., Agemar, T., Althen, A.-J., Kühne, K., Maul, A.-A., Pester, S., Wirth, W., 2007. Aufbau eines geothermischen Informationssystems für Deutschland. *Erdöl Erdgas Kohle* 123, 76-81.

A. Schuster, S. Karellas, R. Aumann, 2010. Efficiency optimization potential in supercritical Organic Rankine Cycles, *Energy*, Volume 35, Issue 2, Pages 1033-1039.

Schwab, G., Benek, R., Jubitz, KB, Teschke, HJ. 1982. Intraplattentektonik und Bildungsprozess der Mitteleuropäischen Senke. *Z. Geol. Wiss.* 10, 397-413.

Schwab, G., 1985. Paläomobilität der Norddeutsch-Polnischen Senke, (unveröff.) Diss. B der AdW der DDR, Berlin, pp. 196.

Senglaub, Y., Brix, M. R., Adriasola, A. C., Littke, R. 2005. New information on the thermal history of the southwestern Lower Saxony Basin, northern Germany, based on fission track analysis, *Int. J. Earth Sci.*, 94, 876-896.

Sirocko, F., Reicherter, K., Lehne, R., Hübscher, Ch., Winsemann, J., Stackebrandt, W., 2008. Glaciation, salt and the present landscape. In: Littke, R., Bayer, U., Gajewski, D., Nelskamp, S. (Eds.), *Dynamics of Complex Sedimentary Basins. The Example of the Central European Basin System*. Springer, 234–245

Sosnicka, M., Lüders, V. 2020. Fluid inclusion evidence for low-temperature thermochemical sulfate reduction (TSR) of dry coal gas in Upper Permian carbonate reservoirs (Zechstein, Ca<sub>2</sub>) in the North German Basin. *Chemical Geology* 534

Sparfeld, K., F., Dreyer, M., 1970. Zusammenfassung der biofaziellen Ergebnisse der makro und mikropaläontologischen Untersuchungen in der Bohrung Sanne 1/64 + Beitrag zum Bericht. Forschungsinstitut für die Erkundung und Förderung von Erdöl und Erdgas, Gommern.

Sparfeld, K., F., Dreyer, M., 1970a. Biofazielle Ergebnisse der makro- und mikropaläontologischen Untersuchungen in der Bohrung Bismark-Ost 1. Forschungsinstitut für die Erkundung und Förderung von Erdöl und Erdgas, Gommern.



Sparfeld, K., F. 1972. Biofazielle Ergebnisse der makro- und mikropaläontologischen Untersuchungen in der Bohrung Waddekath 35. Forschungsinstitut für die Erkundung und Förderung von Erdöl und Erdgas, Gommern.

Sparfeld, K., F. 1973. Ergebnisse der makro- und mikropaläontologischen Untersuchungen der Unterkreide der Bohrung Teetz 1/63. Zentrales Geologisches Institut, Berlin.

Stampfli, G.M., Borel, G.D. 2002. A plate tectonic model for the Paleozoic and Mesozoic constrained by dynamic plate boundaries and restored synthetic oceanic isochrons. *Earth Planet. Sci. Lett.* 196, 17–33.

Stollhofen, H., Bachmann, G. H., Barnasch, J., Bayer, U., Beutler, G., Franz, M., Kästner, M., Legler, B., Mutterlose, J., Radies, D. 2008. Upper Rotliegend to Early Cretaceous basin development. - In: Littke, R., Bayer, U., Gajewski, D., Nelskamp, S. (Eds.), *Dynamics of Complex Intracontinental Basins: the Example of the Central European Basin System*, Springer, 181-210.

Strauss, C., Elstner, F., Jan du Chêne, R., Mutterlose, J., Reiser, H. & Brandt, K.-H. 1993. New microplaeontological evidence on the stratigraphic position of the 'German Wealden' in NW-Germany. *Zitteliana* 20, 389-401.

Stille, H. 1924. *Grundfragen der vergleichenden Tektonik*. Berlin 1924

Tröger, K. A. 1966. Bericht über die Untersuchungen von Megafaunen aus den Kartierungsbohrungen Barth 4/65, Barth 5/65, Pramort1/60 und Darßer Ort 1/60. *Geologische Erkundung Nord, Schwerin*.

Truche L, Jodin-Caumon MC, Lerouge C, Berger B, Mosser R, Giffaut E, Michau N. 2013. Sulphide mineral reactions in clay-rich rock induced by high hydrogen pressure, Application to disturbed or natural settings up to 250 C and 30 bar. *J Chem. Geol* 351: 217–228

Tucker, M. E. 2011. Ch. 3: Siliciclastic sediments II. In: *Sedimentary Petrology*. 3<sup>rd</sup> edition. Blackwell Publishing.

Ulmer-Scholle, D., Scholle, P., Schieber, J., Raine, R. 2015. *A Color Guide to the Petrography of Sandstones, Siltstones, Shales and Associated Rocks*. American Association of Petroleum Geologist 109.

Underhill, J. R., Partington, M. A., 1993. Jurassic thermal doming and deflation in the North Sea: implication of the sequence stratigraphic evidence. In *Petroleum geology of Northwest Europe*. Vol. 1 of Proceedings of the 4th Conference. Geological Society, (Ed. Parker, J. R.), London, 337–346

Van Houten F. B., Arthur, M. A., 1989. Temporal patterns among Phanerozoic oolitic ironstone and oceanic anoxia. In: Young, T. P., Taylor, E. G., (Eds.), *Phanerozoic Ironstones*. *Geol. Soc. Spec. Publ.* 46, 33-49.

Voigt, E. 1963. Über Randtröge vor Schollenrändern und ihre Bedeutung im Gebiet der Mitteleuropäischen senke und angrenzender Gebiete. *Z. dt. Geol. Ges.* 114 (2), 378–418.

Voigt, T., von Eynatten, H., and Franzke, H.-J.: Late Cretaceous unconformities in the Subhercynian Cretaceous Basin (Germany), *Acta Geol. Pol.*, 54, 673–694, 2004.

Voigt, S., Wagreeich, M., Surlyk, F., Walaszczyk, I., Ulicny, D., Cech, S., Voigt, T., Wiese, F., Wilmsen, M., Niebuhr, B., Reich, M., Funk, H., Michalik, J., Jagt, J. W.M., Felder, P. J.,

Schulz, A. S. 2008a. Cretaceous In: *The Geology of Central Europe Volume 2: Mesozoic and Cenozoic* (Ed. McCann, T.), 923–997, Geological Society.

Voigt, T., Reicherter, K., von Eynatten, H., Littke, R., Kley, J., 2008b. Sedimentation during basin inversion. In: Littke, R., Bayer, U., Gajewski, D., Nelskamp, S. (Eds.), *Dynamics of Complex Sedimentary Basins. The Example of the Central European Basin System*. Springer, 211–232

Voigt, T., von Eynatten, H., and Kley, J. 2009. Kommentar zu „Nördliche Harzrandstörung: Diskussionsbeiträge zu Tiefenstruktur, Zeitlichkeit und Kinematik von Volker Wrede (ZDGG 159/2: 293-316). *Zeitschrift der Deutschen Gesellschaft für Geowissenschaften*, 160(1), 93-99.

Voigt, T., Kley, J., Voigt, S. 2021. Dawn and dusk of Late Cretaceous basin inversion in central Europe. *Solid Earth* 12, 1443–1471.

Wentworth, C. K. 1922. A scale of grade and class terms for clastic sediments. *The journal of geology*, 30(5), 377-392.

Wienholz, E. 1967. Mikropaläontologischer Abschlussbericht für die an der Struktur Gorlosen abgeteufften Bohrungen Gorlosen 1/56 bis 9/58. FIWE Gommern.

Wilmsen, M. 2003. Sequence stratigraphy and palaeoceanography of the Cenomanian Stage in northern Germany, *Cretaceous Res.*, 24, 525–568, 2003.

Wilmsen, M., Niebuhr, B., Hiss, M. 2005. The Cenomanian of northern Germany: facies analysis of a transgressive biosedimentary system, *Facies*, 51, 242–263.

Wolburg, J. 1949. Ergebnisse der Biostratigraphie nach Ostracoden im nordwestdeutschen Wealden. In *Erdöl und Tektonik in Nordwestdeutschland* (Ed. Bentz, A.), 349-360 (Amt für Bodenforschung, Celle/Hannover).

Wolburg, J. 1959. Die Cyprideen des NW-deutschen Wealden. In *Senckenbergiana Lethaea* 40, 223-315 .

Wolfgramm, M., Thorwart, K., Rauppach, K., & Brandes, J. 2011. Zusammensetzung, Herkunft und Genese geothermaler Tiefengrundwässer im Norddeutschen Becken (NDB) und deren Relevanz für die geothermische Nutzung. *Z. geol. Wiss*, 339, 173-193.

Wolfgramm, M., Agemar, T. & Franz, M. 2014. Explorationsstrategie tiefer geothermischer Ressourcen am Beispiel des Norddeutschen Beckens (NDB). In: *Handbuch Tiefe Geothermie*. Ed. by M. J. Bauer, W. Freeden, H. Jacobi & T. Neu. Heidelberg: Spektrum Verlag, 463–505.

Wormbs, J., Diener, I., Rusitzka, I., Pasternak, G., Tesch, M., Toleikis, R. 1989. Abschlussbericht Geothermie im Nordteil der DDR (I), Zentrales Geologisches Institut. Berlin. unpublished. 47 pp.

Ziegler, P. A. 1982. *Geological Atlas of western and central Europe*, 239 pp. (Shell International Petroleum, Den Haag)

Ziegler, P. A. 1990. *Geological Atlas of western and central Europe*, 2<sup>nd</sup> edition, 239 pp. (Shell International Petroleum, Den Haag).

Zimmerle, W. 1979. Lower cretaceous Tuffs in Northwest Germany and their Geotectonic Significance. *Aspekte der Kreide. IUGS series A, No. 6*, 385-402. Stuttgart.

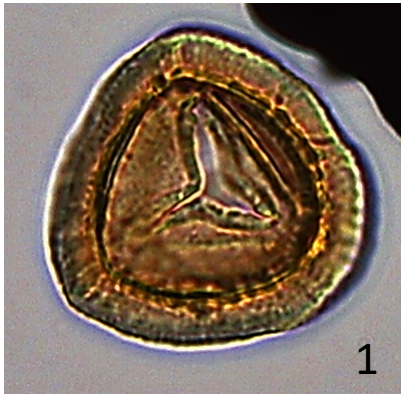
Zimmermann, J., Franz, M., Heunisch, C., Luppold, F.W. Mönning, E., Wolfgramm, M. 2015. Sequence stratigraphic framework of the Lower and Middle Jurassic in the North German Basin: epicontinental sequences controlled by Boreal cycles

Zöllner, H., Reicherter, K., Schikowsky, P. 2008. High-resolution seismic analysis of the coastal Mecklenburg Bay (North German Basin): the pre Alpine evolution. *Geologische Rundschau* 97, 1013-1027.

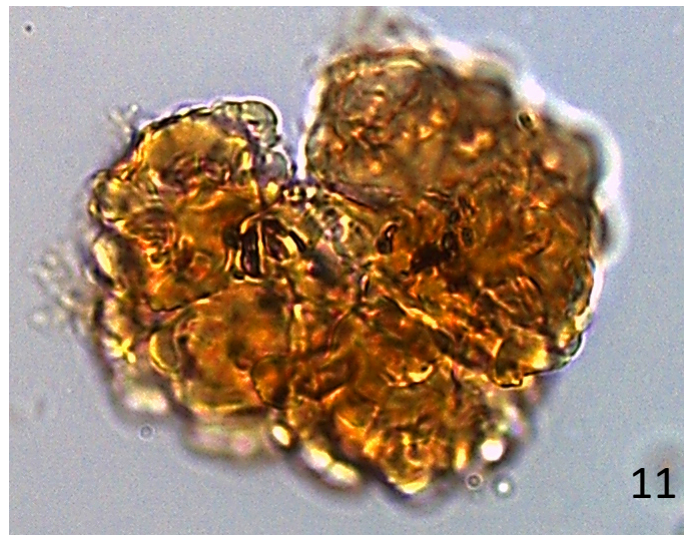
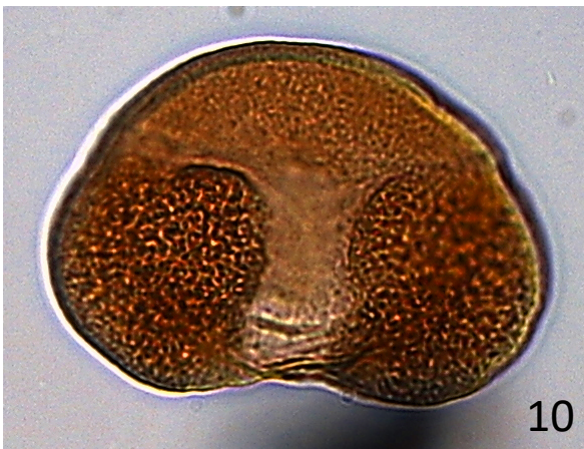
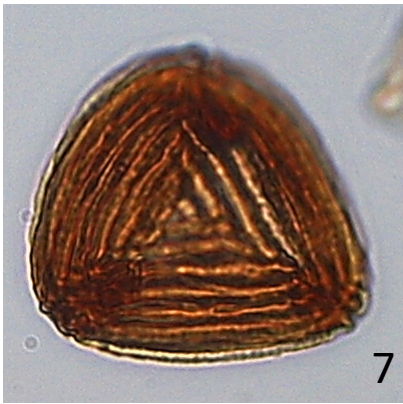
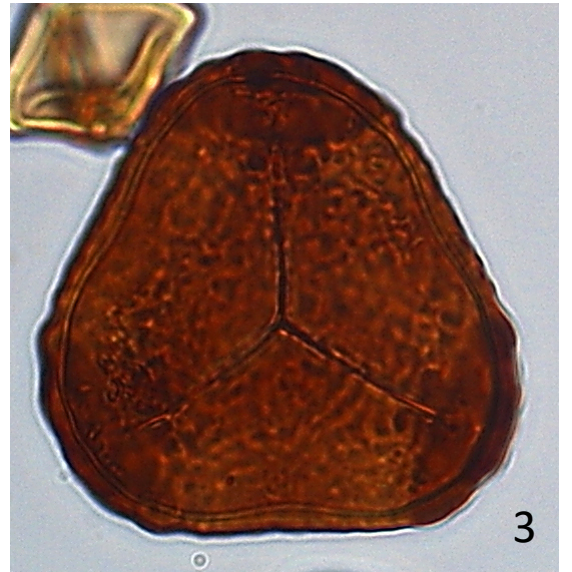
*Appendix*

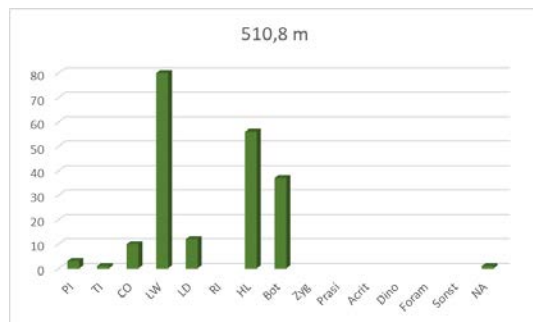
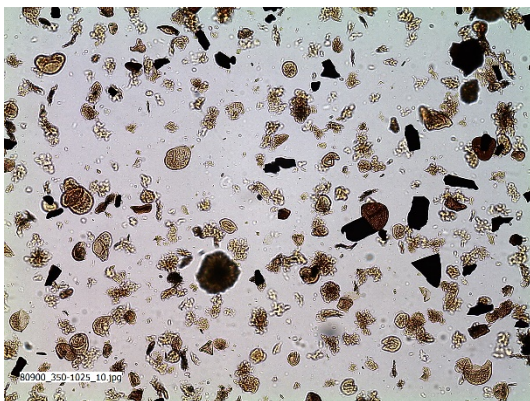
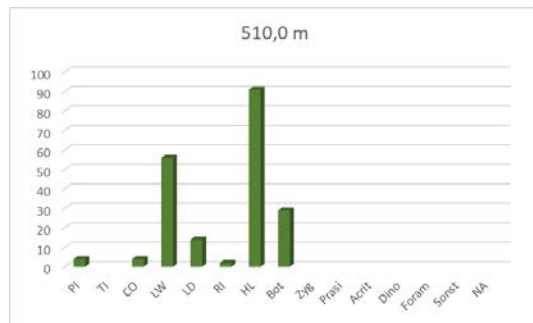
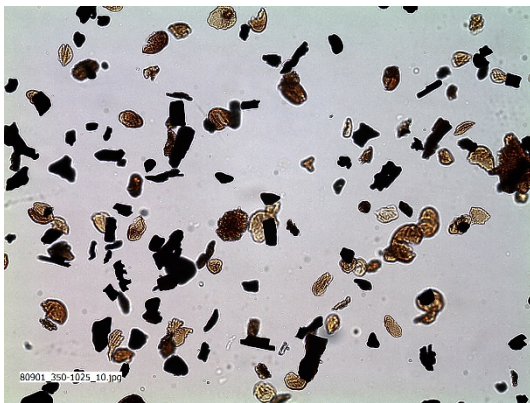
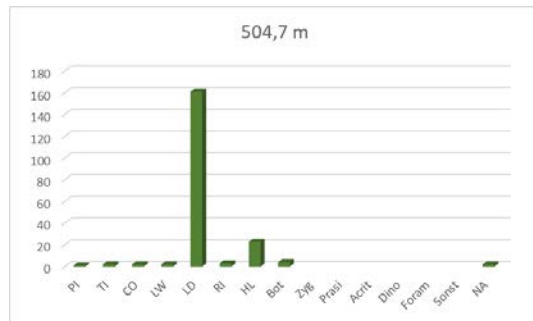
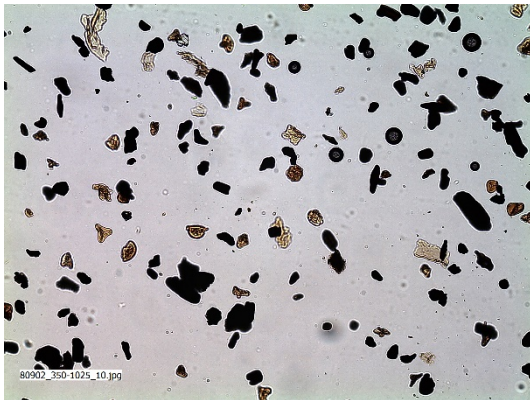
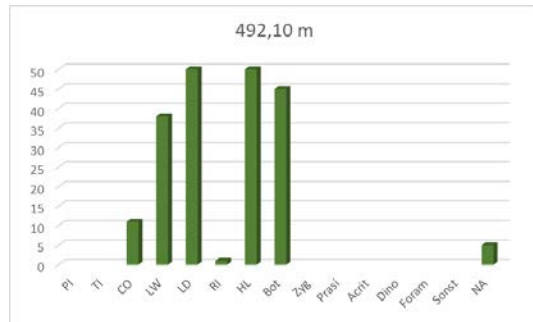
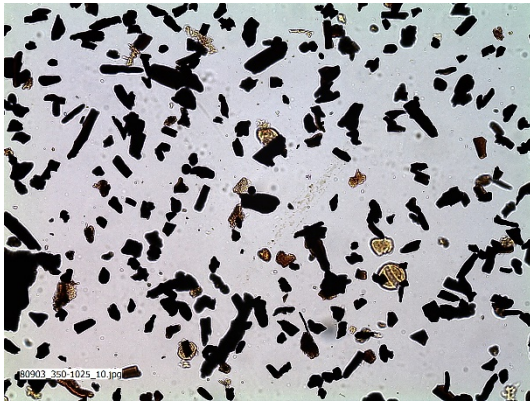
## **Appendix**





50 µm









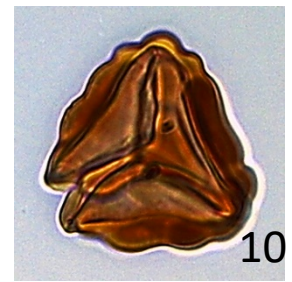
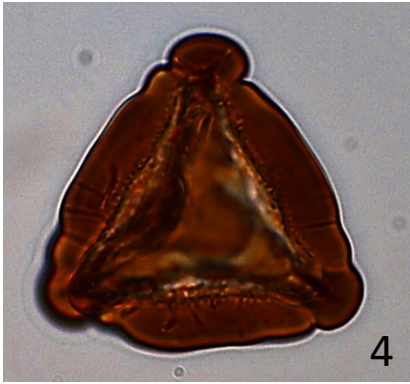
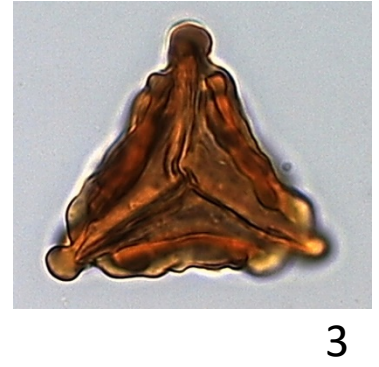
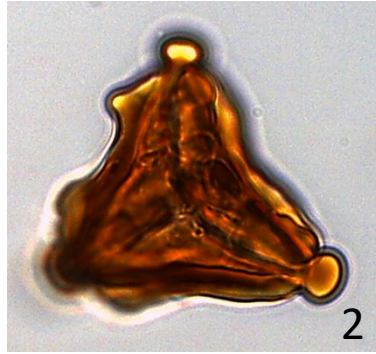
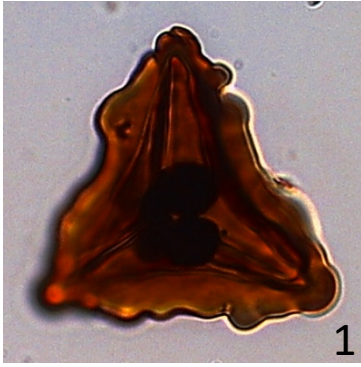


Fundort/ Bohrung	Probenbez. Auftrag.	Probenober-teufe (m)	Probenunter-teufe (m)	P-Nr.	N-Nr.	Biostrat.	terrestrisch_kontinental										ABF		ALB	AM						Summe Plankton marin			
						*: Nannoplankton	PI	TI	CO	LW	LD	RI	HL	NA	Summe e terr.	Bot/Alg	Zygn	SpP u. ABF	Prasi	Acrit	D-prox	D-proxcho	C-chor	D-cavat	Foram		div.		
Bohrung Ückeritz 1/64	16-95	163,7	163,71	80658	16571	krlo3 oder krcu*				2		1		7	3	13			13	4	1	22	93	64	3				187
Bohrung Ückeritz 1/64	16-96	163,8	163,81	80659		kE																							
Bohrung Ückeritz 1/64	16-94	167,8	167,81	80660	16572	krlo3 oder krcu*	5			7	1	67	2	52	7	141	1		142	1	1	13	20	21	1	1			58
Bohrung Ückeritz 1/64	16-93	171,7	171,71	80661	16573	krlo3*	8			3	7	36	3	43	22	122	1		123		3	24	23	25	2			77	
Bohrung Ückeritz 1/64	16-92	171,8	171,81	80662		kru, "Wealden-Fazies"	4				8	70	4	37	21	144	53	1	198	2								2	
Bohrung Ückeritz 1/64	16-91	172,3	172,31	80663		kru, "Wealden-Fazies"	4	4		3	7	90	2	37	11	158	42		200										
Bohrung Ückeritz 1/64	16-89	179,7	179,71	80664K		kru, "Wealden-Fazies"				1		83	1	1	8	94	6		100										
Bohrung Ückeritz 1/64	16-90	179,9	179,91	80665K		kru, "Wealden-Fazies"						73	4	10	8	95	3	1	99					1			1		
Bohrung Ückeritz 1/64	16-88	187,7	187,71	80666		kE																							
Bohrung Ückeritz 1/64	16-87	214,2	214,21	80667	16574	kru	3			9	9	65	5	16	13	120	12		132			21	37	6	2	2	68		
Bohrung Ückeritz 1/64	16-86	220	220,01	80668	16575	kru	1	2		6	13	46	2	23	27	120	1		121			29	20	18	7	5	79		
Bohrung Ückeritz 1/64	16-84	224,1	224,11	80669		kru, "Wealden-Fazies"	4	1		3	12	98	2	29	6	155	45		200										
Bohrung Ückeritz 1/64	16-85	224,4	224,41	80670	16576	krho oder jünger				7	13	38	2	25	31	116	2		118	1	3	39	13	8	11	7	82		
Bohrung Ückeritz 1/64	16-83	235,1	235,11	80671		kru, "Wealden-Fazies"	1	1		2	50	43	4	34	9	144	55		199						1	1			
Bohrung Ückeritz 1/64	16-82	243	243,01	80672		kru, "Wealden-Fazies"	5	3		2	31	87	7	23	7	165	34		199			1				1			
Bohrung Ückeritz 1/64	16-81	248,8	248,81	80673K		kE																							
Bohrung Ückeritz 1/64	16-80	256,2	256,21	80674K		kru, "Wealden-Fazies"		3	5	18	97	6	42	12	183	10			193		1	1	3	2		7			
Bohrung Ückeritz 1/64	16-79	262,4	262,41	80675		kru, "Wealden-Fazies"		1		2	170	2	20	4	199	1			200										
Bohrung Ückeritz 1/64	16-78	270	270,01	80677	16577	kru	3			30	75	20		42	15	185	2		187			12		1		13			
Bohrung Ückeritz 1/64	16-77	278,3	278,31	80676	16578	kru		1	14	4	6			13	29	67	1		68		6	82	23	16	1	4	132		

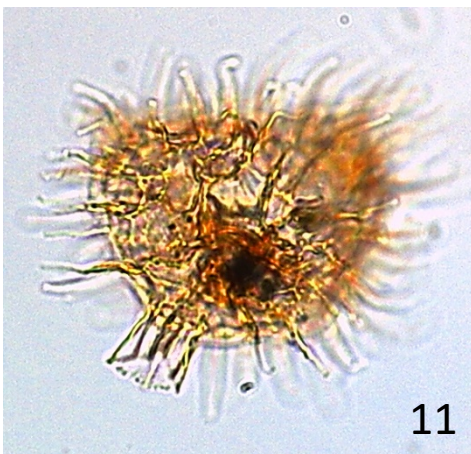
K: KOH

	terrestrisch-kontinentaler Ablagerungsraum
	mariner Ablagerungsraum

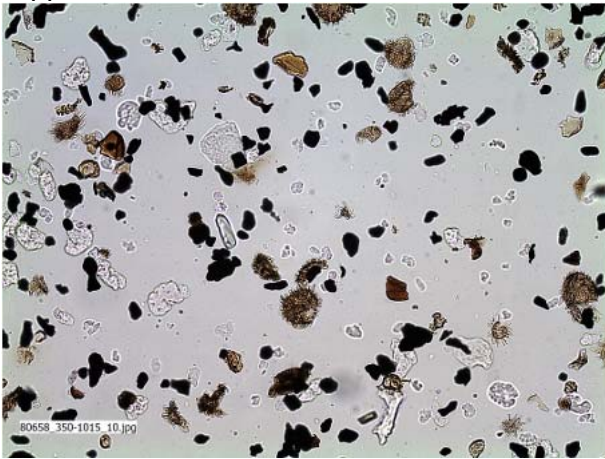
PI: Pionier; TI: Tidal; CO: Coastal; LW: Lowland, wet /Marsch; LD: Lowland, dry / Geest; RI: River; HL: Hinterland; Bot: Botryococcus; Zyg: Zygnemataceen; ABF: aquatisch, brackisch/fluviatil; Prasi: Prasinophyceen; ALB: aquatisch, lagunär/brackisch; AM: aquatisch, marin; Acrit: Acritarchen, D-prox - D-cavat: Dinozysten; Foram: Foraminiferen; Div: divers



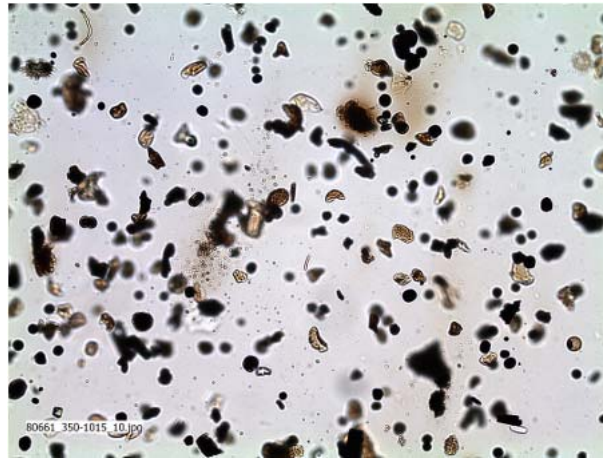
50  $\mu$ m



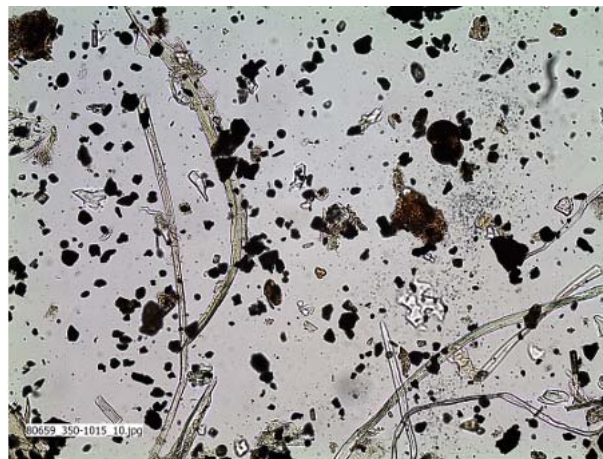
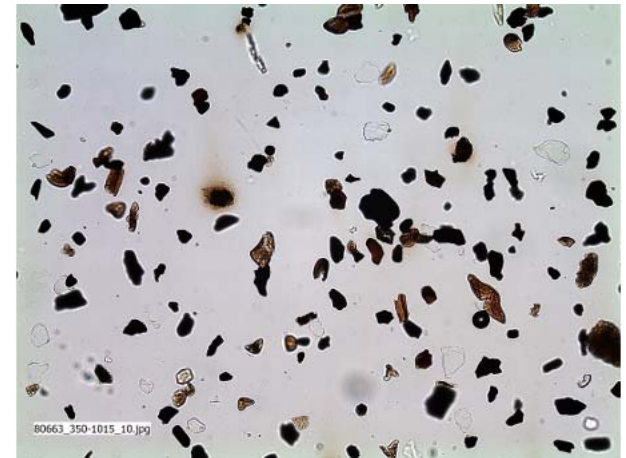
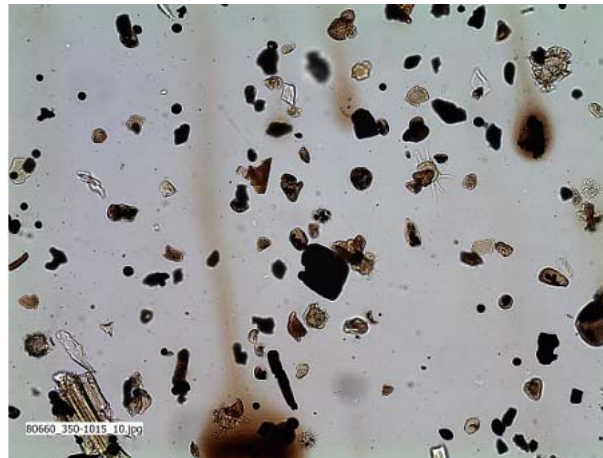
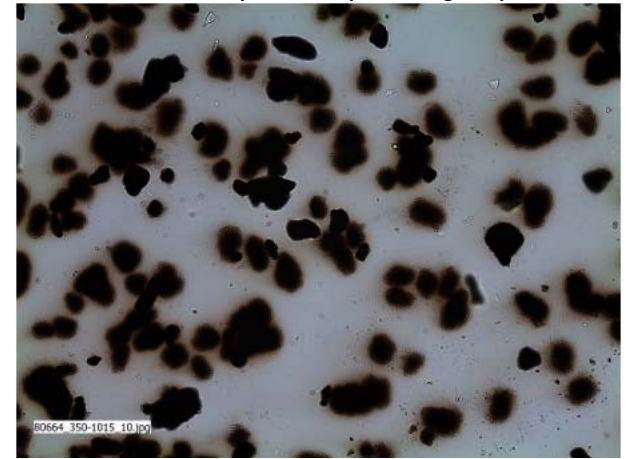
Appendix A



Ückeritz 1



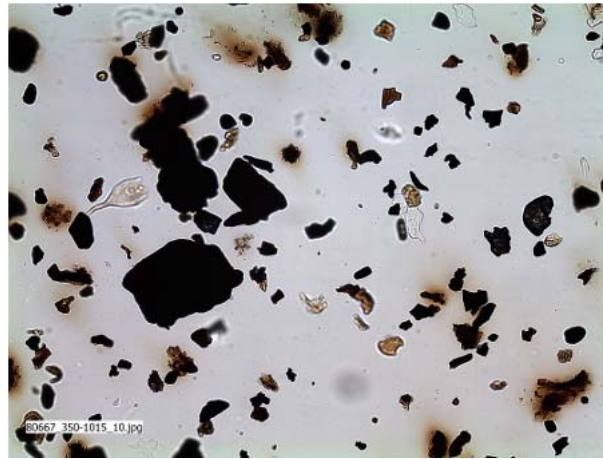
Sporomorph Ecogroup Model



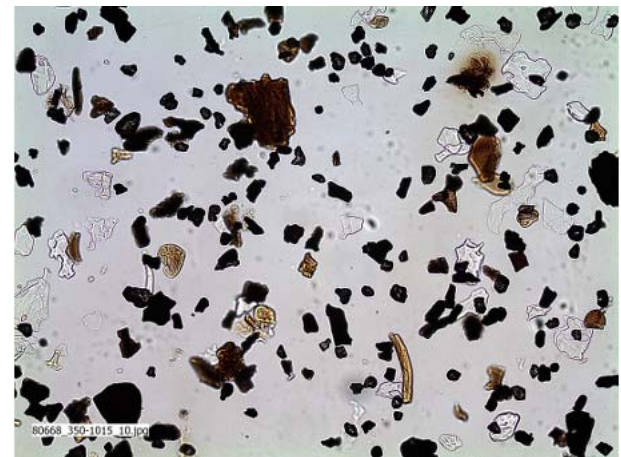
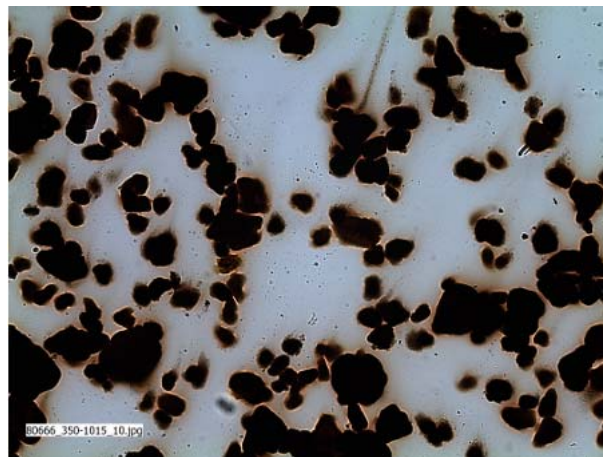
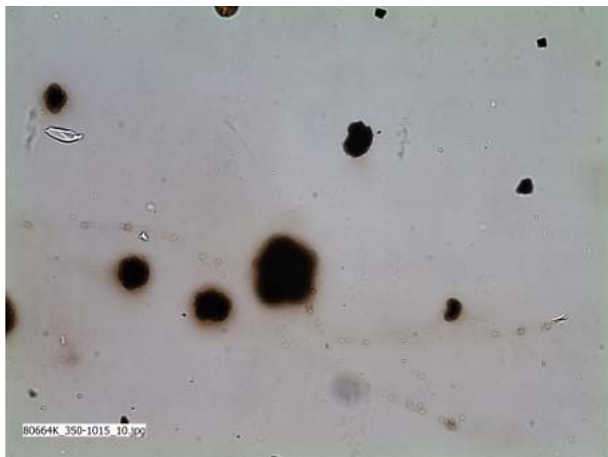
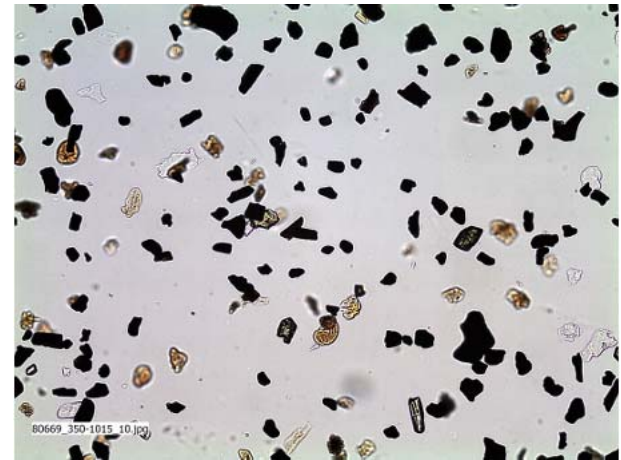
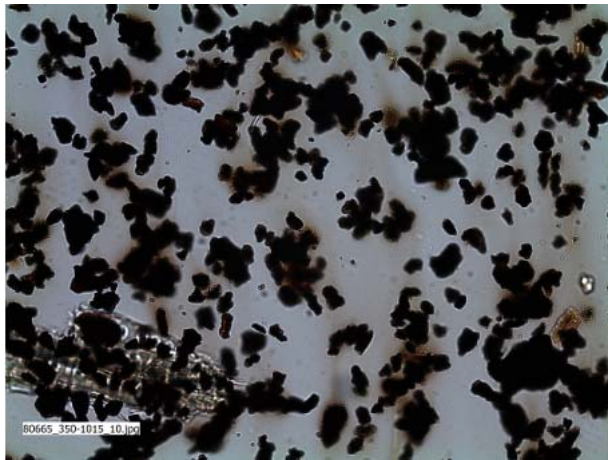
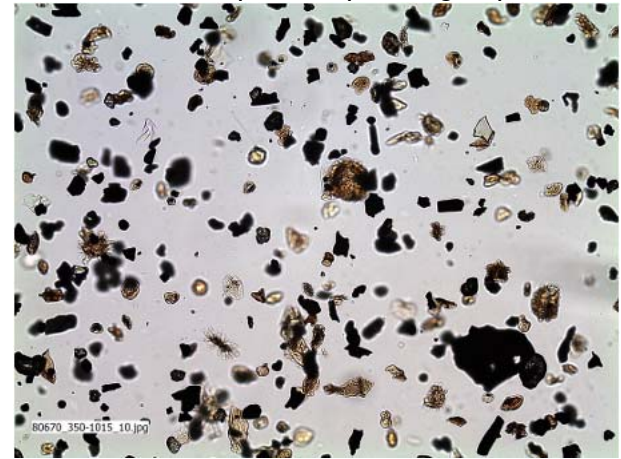
Appendix A



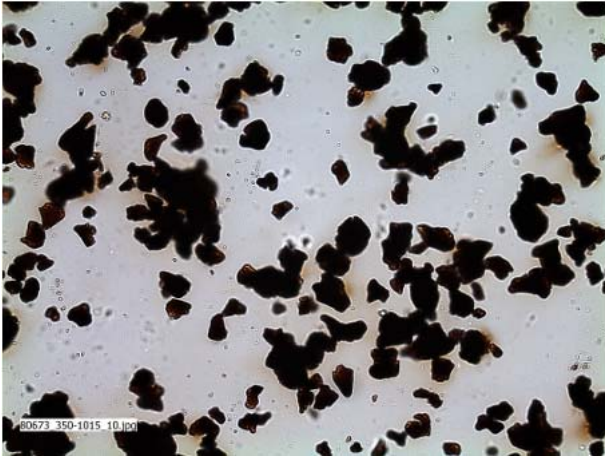
Ückeritz 1



Sporomorph Ecogroup Model



Appendix A



Ückeritz 1



Sporomorph Ecogroup Model

